1968

# A structural model study of load distribution in box-beam bridges, May 1968 Publication 73-44

M. A. Macias-Rendon

D. A. VanHorn

Follow this and additional works at: http://preserve.lehigh.edu/engr-civil-environmental-fritz-lab-reports

A STRUCTURAL MODEL STUDY

OF LOAD DISTRIBUTION

IN BOX-BEAM BRIDGES

by

Miguel Angel Macías Rendón
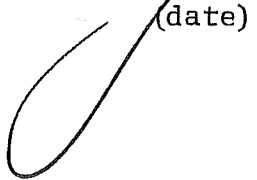
A Dissertation
Presented to the Graduate Committee
of Lehigh University
in Candidacy for the Degree of
Doctor of Philosophy
in
Civil Engineering

Lehigh University
Bethlehem, Pennsylvania
1968

Approved and recommended for acceptance as a dissertation in partial fulfillment of the requirements for the degree of Doctor of Philosophy.

_May 1, 1968_
(date)

_David A. VanHorn_
David A. VanHorn, Professor in Charge

Accepted _May 14, 1968_
(date)

Special committee directing the doctoral work of Mr. Miguel Angel Macías Rendón

_John W. Fisher_
Professor John W. Fisher, Chairman

_David A. VanHorn_
Professor David A. VanHorn

_Le-Wu Lu_
Professor Le-Wu Lu

_Russell E. Benner_
Professor Russell E. Benner

_Lynn S. Beedle_
Professor Lynn S. Beedle

Miguel Angel Macías Rendón

# TABLE OF CONTENTS

## LIST OF FIGURES

# LIST OF TABLES

# ABSTRACT

The major objective of this model study is the design
of a highly efficient structural model system to study the static
live load distribution in a particular type of highway bridge.
The specific bridge type has a beam-slab superstructure consist-
ing of a reinforced concrete cast-in-place slab constructed to
act compositely with precast prestressed concrete spread box
beams.

A thorough examination of the similitude requirements
is presented. The design conditions for the model system are
discussed, and a length scale of 16 is adopted. Particular im-
portance is given to the material properties of the prototype,
and three possible model materials, Plexiglas, aluminum, and
polyvinyl chloride. After careful consideration of the many
factors involved, Plexiglas was selected as the most appropriate
material for this model study.

Special attention was given to the creep phenomenon
in Plexiglas. The creep compensating technique was used and
its mathematical proof is presented. A Plexiglas compensating
load cell was fabricated, and its instantaneous calibration fac-
tor was found by means of a delicate and precise procedure. Two

1

testing frames were designed and fabricated in order to conduct load cell and tensile specimens tests, and the bridge model tests. A model vehicle was also designed, with adjustable axle load ratios, in order to be able to subject the bridge models to design vehicular loads.

Pilot tests were conducted on a model simulating an existing bridge that had been previously tested as part of a series of field tests. These pilot tests served to demonstrate the feasibility of the use of Plexiglas models, and suggested possible improvements in future field and model tests.

The design of the model system is presented. This system enables a systematic evaluation of the most important parameters affecting live load distribution in box-beam bridges. Slabs of various thicknesses had a special pattern of perforations drilled to permit their bolting to the tapped holes in the walls of prefabricated box beams. The box beams were made to represent six different prototype cross-sections. Curb and parapet pieces were bolted to the slab and to the curb, respectively. Midspan and end diaphragms were fitted and held between beams by means of transverse tie rods. To provide uniformity, all of the connectors were tightened with a calibrated torque

wrench. In this manner, dismountable models of a great variety of cross-sections were assembled and tested with considerable saving in time. The experimental data was recorded directly on punched cards, thus permitting the data to be analyzed and all calculations to be performed with a digital computer on the same day of the test.

The tests were designed and conducted so that the experimental data could be subjected to a proper statistical analysis. The small sample method was used and least squares curve fitting was performed using orthogonal polynomials. A procedure was devised to permit the automatic correction of random errors. The main computer program used also included a successive approximations method to obtain equilibrium of moments in the entire cross-section of the model.

Experimental results are presented in graphical form, and the behaviors of the seventeen different cross-sections tested are compared. The influence of beam size, number of beams, slab thickness, and effect of curb, parapet, and diaphragms is also discussed. Finally, recommendations for future investigations are given, having in mind as the main goal a thorough understanding of the structural behavior resulting in the optimum design of box-beam bridges.

# 1.    INTRODUCTION

Numerous theoretical and experimental studies have been carried out on the problem of wheel load distribution in multi-beam bridges.[13,15,21,22]  Due to the high complexity of this problem every theoretical analysis makes use of simplifying assumptions that undoubtedly reduce the accuracy of the solution. An analog computer, either in the form of a structural model system or of a series of singular field tests, is the only practical way to obtain the true response of a multi-beam bridge.

Field studies of existing bridges may be used as a basis for the revision of specifications covering load distribution.  However, due to the many problems involved in field testing, the collection of necessary information and the eventual updating of the specifications is a slow process.  As it is very difficult to substantially shorten the time required for the collection and processing of field test data, consideration should be given to a structural model study.

In the case of box-beam bridges the following paragraph is particularly applicable.[16]

4

"In many such instances (when the general
laws governing the behavior of the system
are unknown and analytical procedures have
not yet been developed) a general formula
is not necessary; all that the engineer re-
quires for the design is an indication of
the relationship of the variables for a
specific design, or within a narrow range
of variation of the significant variables.
Under those circumstances a model may give
the desired result quickly and cheaply."

Although, in recent years, several major model stud-

ies have been made of existing structures and have proved to

be successful,[12, 14, 18, 19] none of these studies has been capable

of producing a systematic investigation of the parameters in-

volved in a particular structural phenomenon. Besides requir-

ing less labor and expense than would be needed to conduct a

series of field tests of prototype bridges, a well-planned

model study enables a more complete investigation with the

adequate variation of the most important parameters.

The major objective of this dissertation is the de-

velopment of a highly efficient structural model system to

study the static live load distribution in prestressed con-

crete spread box-beam bridges. The development of such a sys-

tem should make it possible to investigate the adequacy of cur-

rent design specifications dealing with load distribution in

highway bridge superstructures of the beam-slab type. Collateral objectives are:

    1.  A critical evaluation of the feasibility of the use of model analysis for investigations of load distribution in bridge structures.

    2.  The establishment of design conditions for model studies of this phase, and of similar phases, of structural behavior.

    3.  The further evaluation of three materials, Plexiglas, aluminum, and polyvinyl chloride, for potential use in structural models.

## 2.  SIMILITUDE REQUIREMENTS

### 2.1  Prototype Structure

The specific bridge type to be considered has a beam-slab superstructure with a symmetrical cross-section consisting of a reinforced concrete cast-in-place slab constructed to act compositely with precast prestressed concrete box beams. Curb and parapet sections complete the cross-section.

Over the past few years the box-beam bridge has experienced various changes. Initially, the box beams were placed adjacent to each other, with or without lateral post-tensioning and shear keys designed to provide lateral interaction, and with an asphalt wearing surface applied directly on top of the beams. Later, this design was changed by the placing of a cast-in-place reinforced concrete slab, which acted compositely with the beams, thereby eliminating the need for lateral prestressing, shear keys, and a separate wearing surface. More recently, prestressed concrete box-beam bridges are being constructed with the beams spread apart and equally spaced, and with diaphragms cast integrally with the slab at midspan and at both ends to distribute the live load more uniformly.

## 2.2  Design Conditions for the Model System

The model design conditions are obtained by means
of a dimensional analysis of the phenomenon under considera-
tion. Therefore, it is necessary first to determine the sig-
nificant variables and after careful examination, to assess
their corresponding importance. Depending on the objective
of the investigation, it is often possible to neglect one or
more of the variables in arriving at an adequate and practical
model design.

The static live load distribution in box-beam bridges
is primarily dependent upon the flexural behavior of the super-
structure. Since the slab is subjected to longitudinal and trans-
verse bending moments, two major elastic properties of the slab
material are involved, modulus of elasticity and Poisson's ratio.
In addition, the specific weight and heterogeneity of material
strengths and of support conditions can be considered as sec-
ondary variables.

In the bridge model tests included in this investiga-
tion, the primary measurements are of static loads, distances,
deflections, and normal strains. Therefore, the complete set
of variables involved would be:

| Symbol | Variable | Dimension |
|--------|----------|-----------|
| P | static load | F |
| D | distance | L |
| I | moment of inertia | $L^4$ |
| $E_b$ | modulus of elasticity of beam material | $FL^{-2}$ |
| $\delta$ | deflection | L |
| $\epsilon$ | normal strain | - |
| $\nu$ | Poisson's ratio of slab material | - |
| $\gamma$ | unit weight of material | $FL^{-3}$ |
| $E_s$ | modulus of elasticity of slab material | $FL^{-2}$ |
| S | support conditions | - |

A total of ten variables are involved using only two basic dimensions, force F, and length L. Therefore, according to the Buckingham Pi Theorem, similitude conditions are expressed with eight dimensionless and independent Pi terms. These Pi terms can be readily found by repeating the variables P and D which represent the two basic dimensions:

$$\pi_1 = \frac{D^4}{I} , \qquad\qquad \pi_2 = \frac{P}{D^2 E_b} ,$$

$$\pi_3 = \frac{D}{\delta}, \qquad\qquad \pi_4 = \epsilon,$$

$$\pi_5 = \nu, \qquad\qquad \pi_6 = \frac{P}{D^3 \gamma},$$

$$\pi_7 = \frac{P}{D^2 E_s}, \qquad \text{and} \qquad \pi_8 = S \qquad (1)$$

These eight Pi terms represent the design conditions that should be fulfilled in order to produce a true model. These design conditions are generally expressed as:

$$\left(\pi_i\right)_{model} = \left(\pi_i\right)_{prototype} \qquad (2)$$

## 2.3 Prediction Equations

To determine the load distribution in the model, bending moments carried by individual beams would have to be computed. These individual bending moments can be found from stress blocks determined from strains. Therefore, normal strain is the most important of the model variables to be measured. The prediction equation for normal strain would be

$$\pi_4 = \epsilon = f_4\left( \frac{D^4}{I}, \frac{P}{D^2 E_b}, \frac{D}{\delta}, \nu, \frac{P}{D^3 \gamma}, \frac{P}{D^2 E_s}, S \right) \qquad (3)$$

and interpreted as follows:

If all of the design conditions involving the Pi terms in the right hand side of the prediction equation are fulfilled, then homologous normal strains in the model and in the prototype are identical.

On the other hand, if the deflection is the variable under consideration,

$$\pi_3 = \frac{D}{\delta} = f_3 \left( \frac{D^4}{I} , \frac{P}{D^2 E_b} , e , \nu , \frac{P}{D^3 \gamma} , \frac{P}{D^2 E_s} , S \right) \qquad (4)$$

is the prediction equation for deflection, interpreted as

$$\left( \frac{D}{\delta} \right)_{model} = \left( \frac{D}{\delta} \right)_{prototype} \qquad or \qquad \frac{\delta_p}{\delta_m} = \frac{D_p}{D_m} = n, \qquad (5)$$

where n is the length scale of the model; thus

$$\delta_p = n \, \delta_m \qquad (6)$$

## 2.4 Length Scale

The selection of the length scale depends on several technical, as well as practical, aspects. The magnitude of

quantities to be measured, testing facilities, material prop-
erties, and ease of fabrication and handling, are the pertinent
aspects to consider.

A critical evaluation of the feasibility of the use
of model analysis for the investigation of load distribution in
bridge structures is one of the collateral objectives of this
study; therefore, it follows that the ease of fabrication should
be given special attention. Since all of the bridge elements
are made out of plate components, different plate thicknesses
will be represented by commercial thicknesses of the model ma-
terial. It is known that most materials are sold in thickness
multiples of a certain fraction of an inch, 1/32, 1/16, 1/8,
etc., and it is desirable to directly use an available thick-
ness to represent that of the slab, which is the largest single
plate component of the bridge.

Currently, prestressed concrete bridges are designed
in Pennsylvania according to provisions set forth in the Penn-
sylvania Department of Highways Bridge Division Standards ST-200
through ST-208.[20] In these standards, a minimum slab thickness
of 7-1/2 inches is specified for what can be considered a nom-
inal thickness of 8 inches. This thickness can be scaled down

to 1/4, 1/2, or 1 inch by the use of a length scale of 32, 16,
or 8, respectively. Two-lane traffic requires a clear roadway
of at least 24 feet,[1] and typical simple spans range between
60 and 70 feet. Therefore, the length scale of 16 yields a
slab size of 25 by 50 inches. This size is easily manageable
in a relatively small space, yet large enough to exhibit meas-
urable deformations. Confirmation of this length scale depends
on the material to be used, since its properties influence the
magnitude of the force to be applied by the testing equipment.

## 3. MODEL MATERIAL AND TESTING TECHNIQUE

### 3.1 Pertinent Material Properties

In the selection of the model material, the properties
to be considered are of two kinds; first, the ones directly in-
volved in the design conditions, shown in Table 1; and second,
the properties closely related to the needs for fabrication,
instrumentation, and testing of the model.

According to the design conditions, the properties to
consider in prototype and model materials are, modulus of elas-
ticity of the beam material, Poisson's ratio of the slab material,
unit weight, and modulus of elasticity of the slab material, and
support conditions.

At this point, it would be appropriate to consider the
behavior of the prototype structure under working load conditions,
as related to the appropriateness of choosing a relatively homo-
geneous and isotropic material. The prototype structure is de-
scribed in Section 2.1. When constructed to the design specifi-
cations, the prestressed beams remain uncracked under working
load conditions. Since in many previous laboratory investiga-
tions, elastic behavior has been demonstrated in uncracked pre-
stressed beams, it is certainly appropriate to consider the use
of any elastic material for the model. On the other hand, the
reinforced concrete slab of the prototype does not behave in a

14

full homogeneous and isotropic manner, due to the usual cracking developed under vehicular loadings. Therefore, the use of a homogeneous material in the model slab would actually violate one of the design conditions for a true model. However, it was believed that this cracking would not substantially influence the overall structure behavior, and that a homogeneous model slab would produce an accurate representation of the prototype.

The properties of the prototype are of great influence in the application of the design conditions, and since it is almost impossible to predict with any accuracy the values of the moduli of elasticity for the two different concretes in beams and slab,[11] the ratio of the two moduli is considered instead of their absolute values. Therefore, the dimensionless $\pi_7$ term found in Eqs. 1 is modified by combination with $\pi_2$ in order to obtain a new form for $\pi_7$,

$$\pi_7 = \frac{P}{D^2 E_s} \div \pi_2 = \left(\frac{P}{D^2 E_s}\right) \cdot \left(\frac{D^2 E_b}{P}\right) = \frac{E_b}{E_s} \neq 1, \qquad (7)$$

meaning $\left(\dfrac{E_b}{E_s}\right)_{model} = \left(\dfrac{E_b}{E_s}\right)_{prototype}$ \qquad (8)

This condition cannot be fulfilled in the model by the use of the same material for the beams and slab. Instead, the different modulus of the slab can be simulated by a special scale factor used in the thickness of the slab only. Calling

this special scale factor $n_s$, and using the original $\pi_7$,

$$\left(\frac{P}{D^2 \, E_s}\right)_{model} = \left(\frac{P}{D^2 \, E_s}\right)_{prototype}, \tag{9}$$

where $D^2$, in effect, represents cross-sectional distances in the slab in accordance to typical slab behavior. One of these two distances is measured in a horizontal plane and the other in the vertical direction involving, respectively, the length scale $n$ and the special scale $n_s$. From Eq. 9,

$$\frac{D^2_p}{D^2_m} = n \cdot n_s = \left(\frac{P}{E_s}\right)_p \cdot \left(\frac{E_s}{P}\right)_m, \tag{10}$$

or
$$n_s = \frac{1}{n} \cdot \left(\frac{P_p}{P_m}\right) \cdot \left(\frac{E_m}{E_{sp}}\right), \quad \text{since } E_{sm} = E_{bm} = E_m, \tag{11}$$

Now, using the term $\pi_1$ in Eqs. 1, where $n_s$ does not apply,

$$\frac{P_p}{P_m} = n^2 \left(\frac{E_{bp}}{E_m}\right) \tag{12}$$

and substituting (12) in (11), $n_s = n \left(\dfrac{E_b}{E_s}\right)_p$ (13)

Using the empirical formula proposed by Hognestad,[11]

$$\left(\frac{E_b}{E_s}\right)_p = \frac{1,800,000 + 460\ f'_{cb}}{1,800,000 + 460\ f'_{cs}} \tag{14}$$

where $f'_c$ is the ultimate stress of concrete cylinders in $lb/in^2$. Taking for the beams $f'_{cb} = 5,000\ lb/in^2$, and for the slab $f'_{cs} = 4,000\ lb/in^2$,

$$\left(\frac{E_b}{E_s}\right)_p = \frac{4.10 \times 10^6\ lb/in^2}{3.64 \times 10^6\ lb/in^2} = 1.13, \text{ and } n_s = 1.13n \tag{15}$$

With $n = 16$, as found in Chapter 2, $n_s$ takes a value of 18 which is impractical to fulfill. So, for the time being,

$$n_s \cong n \tag{16}$$

If the results of the model show great discrepancy when compared to the prototype, Eq. 13 can be applied to reduce such discrepancy.

The design condition stated by the term $\pi_5 = \nu$, specifies that Poisson's ratio must be the same in model and prototype. Since all three possible model materials, Plexiglas, aluminum, and polyvinyl chloride, have a Poisson's ratio around 0.33, and Poisson's ratio varies from 0.15 to 0.22 for concrete,[11] it follows that by the use of any of the three

proposed materials a distortion in the model will result. There
are three alternatives:

1. Abandon all three proposed model materials,
   Plexiglas, aluminum, and polyvinyl chloride, and
   search for a material with a Poisson's ratio
   similar to that of concrete.

2. Make use of a factor $\alpha$ as a measure of the de-
   gree of distortion, $\pi_{5m} = \alpha\pi_{5p}$, and of a factor
   $\beta$ in the prediction equation, $\pi_{ip} = \beta\pi_{im}$. The
   value of $\alpha$ has known extreme values, but $\beta$ has
   to be determined by either additional experi-
   mental evidence or by mathematical knowledge of
   how $\pi_5$ affects the behavior of the prototype.

3. Accept the degree of distortion of 2.2 to 1.5
   (in accordance with Poisson's ratio of the pro-
   totype), and study the model as one possible
   extreme behavior of the bridge. This study
   could be later used, with additional tests, to
   determine the value of $\beta$.

For this study, the third alternative was selected.

The $\pi_6$ term establishes the requirement to be fulfilled for true simulation of the unit weight. However, this study being directed toward the distribution of live load will not be handicapped if $\pi_6$ is distorted, unless the bridge's own weight is needed to maintain full contact with the supports. It is interesting to know the weight that the model has to have when made with the three proposed materials, by simply applying the term $\pi_2$ to an estimated prototype weight of 500,000 lb., from Eq. 12,

$$\text{Plexiglas:} \quad \frac{500,000 \times 4.5 \times 10^5}{256 \times 4.1 \times 10^6} = 215 \text{ lb.}$$

$$\text{Aluminum:} \quad \frac{500,000 \times 10 \times 10^6}{256 \times 4.1 \times 10^6} = 4,770 \text{ lb.}$$

$$\text{Polyvinyl chloride:} \quad \frac{500,000 \times 4 \times 10^5}{256 \times 4.1 \times 10^6} = 191 \text{ lb.}$$

It is obvious that the handling of 4,770 lb. in the laboratory should be avoided.

The last design condition, $\pi_8$, specifies similitude of support conditions. The most important conditions are, continuity, fixity, and rigidity.

The prototype bridge to be studied consists of a

simple span with one end fixed by dowels to its support and with
an expansion support at the other end. Neoprene bearing pads,
with durometer hardness of 60 and shape factor (loaded area to
free-to-bulge area) of 3.45 are common values used in Pennsyl-
vania.[10] Their rigidity K has a value close to $2 \times 10^6$ lb/in.,
and its specific $\pi_8$ term requires

$$\left(\frac{K\ D}{P}\right)_m = \left(\frac{K\ D}{P}\right)_p , \qquad (17)$$

or by use of Eq. 12,

$$K_m = \frac{1}{n}\left(\frac{E_m}{E_{bp}}\right) \cdot K_p \qquad (18)$$

Using the values of n, $E_{bp}$, and $K_p$,

$$K_m \cong \frac{E_m}{32} \quad \text{in lb/in. if } E_m \text{ in lb/in}^2 . \qquad (19)$$

This value could be very difficult to fulfill and it is
believed that, for the time being, the conditions of continuity
and fixity of the supports are the most important ones. Their
simulation would not involve additional distortion. Individual
1/2 in. steel rods can be used to support the beams; with
clamped-in-place rods at the south support, and free-to-roll

rods at the north support. Steel end plates can be bolted to the beams in order to eliminate sliding friction with the rods.

3.2  Fabrication Problems

The practical aspect of difficulties of fabrication of the model cannot be disregarded. Each box beam consists of bottom and side walls of 5/16 in. in thickness, and of a 3/16 in. thick top wall. An internal diaphragm 5/8 in. thick and two end blocks 1½ in. thick complete the beam. The beam can be made out of cemented plate elements, or if using aluminum, it can be extruded. Extrusion is impractical due to the high cost, but the cementing of plate elements is a possible alternative.

Plexiglas can be cemented with a number of cements or solvents, such as Ethylene Dichloride. Aluminum can be cemented less easily by means of structural epoxies capable of developing shear strengths of up to 500 lb/in$^3$. Polyvinyl chloride which is not a transparent material, is very difficult to cement, and consequently must be joined by a special process.

Machining is another important aspect of model construction. Plexiglas can be sawed, drilled, and machined like

wood or soft metals, and due to its low weight, it can be stocked and handled more easily than aluminum.

Because of these considerations, Plexiglas was selected as the most appropriate material for this model study. This selection is the last collateral objective of this study.

## 3.3  Compensation for Creep in Plexiglas

Plexiglas has several detrimental properties:

1. It creeps under sustained load, that is, its modulus of elasticity decreases with time under sustained stress. This decrease of E is practically independent of the level of stress, as long as the stress is other than zero.

2. It is a material highly sensitive to temperature. Its modulus of elasticity decreases with an increase in temperature. This calls for a rigorous control of the room temperature in the laboratory.

3. An increase of relative humidity from 20% to 90% produces an expansion of 0.0030 to 0.0055,

in a thickness of 0.25 in., depending on the
grade of the Plexiglas.  Therefore, relative
humidity must be controlled in the laboratory.

4.  Its low coefficient of thermal conductivity,
1.3 BTU per  Hr. x Sq. Ft. x $^\circ$F/in., prohibits
the use of strain measurement circuits with
continuous current flowing through the electri-
cal resistance gages.

5.  Thickness tolerances vary for different grades
of Plexiglas.  Grade II UVA must be used ex-
clusively in order to maintain a better thick-
ness control and a higher degree of consistency.

Creep in Plexiglas is a most undesirable phenomenon.
It has caused numerous model studies to be excessively time
consuming, when the testing technique has been to wait for a
certain time to elapse between the application of the gravity
load and the recording of every gage.  This technique does not
really solve the problem caused by creep.  Instead, it gets a-
round the problem with a resulting waste of the investigator's
time.  The solution is to eliminate the time parameter by the
application of a fixed deformation, and the use of a special

technique to measure the load that would produce such deformation in the absence of creep.[4,6]

In general, strain can be expressed as the product of the activating force P and the flexibility F of the member,

$$\epsilon = P \cdot F \tag{20}$$

Equation 20 indicates that for constant strain the product P x F remains constant also. Creep causes the modulus of elasticity to decrease under the stress produced by the applied strain. A decrease of modulus of elasticity means an increase in flexibility and a decrease in the force necessary to maintain the constant strain. A metallic load cell would show this reduction in the force producing constant strain in a Plexiglas specimen.

A load cell with identical creep characteristics to those of the Plexiglas specimen would have a constant output, even under a force that varies with time. Equilibrium requires that

$$\left(\frac{\epsilon}{F}\right)_{\text{load cell}} = \left(\frac{\epsilon}{F}\right)_{\text{specimen}} , \tag{21}$$

and taking the first derivative of both sides respect to time, and giving indexes c and s to load cell and specimen,

respectively,

$$\frac{F_c\left(\dfrac{d\epsilon_c}{dt}\right) - \epsilon_c\left(\dfrac{dF_c}{dt}\right)}{F_c^2} = \frac{F_s\left(\dfrac{d\epsilon_s}{dt}\right) - \epsilon_s\left(\dfrac{dF_s}{dt}\right)}{F_s^2} \; , \tag{22}$$

constant strain in the specimen means $\dfrac{d\epsilon_s}{dt} = 0,$ therefore

$$\frac{d\epsilon_c}{dt} = \frac{1}{F_c}\left[ \epsilon_c\left(\frac{dF_c}{dt}\right) - \left(\frac{F_c}{F_s}\right)^2 \cdot \epsilon_s\left(\frac{dF_s}{dt}\right)\right], \tag{23}$$

represents the rate of change of the load cell output. For constant output,

$$\frac{d\epsilon_c}{dt} = 0 = \frac{1}{F_c}\left[ \epsilon_c\left(\frac{dF_c}{dt}\right) - \left(\frac{F_c}{F_s}\right)^2 \cdot \epsilon_s\left(\frac{dF_s}{dt}\right)\right]; \tag{24}$$

it follows that $\quad \epsilon_c\left(\dfrac{dF_c}{dt}\right) = \left(\dfrac{F_c}{F_s}\right)^2 \cdot \epsilon_s\left(\dfrac{dF_s}{dt}\right) \quad , \tag{25}$

and using Eq. 21: $\quad \left(\dfrac{F_c}{F_s}\right) \cdot \epsilon_s\left(\dfrac{dF_c}{dt}\right) = \left(\dfrac{F_c}{F_s}\right)^2 \cdot \epsilon_s\left(\dfrac{dF_s}{dt}\right), \tag{26}$

or $\quad \dfrac{dF_c}{dt} = \left(\dfrac{F_c}{F_s}\right) \cdot \left(\dfrac{dF_s}{dt}\right) \tag{27}$

But $F_c = \dfrac{C_c}{E_c}$ and $F_s = \dfrac{C_s}{E_s}$ , where $E_c$ and $E_s$ are the moduli

of elasticity of the load cell and the specimen respectively,

and $C_c$ and $C_s$ are individual geometrical constants;

therefore, $\quad \dfrac{dF_c}{dt} = -\left(\dfrac{C_c}{E_c^2}\right) \cdot \left(\dfrac{dE_c}{dt}\right)$ , $\quad \dfrac{dF_s}{dt} = -\left(\dfrac{C_s}{E_s^2}\right) \cdot \left(\dfrac{dE_s}{dt}\right)$ (28)

and $\quad \dfrac{F_c}{F_s} = \left(\dfrac{C_c}{C_s}\right) \cdot \left(\dfrac{E_s}{E_c}\right)$ . (29)

Substitution of Eqs. 28 and 29 into Eq. 27 results in

$$-\left(\frac{C_c}{E_c^2}\right) \cdot \left(\frac{dE_c}{dt}\right) = \left(\frac{C_c}{C_s}\right) \cdot \left(\frac{E_s}{E_c}\right)\left[-\left(\frac{C_s}{E_s^2}\right) \cdot \left(\frac{dE_s}{dt}\right)\right] \quad (30)$$

and finally, $\quad \dfrac{dE_c}{dt} = \left(\dfrac{E_c}{E_s}\right) \cdot \left(\dfrac{dE_s}{dt}\right)$ . (31)

Equation 31 is fulfilled if load cell and specimen have the same modulus of elasticity and the same creep characteristics. A Plexiglas load cell placed between a mechanical jack and the Plexiglas model would be, in effect, a compensating load cell. Hydraulic jacks are to be avoided due to the possible presence of compressible air bubbles in the fluid.

The load cell, shown in Fig. 1, is of the compression type. It has adequate cross section and sensitivity, and

a stable output is developed from its four strain gages. It

is made out of a cast Plexiglas tube, 1.50 in. O.D. and 1.25

in. I.D., which showed almost identical modulus of elasticity

and creep characteristics as those of standard tensile

specimens taken out of the same Plexiglas sheet used for the

slab of the pilot model described in Section 4.3.


## 3.4 Calibration of the Plexiglas Load Cell

To obtain the instantaneous calibration factor of

the load cell, precise dead weights had to be applied with

equal increments, and output readings had to be taken at iden-

tical time intervals from the instant of application of the

full load. This permitted the use of orthogonal polynomials

in the regression analysis of the data.[24] In order to guaran-

tee the linearity of the load cell up to a high level of load

it was necessary to construct a dead-weights testing machine

with a calibrated lever arm which produced a magnification

ratio of five. Figure 2 shows the calibration of the load

cell.

The calibration was performed at two different tem-

peratures, 75°F and 76°F. For each temperature, the load cell

was loaded and unloaded three times. Figures 3 and 4 show

the regression analysis used for each determination. The sample of six values of instantaneous calibration factor was subjected to a statistical analysis, where the outliers were rejected in accordance with the Dixon criterion.[9,10,17] The instantaneous calibration factor of the load cell was found to be 0.0814 ± 0.0001 lb./microoutput at 75°F.

After the load cell had been calibrated, tests were performed on Plexiglas specimens taken from sheet stock used in the specimens described in Chapter 6. The tests, in conformance with the ASTM D 638-64T Standard,[3] were conducted by placing the load cell in series with the specimen and a straining turnbuckle, as shown in Fig. 5. The instantaneous modulus of elasticity, based on seven specimens, was found to range from 466,000 lb/in.$^2$ to 500,000 lb/in.$^2$, with a mean value of 484,000 lb/in.$^2$

## 3.5 Testing Frame and Vehicle

The testing frame was designed with the following objectives in mind:

1. Safe capacity for the application of a maximum load of twenty times the model vehicular load.

With Plexiglas as model material the standard

AASHO[1] HS20-44 truck trailer would be simulated

by a load of 32 lb. (Eq. 12), provided that the

modulus of elasticity for the concrete of the

beams has the value used in Eq. 15. The pro-

cedure of subjecting the model to twenty, or

perhaps more, times the rated load in several

increments has three obvious advantages over

making observations for the rated load only.[16]

First, gross errors of observation may be de-

tected and eliminated; second, errors due to an

initial lag or slippage may be eliminated; and

third, it is unnecessary to apply the rated load

to the model. The behavior under the rated load

can be found by interpolation. The allowable

capacity of the load cell is almost 3,000 lb.,

and a load twenty times the rated load would pro-

duce admissible stresses in the model.

2. Adequate rigidity to provide fixed reference to
   dial gages.

3. Bolted connections to permit changes in the
   assembly.

4. Versatility to test models with angle of skew
   varying from $45^{o}$ to $90^{o}$.

5. Facility to position the mechanical jack at any
   longitudinal or transverse location.

6. Small capacity mechanism to lift the model for
   possible work on the supports, deflection gages,
   etc.

The testing frame was designed with two levels of
longitudinal members connected by four vertical members. The
lower longitudinal members and the piers for the models were
fabricated from a 6 x 1-7/8 JR A7 steel rolled shape, while a
2-5/8 x 1-7/8 special I-shape was used for the members of the
upper level and the four vertical members. They were assembled
with 1/4" x 20 bolts and bevel washers, and tightened under a
test load of approximately 700 lb. Cross-bracings were used to
stabilize the frame. The overall dimensions of the frame are
approximately 86 in. long, 34 in. wide, and 38 in. high. Figure
6 shows the chain-driven mechanism used to change the longi-
tudinal position of the jack. Figure 7 is a close-up of the
mechanical jack, showing the ball-bushing system used to change
the transverse location.

In order to directly study the vehicular load distribution in the models, a model vehicle was needed. This model vehicle, shown in Fig. 8, was fabricated from slotted steel angle which permitted the lever arms to be easily changed. The front transverse member carries the front wheels and the lower longitudinal members carry the drive and rear wheels. All of the wheels and members are connected by pairs of bearings, each pair consisting of one regular ball bearing and one self-aligning bearing. The load cell rests on the loading plate in the upper longitudinal member. The webs of the members are stiffened with aluminum blocks. The contact area under the tires is represented by rectangles of aluminum,[2] and rubber pads cemented to these rectangles eliminate any damage to the model slab.

## 4.   PILOT TESTS

### 4.1  Description of the Prototype Bridge

In the period 1964-66, five existing box-beam bridges
were tested as part of an investigation being conducted by the
Structural Concrete Division of the Civil Engineering Department
of Lehigh University.  One of these bridges, located near Berwick,
Pennsylvania, was chosen as the prototype structure for the pilot
tests of this study.

The prototype has an angle of skew of 88° and was se-
lected to represent a 90° skew bridge in the field tests.  Figs.
9 and 10 show the elevation and the cross-section of the center
span, respectively.[8]  The section of maximum moment, which could
be produced by the northbound test vehicle, was located 3.55 feet
north of midspan, and gaged as shown in Fig. 11.

### 4.2  Test Vehicle

A photograph of the Bureau of Public Roads Bridge Re-
search Test Vehicle used in the field test is shown in Fig. 12,
along with the wheel spacings and axle loads.  The truck was a
three-axle Diesel tractor semi-trailer combination, which was
loaded with crushed stone to approximate the AASHO HS20-44 de-
sign vehicle.

32

## 4.3  Description of the Pilot Study Model

The pilot model A1, to simulate the Berwick bridge, was cemented with Ethylene Dichloride.  This adhesive was not only used to cement together the plate components of the beams, but to cement the entire model.  It was impossible to completely eliminate the air bubbles trapped in the adhesive between beams and slab, mainly because of the large contact areas.  No particular problem was encountered in the cementing of the curb and parapet sections, nor in the cementing of the nine diaphragm pieces.  This produced a permanent pilot model A1, with a midspan cross-section as shown in Fig. 13.  This figure clearly indicates the configuration of plate components in the beams.

The section of maximum moment was located at 2.66 in. north of midspan in the model.  This maximum moment location occurs under the drive axle of the northbound test vehicle. The section of maximum moment was gaged with eight strain gages on the beams, six gages on the curb and parapet, and three gages on top of the slab.  The strain gages are 120-ohm, wire-resistance gages, with the sensing element 1/2 in. long, and all are mounted in the longitudinal direction.  With gages on half of the cross-section only, each beam had two bottom gages and two gages 15/16 in. above the bottom fiber.  Two dial gages per beam were used in eastern beams A and B to measure deflections and rotations.  No transverse or diaphragm gages were used.  Figure 14 shows the final setup of the pilot tests.

## 4.4  Test and Results from Pilot Study

In trial tests of model Al, the performance of all gages was excellent, and an almost perfect linear strain distribution from bottom of beam to top of slab was exhibited. To develop a consistent, reproducible response, it was found necessary to shake down the model a minimum of three times before starting a formal test. Experimental values of the modulus of elasticity of the prototype, taken from the northbound runs, have an average of $7.5 \times 10^6$ lb/in$^2$.[8] The model truck load was reduced to 17.89 lb., instead of the value of 32 lb. mentioned in Section 3.5. The high ratio of moduli of elasticity does not affect the behavior of the model, but it linearly affects the prediction values for the prototype.

The comparison of moments and slab widths between model Al and the prototype is carried out in Chapter 9, after the computational assumptions are formulated in Chapter 8. It is possible to compare now the homologous values of deflections and rotations of the beams. Table 2 shows large differences between model and field test values due to distortions of various design conditions in the model. However, these differences suggest a much lower value for the prototype modulus than the one found in the field tests.

# 5. DESIGN OF THE MODEL SYSTEM

## 5.1 Description of the System

A highly efficient structural model system, which provides the capability for studying the most important parameters of load distribution in box-beam bridges, is not economically possible with the use of a set of permanent models such as Model A1. Instead, a much more practical system was chosen, involving prefabricated beam, slab, curb, parapet, and diaphragm elements which can be interchanged to produce an extensive family of related model structures.

The box beams were prefabricated in various widths and depths with their components cemented to one another. The rest of the model elements are simply cut out of Plexiglas plates.

With holes drilled and tapped in the walls of the beams, a pattern of perforations was drilled in the slab, permitting the attachment of the slab to the beams at predetermined locations. Curb and parapet pieces were bolted to the slab and to the curb, respectively. In this manner a cross section such as the one shown in Fig. 13 could be assembled in several stages, each representing a different model. First, the simplest model results after bolting the slab to the beams;

35

second, the curb sections are installed; third, the parapet
pieces are mounted; and fourth, the diaphragms are fitted and
held between beams by means of transverse tie rods. Further-
more, by varying the thickness of slab, and the spacing and
number of beams, the effects of these parameters are also in-
vestigated with this system of interchangeable elements.

## 5.2  Connectors

The main problem encountered in a dismountable model
is that of adequate connections, in order to develop full com-
posite action throughout the entire cross-section. The 5/16
in. thick walls of the model box beams permit the use of No.
6-32 screws in order to bolt the slab to the beams. The curbs
can be bolted to the slab using No. 10-24 screws, and the para-
pets can be bolted to the curbs with either No. 6 or No. 10
screws. Diaphragms can be fastened to the beams by means of
1/8 in. Ø tie rods. To provide uniformity, screws and tie rods
were tightened with a calibrated torque wrench, such as the one
shown in Fig. 15.

## 5.3  Most Versatile Pattern of Slab Perforations

Ideally, it should be possible to use the same slab

with model beams representing prototype widths of either 4 or
3 feet. The slab should be capable of accommodating the beams
in symmetric cross sections with even or odd number of beams.
The pattern of perforations must be fine enough to permit
small variations of spacing and at the same time, must not
reduce the slab stiffness by more than 13%. It should be
noted that this reduction of stiffness compensates the distor-
tion of the $\pi_7$ term discussed in Section 3.1.

The center-of-wall to center-of-wall distances in
the 4 ft. and 3 ft. wide prototype beams, are in the model:

$$w_{(4)} = \frac{4 \cdot 12}{16} - \frac{5}{16} = 2\frac{11}{16} \text{ in.} = 2.6875 \text{ in.} \text{ and}$$

$$w_{(3)} = \frac{3 \cdot 12}{16} = \frac{5}{16} = 1\frac{15}{16} \text{ in.} = 1.9375 \text{ in.}$$

A No. 6-32 screw has a diameter 0.138 in., and
leaves a cover of 0.087 in. when centered in a 5/16 in. wall.
A minimum cover of 0.030 in. permits a maximum eccentricity
of 0.057 in. With this eccentricity, the above values of $w_{(4)}$
and $w_{(3)}$ become:

$$w_{(4)} = 2.6875 \pm 0.1144 \text{ in.} \text{ and}$$

$$w_{(3)} = 1.9375 \pm 0.1144 \text{ in.} \tag{32}$$

Their ratio can vary from $\left[\dfrac{w_{(4)}}{w_{(3)}}\right]_{min} = \dfrac{2.5731}{2.0519} = 1.254,$

to $\left[\dfrac{w_{(4)}}{w_{(3)}}\right]_{max} = \dfrac{2.8019}{1.8231} = 1.537.$

Both, $w_{(4)}$ and $w_{(3)}$ must be even multiples of the transverse spacing x of the pattern of perforations in the slab. Therefore it is necessary to choose a ratio of $w_{(4)}/w_{(3)}$ equal to 1.500, satisfied with $w_{(3)} = 4x$ and $w_{(4)} = 6x$.

The best transverse spacing is found by setting the same minimum cover in both beam widths. In the 4 ft. beam the minimum cover results at the outer face, while in the 3 ft. beam the minimum cover is at the inner face. Therefore,

$$1.9375 - 4x = 6x - 2.6875, \quad \text{or } x = 0.4625 \text{ in.} \quad (33)$$

This transverse spacing gives a minimum cover of 0.0435 in., which is acceptable. It is important to note that one line of perforations in the slab must coincide with the centerline of the roadway.

The perforations in the slab can be drill size No. 29, which has a diameter of 0.136 in., since the actual diameter of commercial No. 6-32 screws is effectively less than the nominal diameter of 0.138 in. and slightly less than drill

size No. 29. In this manner the play of the screw in a No. 29 hole is almost negligible; however a very strict tolerance is required in the drilling of slab and beams.

With the transverse spacing of 0.4625 in., the slab width of 25 in. accommodates 53 lines of perforations which represent a total width of perforations of 7.22 in., or close to 29% of the slab width. As one third of this percentage would be desirable the perforations are staggered longitudinally, every three rows.

The optimum practical longitudinal spacing between rows should produce an almost homogeneous pattern of perforations. The center-to-center distance from one perforation to its closest neighbor along one of the diagonals should be approximately three times the transverse spacing of 0.4625 in., or 1.3875 in. This requirement results in a longitudinal distance y of

$$y = \sqrt{(1.3875)^2 - (0.4625)^2} = 1.31 \text{ in.} \tag{34}$$

A longitudinal spacing of 1.5 in. was adopted, producing a longitudinal distance of 4.5 in. between consecutive perforations in the same line. The resulting pattern has 583 perforations in the entire slab, and is illustrated in Fig. 16.

## 5.4 Beams

Each beam required 33 No. 6-32 threaded holes per
wall. Because of the staggered hole pattern in the slab only
11 pairs of holes were used at any one transverse location of
the beam. Number 6-32 steel screws have an allowable shearing
strength of 90 lb.; therefore, each pair of screws provides a
connection capacity greater than the maximum shearing stress
expected in a beam-slab bridge model.

## 5.5 Curbs and Parapets

Since in some instances the edge beams are posi-
tioned partly under the curbs, the curbs cannot be bolted
from under the slab. Holes in lines No. 24, 25, and 26, at
both edges of the slab, can be tapped with No. 10-24 thread.
Each curb can be bolted to any two of these three lines while
the third line is used to bolt the exterior wall of the edge
beam.

Each parapet consists of five identical segments
assembled in line and leaving gaps of 1/16 in. which simulate
the 1-inch gaps in the prototype. In order to provide good
connection with the curb, four No. 6-32 screws are used per
segment of parapet. The screws are located along the center

line of the parapet as shown in the plan view and elevation
of one piece in Fig. 17. If screws along a single line do not
produce a satisfactory connection between parapet and curb, it
is always possible to increase the connection with a few addi-
tional screws in a zig-zag pattern, 1/2 in. or 5/8 in. wide.

## 5.6  Diaphragms

Diaphragms of two different thicknesses and three
different depths are utilized in an actual box-beam bridge
with a span of over 45 ft.[20] With a model length scale of 16,
end diaphragms are 3/4 in. thick, and midspan diaphragms are
5/8 in. thick. Full depth and shallow diaphragms are used at
the fixed end, while only shallow diaphragms are used at the
expansion end. Intermediate depth diaphragms are used at
midspan.

An intermediate depth of 9/16 in. less than the
depth of the model beam was adopted for the midspan diaphragms,
and shallow diaphragms were used with a depth of approximately
half the intermediate depth.

In assembling the diaphragms in the model, it is
possible to pass the 1/8 in. Ø steel tie rods through beams

and diaphragms at both ends and at midspan. Whenever possible,
two tie rods at different levels were used at each line of
diaphragms. The tie rods for the end diaphragms were located
5/8 in. from the ends of slab and beams. The amount of tight-
ening applied to the tie rods was determined by trial and error
such that uplift does not occur at the supports of the interior
beams.


5.7  Tests of T-Beam

In the assembly and testing of the various models,
it was necessary to ensure full interaction between beam and
slab when No. 6-32 screws were used in the connection. It was
also appropriate to evaluate the accuracy of axle load ratios
produced by the model vehicle described in Section 3.5. For
these purposes, a T-Beam was fabricated and subjected to two
series of tests. The T-Beam was made up of a model beam, repre-
senting a 4 ft. by 39 in. beam prototype, bolted to a 1/2 in.
slab 6 in. wide. The 22 screws used to attach the slab to the
beam were tightened under a controlled torque of 10 in.-lb.

In the first series of tests, twenty strain gages
were mounted on the T-Beam at different cross-sections and in
a variety of locations and orientations. Two dial gages were

used to measure the midspan deflection, and one dial gage was positioned at each end in order to measure relative slip between beam and slab. The load was applied at the third points with four total load increments of 75 lb.

The end dial gages indicated an abrupt slip of 0.0001 in. at a load of over 150 lb. With the sole exception of one strain gage mounted on the slab in the immediate vicinity of one of the holes, the strain and deflection gages exhibited almost perfectly linear load-deformation relationships. The gage which showed a non-linear relationship indicated an abrupt increase in strain at the increment of load after 150 lb., when the slip occurred. The cross-section at that gage was the only one which did not give evidence of an excellent composite action of the T-Beam.

To achieve good composite behavior it was necessary to tighten the screws while the beam was under some test load. The test load used was approximately 40% of the maximum load. It was found advisable not to mount strain gages near holes or diaphragms since stress concentrations affect the normal stress flow. In an attempt to increase the friction developed in the connection between beam and slab, sand paper was glued on top of the beam. However, the creep in the sand paper caused the

load cell output to be unstable, and the idea was dropped.

In the second series of tests, a similar T-Beam was gaged at three different cross sections. The Standard AASHO HS20-44 truck was simulated with the distances between axles at the minimum of 10.5 in., in order to produce the largest bending moment possible under the drive axle. The truck was positioned heading northbound with its drive axle 1.75 in. north of midspan.

The three sections gaged were identified as: 1, Nominal Maximum Moment, 3.75 in. north of midspan; 2, Nominal Third of the Span, 6.75 in. south of midspan; and 3, Nominal Sixth of the Span, 17.25 in. south of midspan. The theoretical bending moments at the three sections are:

$$M_1 = 8.675 \ P, \quad M_2 = 8.605 \ P, \quad \text{and} \quad M_3 = 3.868 \ P \quad (35)$$

in units of Force·inches, and where P is the total truck load.

Under the theoretical moments $M_1$, $M_2$, and $M_3$, bottom fiber strains $\epsilon_1$, $\epsilon_2$, and $\epsilon_3$ are produced in accordance with the flexural formula

$$\epsilon = \frac{Mc}{EI} \ , \quad (36)$$

where c = 1.940 in., is the distance from the bottom fiber to

the centroid of the cross-section; and I = 5.727 in.[4] is the

moment of inertia with respect to the horizontal centroidal

axis. These two values correspond to sections away from the

midspan and the end diaphragms; therefore, they are applicable

to the three sections under consideration. As in the slab ma-

terial, $E = 4.66 \times 10^6$ lb./in.[2], the microstrains are expressed

as

$$\mu\epsilon = 0.7268\ M, \quad (M \text{ in lb.in.}) \tag{37}$$

The T-Beam was tested four times, and each test was

performed with four increments of 25 lb., starting from a

"zero" load of 25 pounds. Prior to testing, the T-Beam was

subjected to three shakedown loads of 125 pounds. The experi-

mental data of bottom fiber strains was reduced using the sta-

tistical analysis described in Chapter 7. Since the experimental

values are expressed in microstrains per load number, the load P

takes the form of any positive integer, from one to four, mul-

tiplied by 25 pounds. For simplicity, P = 25 pounds.

With this value of P in expressions (35), and using

the average experimental values due to one load increment, it

is possible to have a comparison with the theoretical micro-

strains:

|                 | Theoretical | Experimental | Difference (%) |
|-----------------|-------------|--------------|----------------|
| Cross-section 1 | 157.5       | 157.2        | -0.19          |
| Cross-section 2 | 156.3       | 157.5        | +0.77          |
| Cross-section 3 | 70.3        | 66.3         | -5.70          |

The previous values, with an absolute average of 2.22%, indicate an acceptable degree of accuracy in the axle loads produced by the model vehicle.

# 6. SPECIMEN ELEMENTS AND INSTRUMENTATION

## 6.1 Beam Sizes and Properties

As mentioned in Section 5.3, two prototype beam widths, 4 ft. and 3 ft., were investigated. Since the standard depth of prototype box beams ranges from 21 in. to 48 in., in increments of 3 in.,[20] it was necessary to study the properties of all of the available sections in order to determine the most appropriate sizes to be used in the model system. Table 3 shows the theoretical values of I and J, the flexural and torsional moments of inertia respectively, of box-beam sections of ten different depths in the two widths. The thicknesses of the four walls of all beam sections are the same, as shown in Fig. 10.

Six sections were chosen in an attempt to cover the range of depths. These sections were: 3 x 24 (3 ft. in width by 24 in. in depth), 3 x 33, 3 x 42, 4 x 30, 4 x 39, and 4 x 48. With these six sections it was possible to take advantage of the three matches of I's and J's indicated in Table 3. Furthermore, Table 4 shows that with these six sections, 7 matches, 3 of I's and 4 of J's, underlined, were found to be within $\pm$ 4% of an integer. It was believed that these matches would be of great help in future comparisons of beam

47

behavior. Figure 18 shows the family of elements to be used with one slab thickness.

## 6.2 Slab Thicknesses

With commercial thickness of Plexiglas plate varying in eighths of an inch, the choice of possible slab thicknesses was limited to 3/8 in., 1/2 in., and 5/8 in.; which simulate 6 in., 8 in., and 10 in. in the prototype, respectively.

The slabs were subjected to flexural tests before and after the pattern of perforations was drilled. It was found that the stiffness of the slabs was reduced by approximately 8% to 15%.

## 6.3 Assembled Models

A complete description of the assembled models tested in this investigation is contained in Section 9.1.

## 6.4 Instrumentation

To facilitate the testing of the dismountable models, all of the elements were instrumented individually with resistance strain gages; and their leads, soldered carefully with a low temperature iron, were systematically arranged in male multiple electrical connectors. A battery of corresponding female connectors was used to rapidly complete the circuit to the switching boxes. A digital strain indicator, with an

excitation voltage of only 3.5 volts across the Wheatstone bridge, was used for the specimen gages. A higher sensitivity digital strain indicator, with an excitation voltage of 1.5 volts, was always used with the circuit of the load cell.

The observations mentioned in Section 5.7, in reference to the performance of the two T-Beams tested, were used advantageously in the instrumentation of the bolted models. The same three sections were gaged: 1, Nominal Maximum Moment; 2, Nominal Third of the Span; and 3, Nominal Sixth of the Span. Four strain gages were mounted on one beam at each section; two gages near the edges of the bottom wall, and one gage at middepth of each wall. Six $90^\circ$ rosettes were mounted at each section on top of the 1/2 in. slab; in addition, 6 transverse gages were mounted on the same slab near the fixed end in an attempt to investigate the presence of transverse moments. The transverse spacing of the six lines of slab gages was half the spacing of the loading lanes used in the bolted models. From lane 1 to lane 5 the truck covered the entire clear roadway, with a lane spacing of 3.72 in. The slab gages, however, were not used in this study since the slab strains were assumed to be in the same plane as the strains of the beams. Future investigations of detailed slab behavior will include use of the slab strain gages, (see Section 8.1).

Special attention was given to the cement used to
mount the paper-base strain gages to the Plexiglas specimens.
After an extensive literature survey on this subject,[5,33]
was decided that a carefully machined long tensile specimen
should be tested with gages of the same lot mounted with three
different cements:   (1) the cement recommended by the gage
manufacturer regardless of the specimen material,   (2) an in-
dustrial epoxy, and   (3) Ethylene Dichloride.  The tensile
test indicated that the gages mounted with the cement recom-
mended by the gage manufacturer were the ones that showed a
more uniform output.  Therefore, this cement was used for
all of the specimens.

Dial gages were used at sections 1 and 2 to measure
deflections and rotations of the beams.  Two dial gages were
used per section in each beam, with stems placed against
aluminum brackets mounted with set screws on the bottom wall
in order to leave the bottom strain gages undisturbed.  De-
tails of the instrumentation and wiring, as well as a complete
view of the test setup, are shown in Figs. 19, 20, and 21.

# 7. STATISTICAL ANALYSIS OF DATA

## 7.1 Small Sample

In order to increase the reliability of the experimental results it was decided to repeat each test a number of times. This made it possible to perform a statistical analysis of the data, and thus, to obtain a set of test values that more accurately represents the true behavior of the model specimen. It was necessary to select the size of the sample to be compatible with the mathematical treatment to be given to the data. If single measurements were to be taken, it would have been possible to produce a sample of size ten, without exceeding a practical testing time for one specimen. However, this was not the case. Instead, the load was applied in four increments up to a level of twenty times the rated load, as explained in Section 3.5. Furthermore, the data from each of the five loading lanes was needed in order to analyze the three cross sections 1, 2, and 3 (Section 6.3) of the bridge. Finally, the possibility existed that more than one load position of the vehicle along the span could be used if found advantageous to do so. One position of the vehicle was already described in Section 5.7, in the testing of the second T-beam. A second

position was chosen so that the section located at one-sixth
of the span from the south support would be subjected to the
maximum bending moment possible. In total, twenty load incre-
ments per test were necessary to study the response of the model,
under each of the two longitudinal positions. In a model with
an expected maximum number of seven beams, and with curb and
parapet, it would have been necessary to record sixty-six strain
gages and sixteen dial gages per load increment. Therefore, the
sample to be taken could not be large. In fact, it had to be
the smallest possible sample which would accept a statistical
analysis of any dependability.[10] The size selected was four.
In this manner, with the presence of two rejectable outliers,
two acceptable values could still be averaged.


## 7.2  Orthogonal Polynomials

The most convenient way to minimize mistakes in the
testing of a specimen with linear behavior, is to use identical
increments of load. This permits the use of orthogonal poly-
nomials when any curve fitting by least squares is to be done
on the experimental data. Since it was necessary to measure
the linear response of each strain and dial gage, orthogonal
polynomials up to the first degree were used. The formulation

for the computer program was simplified in this aspect.[24]
Since the readings under a "zero" load of one increment were
not recorded, the expression for the dependent variable, either
strain or deflection represented as the ordinate v, takes the
form

$$v = \frac{1}{4}\left(\sum_{u=1}^{u=4} v + 3\sum_{u=1}^{u=4} vP_{31}(u)\right) - \left(\frac{3}{10}\sum_{u=1}^{u=4} vP_{31}(u)\right)u \qquad (38)$$

where $P_{31}(u)$ is the polynomial of first degree in a four-incre-
ment set of abscissae u, and is expressed as

$$P_{31}(u) = 1 - \frac{2}{3}(u-1) = \frac{1}{3}(5 - 2u) \qquad (39)$$

The slope $\frac{dv}{du}$, which is a measure of the response of
each gage, is obtained from Eqs. 38 and 39:

$$\frac{dv}{du} = -\frac{1}{10}\sum_{u=1}^{u=4}(5 - 2u)\cdot v \qquad (40)$$

Then, all that is needed is the substitution of the four exper-
imental values of strain or deflection $v_1$, $v_2$, $v_3$, and $v_4$;

or

$$\frac{dv}{du} = -\frac{1}{10} \ (3v_1 + v_2 - v_3 - 3v_4) \tag{41}$$

## 7.3 Rejection Criterion of Outliers

The Dixon Criterion was used to reject both of the extreme values of the four slopes for each gage found from the data of the four tests. This criterion is applicable when the population mean and the standard deviation are unknown, and the sample in hand is the only source of information.[17]

For the case of a sample of size four, the smallest or largest observations are rejected if their relative values of outliers exceed a certain percentile. This percentile is tabulated as a function of the risk of rejecting an observation which really belongs in the group. For the risk of 50% which was adopted, the limiting percentile is 0.51.

After arranging the four observations in increasing order $X_1$, $X_2$, $X_3$, and $X_4$, the extremes $X_1$ and $X_4$ are rejected if

$$\frac{X_2 - X_1}{X_4 - X_1} > 0.51, \text{ and } \frac{X_4 - X_3}{X_4 - X_1} > 0.51 \tag{42}$$

7.4  Correction of Random Errors

In the first trial tests of the pilot model Al, it was found that regardless of the systematic execution of each test and of the high degree of care with which all of the operations were performed, recording mistakes and random errors in general could not be avoided.  This was verified whenever the data was reduced by hand with the objective of debugging the computer programs.

The mistakes were so noticeable in some cases, that there was no doubt about the type of error committed:  the minus sign was missing, digits had been transposed, the digit in the hundreds or in the thousands had been obviously misread or misrecorded, the load had been given a wrong increment, the circuit of one strain gage had been disturbed in the middle of a test, and others.  Once the diagnosis was given the error was corrected by hand.  The problem was to incorporate this correction of random errors in the computer program, so that the experimental data could be given directly to the computer.

The procedure to correct random errors was devised with the following assumptions in mind:  (1) there exist at least two correct data points in each set of four load points in a test; (2) there exist at least two correct sets of four

load points in each gage; and (3) even after three shakedowns, the stress memory of Plexiglas results in non-repeatable absolute readings.

It was therefore necessary to use relative values in terms of the ratio of increment in the readings to the general slope of the gage in study. A value had to be established in order to define a possible mistaken datum point as admissible or not. Equation 41 clearly indicates that in a four-point set, an error in an exterior point, $v_1$ or $v_4$, influences the resulting slope three times as much as does an error in an interior point, $v_2$ or $v_3$. It was found later that a criterion with the limiting values of error for exterior points and interior points in a ratio of 3 would be too rigid for the exterior points or too mild for the interior points. A compromise ratio of 1.5 was then successfully adopted.

The logic in the procedure to correct random errors in each gage is as follows:

1.  With the sixteen data points, four per test, determine the four slopes.

2.  Apply the Dixon Rejection Criterion to those four slopes and find the average slope of the non-rejected values.

3. Return to the original data points to examine the four points of one test at a time. Analyze the six possible binary combinations to determine which pair of correct points are in a slope closest to the average slope found in 2. The test under examination is entirely rejected when the difference between the closest slope and the average slope has an absolute value of more than 50%, 25%, or 17% in one, two, or three abscissa increments, respectively.

4. Check the possibly mistaken points, one at a time, to see if, according to the individual location, the limiting value is exceeded and the point is actually mistaken. To do so, the closest correct point is used as a reference, and the mistake is expressed as the ratio of the deviation from the position along the average slope, to the average slope itself. If the mistake exceeds 1.0 in an interior point, or 1.5 in an interior point, the mistaken datum is automatically replaced

by the position along the average slope.

5. The procedure is completed with the performing of a second and final cycle of steps 1 and 2.

# 8. ASSUMPTIONS IN THE COMPUTATIONS

## 8.1 Linear Variation of Slab Strains

It was mentioned in Section 6.3 that the slab strains were assumed to be in the same plane as the strains of the beams. This is equivalent to saying that Bernoulli's (often referred to as Navier's) hypothesis holds for individual beam-slab units. There is no doubt that this hypothesis is correct for a single beam-slab, as proven by the results of the second T-Beam reported in Section 5.7. In a bridge cross-section with more than one beam, this hypothesis could not be 100% correct; and the only way to exactly analyze the experimental data would be to mount a large number of strain gages on both slab surfaces. This could not possibly be done on the bottom surface of the slabs used in a system such as the one described in Chapter 5. Strain gages could have been mounted on the top surface of the slab, provided they are located in the cross sections 1, 2, and 3, away from the vehicle wheels, and mounted in the manner described also in Section 6.4. However, this would result in a total of 108 strain gages in the seven-beam model exemplified in Section 7.1. Since automatic data acquisition equipment, featuring single gage current input (see property 4 in Section 3.3) was not available, it was decided not to use the slab gages in this investigation.

59

It was then necessary to make the assumption that the slab strains vary linearly over the width of slab that corresponds to each beam. This is in every case an upper bound of the slab contribution to the equilibrium of the cross-section; and the error involved should be reduced as the clear spacing between beams decreases.

## 8.2 Support Restraints

The cross-sectional equilibria are completely disfigured if existence of support restraints is not considered. The possible presence of longitudinal and transverse reactions could not be neglected in the preparation of the computer program used to analyze the experimental data to ultimately produce, as the main output, the moment percentages and individual slab widths of all of the beams in the cross-section of the bridge.

It was assumed that the longitudinal reaction was distributed among the beams in proportion to the individual moment percentages.

## 8.3  Cross-Sectional Moments

The cross-sectional moments of individual beam-slab units were corrected by the elimination of the contribution of the corresponding portion of longitudinal reaction assumed in Section 8.2.  It was assumed that the jack and model vehicle did not impose any longitudinal restraint, and that the longitudinal reaction was acting at the support level.

## 8.4  Slab Widths

In order to compute the total longitudinal reaction, initial individual slab widths were assumed to cover: edge of slab to midspacing of beams for exterior beams, and midspacing to midspacing for interior beams.  Consequently, with these assumptions, the value computed for the total longitudinal reaction was an upper bound of the reaction.

## 8.5  Equilibria with External Forces

Normal forces and longitudinal bending moments (in vertical planes) were primarily considered in the equilibrium of the bridge cross-section.  In addition, the resulting transverse bending moments (in horizontal planes) were set in

equilibrium with the south transverse reaction at the fixed-
end support, as long as the expansion end was not free to
move in the transverse direction.

From the experimental strains, already statistically
analyzed, stress blocks were computed with the resulting
equivalent forces. The sum of all of these forces produced
the longitudinal reaction, while sums of moments in individual
beam-slab units gave the initial values of bending moments.
Successive approximations were then used on the individual
bending moments in a number of cycles from three to five.
From the second cycle on, a correction on the moment was car-
ried out as described in Section 8.3. That correction changed
the moment percentages and also changed the individual longi-
tudinal reaction. After the third cycle had been completed
(with the second correction performed), the moments of the
third cycle were changed to linearly extrapolated values deter-
mined with the expression

$$M_3 = \frac{\Delta_1 \cdot M_2 - \Delta_2 \cdot M_1}{\Delta_1 - \Delta_2} \qquad (43)$$

where $M_1$ and $M_2$ are the moments found in the first and second
cycles, and $\Delta_1$ and $\Delta_2$ are the changes in moments due to the
corrections in the second and third cycles.

It was found that the moments converged very rapidly, and that a total of four cycles, with a second extrapolation, produced values which were very close to the final moments and final moment percentages. With these moments, the final individual slab widths were determined, together with transverse bending moments and south support reaction.

The main computer program I-23 was written in LEWIZ language and believed completely debugged after one year of programming struggle. It resulted in a segmented program in order to comply with the capacity of the G.E. 225 digital computer. During the main testing program, the program was saved on two magnetic tapes, and called to execution for each new set of experimental data. It was possible to have available the results for a model test on the same day of the test. This program is filed, together with all of the programs and test data used, in Fritz Lab Project 322 entitled "A Structural Model Study of Load Distribution in Highway Bridges".

Section 12.1 in the Appendix shows synthetic description of Program I-23 in all of its nine segments.

## 9.   PROGRAM OF TESTS

### 9.1   Basic Cross-Sections

Sixteen different bolted models were tested and ana-
lyzed at an average rate of four models per week.  One of the
first bolted models tested was almost identical to the pilot
model Al.  The only difference in the cross-section was that
of a slightly closer spacing of beams as a result of the trans-
verse spacing of the pattern of holes in the slab.  Three addi-
tional differences were built-in as a result of the planning of
the model system.  First, the section of Nominal Maximum Moment
was farther from midspan in order to be as far from holes and
midspan diaphragm as possible; second, the transverse spacing
of the loading lanes was larger; and third, the track of the
standard design vehicle was slightly narrower.  Nevertheless,
it was convenient to test this model as a complete pilot bolted
model.  It was during the pilot tests of this bolted model that
the torque specifications for the assembly operations were de-
fined.  This model was identified as B4.

The torque specifications, together with all of the
information necessary to conduct a bolted model test, are a

part of the computer program I-23. They are arranged in the
first page of the output, which can be found in Section 12.2 of
the Appendix.

The program of tests is schematically represented in
Fig. 22 where the midspan cross-sections are all drawn at the
same scale. In summary, seven basic cross-sections of bolted
models were used. It can be seen that four models were tested
out of each of the first three basic cross-sections.

Figures 23, 24, and 25 show a graphical comparison
of moment percentages and slab widths between model A1 and the
prototype, with the vehicle on the three different loading lanes
1, 2, and 3, respectively.[8]  It is evident that the exterior
beams A and D carry more moment in the model than in the pro-
totype; and that the sum of the individual slab widths in the
prototype beams is always less than the total widths of the
slab by a large percentage. The sums of individual slab widths
are approximately 66%, 72%, and 86%, respectively for lanes 1,
2, and 3. The substantial and consistent differences of moment
percentages and of individual slab widths, between model A1 and
prototype, could be explained in the following manner:

1.  It is possible that the interaction between
    curb and slab, and between parapet and curb

is better in the model A1 where a continuous adhesive was used, than in the prototype where reinforcing bars provide a somewhat discontinuous connection.

2. The neoprene bearing pads used in the prototype supports actually do not permit fully unrestrained stretching of the bottom fibers of the beams. A compressive force is developed, resulting in a combined flexure-compression behavior of the prototype. In an equilibrium analysis of any cross-section, the computed compressive stress blocks in the slab are greatly reduced when the combined behavior is taken into account. Therefore, the resulting individual slab widths do not add up to the total transformed width of the slab. The total theoretical transformed width of the slab would be about 13% less than the total actual width, (see Eq. 15, Section 3.1), if the theoretical ratio of moduli is based on Eq. 15. Furthermore, the moments carried by the beams are also reduced if the compressive restraining force is not included

in the analysis. A large value of the mod-
ulus of elasticity (see Section 4.4) is ob-
tained when the sum of interior moments is
equated with the external moment. Although
the moments of individual beams are all re-
duced, the reduction is not uniform. Because
of a higher value of section modulus due to
the presence of curb and parapet, the moments
in the exterior beams are reduced by the com-
pressive force in a larger proportion than the
reduction in the interior beam moments. Con-
sequently, the moment percentages in the model
differ from those computed in the prototype
study, as shown in Figs. 23, 24, and 25.

## 9.2 Sequence of Bolted Models

It was decided to test, first of all, three families
of four-beam bridges, having the same center-to-center spacing
of 6.48 in. for the beams. This spacing was the closest pos-
sible to the beam spacing of 6.56 in. in model Al. The three
beam sizes to be used were selected such that the flexural mo-
ment of inertia of the 4 x 39 could be approximately duplicated

by the 3 x 42.  The torsional moment of inertia of the 3 x 42 could, in turn, be duplicated by the 4 x 30.

Each family of four models was formed as a result of the assembly steps mentioned in Section 5.1.  The first model had only the four beams and slab; the second had beams and slab with curb and parapet pieces; the third had beams and slab with diaphragm pieces; and the fourth had beams and slab with curb, parapet and diaphragm pieces.  The same 1/2 in. slab was used throughout all of the twelve tests of the 4 x 39, 4 x 30, and 3 x 42 families.  In addition to these twelve tests, two tests involving 3/8 in. and 5/8 in. slab thicknesses were performed on complete models with 4 x 39 beams; and two final tests without curb, parapet, and diaphragm pieces were carried out, first in a four-beam bridge with 3 x 42 and 4 x 39 beams, and last in a seven-beam bridge with 3 x 24 beams, which were the smallest beams used in the system.

Table 5 gives a synthetic description of all seventeen models tested, including A1, with the corresponding file numbers.

Several modifications were made to the testing program as a result of the experience obtained while testing model B1.

With the vehicle at position one (see Section 7.1), the signal from the strain gages in the third section gaged (see Section 6.4) did not show the same consistency as the signal from gages in the first two sections. This was confirmed by the program output for the three sections which showed that, although the uniformity of load distribution decreased consistently from midspan toward the support, the inaccuracy of the computations for the third section gaged was being magnified due to the assumptions mentioned in Chapter 8. Furthermore, it was clear that the individual maximum moments in the beams were occurring at a location somewhere between the first two sections gaged. Therefore, it was decided that the strains from the third section should not be recorded. It was also found that the overall response of the bridge did not change substantially with the vehicle at the second position. Besides, this second position was selected with the intention of producing the maximum moment at the third section gaged. Therefore, since the gage response from the third section was not to be recorded, the use of the second position of the vehicle was abandoned.

# 10.    DISCUSSION OF RESULTS

## 10.1  Effect of Diaphragms

Table 5 suggests that two possible distinctions can be made among the sixteen bolted models tested.  One distinction is that of cross-sections with, and without, curb and parapet sections, and the second distinction is that of cross-sections with, and without, diaphragms.

Since the effect of curbs and parapets is of a more localized nature, affecting primarily the exterior beams, greater importance was given to the study of the effect of diaphragms. This was the policy used in the preparation of most of the Figs. 26 through 47.

The effect of the disphragms is shown for the three families of four-beam cross-sections, involving 4 x 39, 4 x 30, and 3 x 42 beams, in Figs. 26 through 31, 36 through 41, and 42 through 47, respectively. Without exception the presence of diaphragms substantially improves the uniformity of the lateral load distribution.

It was appropriate to present Fig. 32 immediately after the figures pertaining to the family of models with four

4 x 39 beams. Figure 32 compares model B4 with model A1 and the prototype, and shows less disagreement between the prototype and B4 than between the prototype and A1. The parapet strains in model B4 showed less parapet interaction than the parapet strains in model A1.[7] This is a verification of the statement mentioned in Section 5.5, regarding the possibility of increasing the parapet connection with additional screws. It should be noted that the study of the effects of a single diaphragm was not included in this program of tests. However, the particular effect of the midspan diaphragm only, can be easily studied with this model system.

## 10.2  Effect of Curbs and Parapets

Figures 33, 34, and 35 show the typical effect of the presence of curb and parapet pieces on the lateral load distribution. The exterior beam closest to the load carries a larger percentage of moment, and the moment in the other exterior beam is thereby reduced.

## 10.3  Effect of Beam Cross-Section

A comparison of the maximum and minimum values of the moment percentages for the 4 x 39, 4 x 30, and 3 x 42 families of cross-sections, shows that appreciable differences exist.

The differences are of a consistent nature, and the complete models B4, B8, and B12 can be properly used as representative of cross-sections utilizing 4 x 39, 4 x 30, and 3 x 42 beams, respectively.

With the load on lane 1, Fig. 29 shows a maximum of 47% and a minimum of 10% for model B4; Fig. 39 shows a maximum of 47% and a minimum of 13% for model B8; and Fig. 45 shows a maximum of 51% and a minimum of 7% for model B12. Similar comparisons for the cases with the load on lane 2 and 3 would yield similar responses. Of the three cross-sections, the model with 4 x 30 beams had the most uniform lateral load distribution while the model with 3 x 42 beams had the least uniform distribution. The 4 x 30 and 3 x 42 beams have the same J, but the 3 x 42 has a larger I. The clear spacing between the 3 x 42 beams was more than 1.2 times the clear spacing between the 4 x 30 beams. All of these observations indicate, among other things, that the magnitude of the transverse span of the slab plays an important role in lateral load load distribution. Figures 48 through 51, which will be analyzed in Section 10.4, show the effect of slab thickness.

Figures 52, 53, and 54 compare models B4, B8, and B12 with the load on lanes 1, 2, and 3, respectively. Model B15 was assembled with two exterior 3 x 42 beams and two interior 4 x 39 beams, and its behavior is shown, for the three separate lanes of loading, in Fig. 55. Figures 56, 57, and 58 show an improvement of B15 over B9 as compared with B1.

## 10.4  Effect of Slab Thickness

Models B13 and B14 are identical in every respect except slab thickness. Figures 48, 49, and 50 show, in every case, that the model with the thicker slab exhibits a more uniform lateral load distribution.

As an item of interest, Fig. 51 is included to show that model B13, with a 3/8 in. slab exhibits a behavior somewhat closer to that of the prototype of model A1. (See Section 3.1)

Figures 48, 49, and 50 could have included model B4 which had the 1/2 in. slab. However, the performances of models B4 and B14 were very similar, indicating that slab thickness, in the range 1/2 in. to 5/8 in., has little effect on lateral distribution.

## 10.5  Effect of Number of Beams, and Section Gaged

One model with seven 3 x 24 beams was tested as a final check on the computer program. The results shown in Fig. 59 are a clear indication of the uniformity achieved in the lateral load distribution.

The complete output of results of the test of model B16 constitutes Section 12.2 of the Appendix.

Finally, Figs. 60, 61, and 62 are presented to show the typical difference in response exhibited between the section at the Third of the Span and the Section of Maximum Moment.

## 11.  SUMMARY AND CONCLUSIONS

### 11.1  Present Achievements

A model system was designed and proven to be highly efficient in the study of the most important parameters affecting load distribution in box-beam bridges of the beam-slab type.  The system incorporates concepts and techniques which were responsible for the efficiency and versatility evidenced during the program of tests.  The achievements of this investigation were primarily the result of the appropriate use of these concepts and techniques.

The analytical treatment of the data, presented in Chapters 7 and 8 proved most useful, and certainly applicable, within the limitations of the assumptions made, to all of the cases tested, and later discussed in Chapter 10.  In particular, the correction of random errors (Section 7.4), and the method of successive approximations on the individual bending moments (Section 8.5) are original contributions.

The results from the seventeen models tested show the qualitative and quantitative effects of (1) size and number of beams, (2) slab thickness, (3) curb and parapet sections, and

(4) diaphragms. The understanding of the behavior of the bridge type studied is greatly improved when these effects are correctly assessed.

A main computer program was written in order to fully analyze the experimental data. The program contains all of the analyses and techniques presented. The program output gives the results in a complete and detailed manner.

Finally, the creep compensating technique for the testing of viscoelastic material specimens is effectively incorporated, with a high degree of reliability, into a formal investigation. Although the use of the concept of creep compensation is not original, the practical use of this technique is presented as a powerful tool in Structural Model Analysis.

## 11.2 Recommendations for Future Work

As a result of the experience gained during this investigation, it is appropriate to include a series of recommendations for future experimental studies.

Starting with the test setup, it is advisable to make an attempt to measure the individual beam reactions. This

can be accomplished through use of calibrated creep compensating tripods, two at each end of a beam. The tripods would give the three components of the reaction force, and the overall equilibrium could be correlated. In addition, a thrust bearing can be easily placed between the mechanical jack and the load cell to completely eliminate any restraint from the jack.

With respect to the instrumentation, it is necessary to collect more information on the strain variation in the slab of the bridge models. Even with the use of smaller foil-resistance strain gages, it would be impractical to mount a large number of gages, and this would certainly affect the behavior of the specimens. The answer may be in the use of the incipient applicability of laser beams which could be capable of detecting the strain surface for the entire cross-section.

Finally, with reference to the parameters to be studied, much work is yet to be done. This additional work could include, among other items, an exhaustive investigation of the effect of beam spacing and of angle of skew of the bridge.

12.    APPENDIX

12.1  Synthetic Description of the Main Computer Program

The main computer program I 23, filed under I 23h, consists of nine segments, plus a common portion.  The description of the program is divided into ten parts:

Common Portion - Dimensions are set for fixed-point and floating-point arrays and inter-segmental variables.

Segment 1 - Information about typical characteristics of the model, material properties, prototype load, model beam sizes, load increment used in the test, and beam spacings is read.  The cross-sectional properties are computed.  Initial individual slab widths are assumed.

Segment 2 - The number of the load position is read.  Segments 2 through 9 are repeated for each load position.

Segment 3 - All of the experimental data of strains and deflections for one section gaged

is read. The complete statistical analysis on the data is performed. Segments 3 through 8 are repeated for each section gaged.

Segment 4 - Invariant forces and moment components are computed for beams, with curb and parapet, if present in the cross-section. Beam deflections and rotations are also computed.

Segment 5 - Computations for equilibrium of normal forces, and for bending moments in a vertical plane using successive approximations, are carried out.

Segment 6 - Slab widths and bending moments in a horizontal plane are computed. Testing instructions are printed in the output.

Segment 7 - Symmetrically located values are combined to form the arrays of response for the entire cross-section under load on three different lanes only. Strains, deflections, and location of neutral axes can be printed as secondary output number one. Coefficients

of $M_x$, $M_y$, mid-width deflections, and rotations, together with slab widths can be printed as secondary output number two.

Segment 8 - Computations of moments, moment percentages, reactions, and percentage of total slab width are performed. These values can be printed, together with cross-sectional profiles of deflections and rotations as secondary output number three.

Segment 9 - This last segment commands the printout of the main output containing moment percentages and slab widths of all of the section gages for the load on three different lanes. A brief description of the model analyzed is also printed. A final check is performed to verify if the data contained the exact number of data points.

## 12.2 Example of the Main Computer Program Output

The entire output for model B16 is included in the following pages.

          MAIN COMPUTER PROGRAM I-23 FOR FRITZ LAB PROJECT 322.  IT CONTAINS THE MOST RECENT IMPROVEMENTS, AS OF
MARCH 1968, DEVELOPED IN THE PROGRAMMING OF THIS PROJECT.  THIS PROGRAM CAN HANDLE BOX BEAM BRIDGE MODELS WITH A SYMMET-
RIC CROSS SECTION OF TWO TO SEVEN IDENTICAL OR DIFFERENT BEAMS.  CURBS, PARAPETS, OR DIAPHRAGMS MAY OR MAY NOT BE PRES-
ENT, AND THE EXPANSION END MAY OR MAY NOT BE FREE TO MOVE IN THE TRANSVERSE DIRECTION.  THE INTERCHANGEABLE MODEL COMPO-
NENTS, MADE OUT OF PLEXIGLAS, ARE BOLTED TOGETHER UNDER 40% OF THE MAXIMUM LOAD TO BE APPLIED USING THE FOLLOWING TORQUE
SPECIFICATIONS.. 10 IN.LB. IN THE SCREWS CONNECTING THE BEAMS AND DIAPHRAGMS TO THE SLAB, 15 IN.LB. IN THE SCREWS CON-
NECTING THE CURBS TO THE SLAB, 20 IN.LB. IN THE SCREWS CONNECTING THE PARAPETS TO THE CURBS, AND 5 IN.LB. IN THE TIE
RODS CONNECTING THE DIAPHRAGMS TO THE BEAMS.  AFTER THE MODEL IS ASSEMBLED FULL CONTACT WITH THE SUPPORTS IS ACHIEVED BY
THE USE OF STEEL SHIMS BETWEEN THE STEEL PLATES BOLTED TO EACH BEAM AT ITS ENDS AND THE NORTH AND SOUTH SUPPORTS.

          THE INPUTS TO THIS PROGRAM ARE THE EXPERIMENTAL READINGS OF MICROSTRAINS AND DEFLECTIONS IN TENTHOU-
SANDTHS OF AN INCH DUE TO STATIC TRUCK LOADINGS ON THE FIVE LOADING LANES FOR ONE OR TWO LOAD POSITIONS.  THE STANDARD
HS20-44 AASHO TRUCK TRAILER IS SIMULATED WITH THE DISTANCES BETWEEN AXLES AT THE MINIMUM OF 10.5 IN. IN ORDER TO PRODUCE
THE LARGEST BENDING MOMENT POSSIBLE UNDER THE DRIVE AXLE.  THE FIVE LOADING LANES COVER THE ENTIRE CLEAR WIDTH OF 20.88
IN. OF THE ROADWAY, ARE EQUALLY SPACED 3.72 IN., AND ARE NUMBERED 1 THROUGH 5 FROM THE EAST WESTWARD.  ON LOAD POSITION
NUMBER ONE THE DRIVE AXLE OF THE TRUCK IS LOCATED 1.75 IN. NORTH OF MIDSPAN, AND ON LOAD POSITION NUMBER TWO THE REAR
AXLE OF THE TRAILER IS AT THE SIXTH OF THE SPAN CLOSE TO THE SOUTH SUPPORT.  THE TRUCK HEADS ALWAYS TOWARD THE NORTH.

          THE LOAD HAS TO BE APPLIED IN FOUR IDENTICAL INCREMENTS EQUAL TO ONE FIFTH OF THE TOTAL FORCE REQUIRED TO
DEFLECT THE MIDSPAN A MAXIMUM OF ABOUT TWO TENTHS OF AN INCH WITH THE TRUCK ON LANE ONE OR FIVE.  LOAD NUMBER ZERO IS
THUS EQUAL TO ONE INCREMENT.  THE LOAD IS MEASURED WITH A PLEXIGLAS COMPENSATING LOAD CELL PLACED BETWEEN THE HEAD OF A
MECHANICAL JACK AND THE BEARING-JOINTED FRAME THAT SIMULATES THE TRUCK TRAILER.  THE INSTANTANEOUS CALIBRATION FACTOR OF
THE LOAD CELL IS, AT 75 DEGREES FAHRENHEIT, EQUAL TO 0.0814 LB./MICROOUTPUT.  BEFORE TESTING EACH MODEL IT IS NECESSARY
TO SUBJECT IT TO AT LEAST THREE SHAKEDOWN LOADS EQUAL TO THE MAXIMUM LOAD TO BE APPLIED.  DURING THE TESTS THE SEQUENCE
OF LOADING LANES IS 3, 4, 2, 1, AND 5.

          THE READINGS ARE PUNCHED DIRECTLY IN DATA CARDS USING AN IBM ±0 CARD PUNCH.  SINCE THE CROSS SECTIONS OF
THE BRIDGES ARE SYMMETRIC, GAGES ARE NECESSARY ONLY ON HALF OF EACH MODEL.  EACH BEAM GAGED HAS FOUR STRAIN GAGES IN
EACH OF THE THREE SECTIONS GAGED ( MAX. MOMENT, THIRD OF THE SPAN, AND SIXTH OF THE SPAN ), AND TWO DIAL GAGES IN EACH
OF THE FIRST TWO SECTIONS GAGED.  THE FORTY-TWO STRAIN GAGES ON TOP OF THE SLAB WILL NOT BE USED IN THIS PROJECT, BUT IN
FUTURE STUDIES.  IT IS OF UTMOST IMPORTANCE TO ELIMINATE OXIDATION IN THE CONTACTS OF THE MULTIPLE CONNECTORS OF THE
STRAIN GAGES BEFORE STARTING TO TEST A MODEL.  THE READINGS TO BE RECORDED ARE THOSE UNDER LOAD NUMBERS 1, 2, 3, AND 4.

          FOR STATISTICAL ANALYSIS PURPOSES THE TESTS ARE TO BE PERFORMED FOUR TIMES, AND ANY SIGNIFICANT RANDOM
ERROR IN THE DATA WILL BE AUTOMATICALLY CORRECTED IN THIS PROGRAM.  THE SLOPES OF LOAD VS. STRAIN AND OF LOAD VS. DE-
FLECTION ARE FOUND BY FITTING ORTHOGONAL POLYNOMIALS USING LEAST SQUARES.  THE DIXON CRITERION TO REJECT OUTLIERS IS
USED WITH A 50% RISK OF REJECTING AN OBSERVATION THAT REALLY BELONGS IN THE SAMPLE.  REFERENCES.. FIT OF ORTHOGONAL POL-
YNOMIALS BY LEAST SQUARES, C. R. WYLIE JR., ADVANCED ENGINEERING MATHEMATICS, MCGRAW-HILL, 1960, PP. 179 TO 183., SMALL
SAMPLE METHOD, P. G. HOEL, INTRODUCTION TO MATHEMATICAL STATISTICS, JOHN WILEY AND SONS, 1965, PP. 262 TO 292., DIXON
REJECTION CRITERION, M. G. NATRELLA, EXPERIMENTAL STATISTICS, NATIONAL BUREAU OF STANDARDS HANDBOOK 91, 1966, P. 17-3.

          THE MAIN OUTPUT OF THIS PROGRAM IS AN ARRAY OF MOMENT PERCENTAGES AND SLAB WIDTHS IN INCHES FOR ALL BEAMS
AT ALL SECTIONS GAGED, WITH THE LOAD ON THREE DIFFERENT LANES, AND FOR EACH OF THE LOAD POSITIONS USED.  SECONDARY OUT-
PUTS PER SECTION GAGED THAT CAN BE PRINTED.. STRAINS, DEFLECTIONS AND NEUTRAL AXIS ORDINATES, COEFFICIENTS AND SLAB
WIDTHS FOR ALL THE BEAMS, AND SUMMATIONS OF MOMENTS AND SLAB WIDTHS WITH VALUES OF THE NORTH LONGITUDINAL REACTION, OF
THE MODULUS OF ELASTICITY NECESSARY FOR EQUILIBRIUM, AND OF THE SOUTH TRANSVERSE REACTION, PLUS CROSS SECTIONAL DEFLEC-
TION AND ROTATION PROFILES.

          SPECIAL CODE IN THE FIRST TWO DATA CARDS.. IN EITHER CURB, PARPT, DIAPH, EXEND FREE, PRINTS01, PRINTS02,
AND PRINTS03, A ZERO MEANS NO AND A ONE MEANS YES.  MODEL DIMENSIONS IN INCHES BUILT INTO THIS PROGRAM.. LENGTH 50, SPAN
48.44, WIDTH OF SLAB 25, BEAM BOTTOM AND SIDE WALLS THICKNESS 5/16, BEAM TOP WALL THICKNESS 3/16, CURB WIDTH 2 1/16,
CURB THICKNESS 1/2, PARAPET WIDTH AND THICKNESS 0.95, THICKNESS OF STEEL END PLATES 1/8, AND DISTANCES FROM THE SOUTH
SUPPORT TO THE FIRST SECTION GAGED 28.22, TO THE SECOND SECTION GAGED 17.72, AND TO THE THIRD SECTION GAGED 7.22.

I
23t

TENTHS OF MICROSTRAINS AND DEFLECTIONS IN HUNDREDTHOUSANDTHS OF AN INCH.  AVG. E MODEL=   4.6583245+05 LB: PER SQ.IN.

LOAD POSITION        1

| CASE NUMBER | SECTION GAGED | LOAD ON LANE 1 | LOAD ON LANE 2 | LOAD ON LANE 3 | LOAD ON LANE 4 | LOAD ON LANE 5 | TYPE |
|---|---|---|---|---|---|---|---|
| 1 | 1 | 630 | 434 | 316 | 243 | 181 | BEAM STRAIN |
| 2 | | 240 | 171 | 123 | 100 | 79 | BEAM STRAIN |
| 3 | | 669 | 458 | 326 | 241 | 173 | BEAM STRAIN |
| 4 | | 268 | 175 | 115 | 64 | 52 | BEAM STRAIN |
| 5 | | 540 | 470 | 358 | 274 | 214 | BEAM STRAIN |
| 6 | | 200 | 172 | 141 | 113 | 88 | BEAM STRAIN |
| 7 | | 540 | 458 | 350 | 264 | 190 | BEAM STRAIN |
| 8 | | 235 | 191 | 130 | 85 | 49 | BEAM STRAIN |
| 9 | | 432 | 448 | 403 | 326 | 266 | BEAM STRAIN |
| 10 | | 141 | 156 | 153 | 123 | 87 | BEAM STRAIN |
| 11 | | 424 | 447 | 408 | 330 | 256 | BEAM STRAIN |
| 12 | | 182 | 170 | 122 | 90 | 42 | BEAM STRAIN |
| 13 | | 352 | 418 | 427 | 391 | 326 | BEAM STRAIN |
| 14 | | 95 | 119 | 149 | 157 | 123 | BEAM STRAIN |
| 15 | | 336 | 399 | 400 | 371 | 308 | BEAM STRAIN |
| 16 | | 134 | 157 | 156 | 138 | 99 | BEAM STRAIN |
| 17 | | 1324 | 950 | 668 | 489 | 344 | BM: DEFLECTION |
| 18 | | 1220 | 948 | 704 | 525 | 390 | BM: DEFLECTION |
| 19 | | 1128 | 927 | 706 | 545 | 415 | BM: DEFLECTION |
| 20 | | 1020 | 917 | 749 | 605 | 480 | BM: DEFLECTION |
| 21 | | 1000 | 942 | 816 | 673 | 546 | BM: DEFLECTION |
| 22 | | 873 | 898 | 841 | 737 | 628 | BM. DEFLECTION |
| 23 | | 781 | 839 | 817 | 750 | 655 | BM: DEFLECTION |
| 24 | | 672 | 757 | 819 | 827 | 775 | BM: DEFLECTION |

DISTANCES IN INCHES FROM THE TOP FIBER TO THE NEUTRAL AXIS IN THE BEAMS GAGED.  AVG. EM =   4.6583245+05 LB: PER SQ.IN.

(AFTER CORRECTION FROM THE EFFECTS OF ANY LONGITUDINAL REACTION)

| BEAM NUMBER (FROM THE EAST EDGE WESTWARD) | LOAD ON LANE 1 | LOAD ON LANE 2 | LOAD ON LANE 3 | LOAD ON LANE 4 | LOAD ON LANE 5 | BEAM WALL |
|---|---|---|---|---|---|---|
| 1 | 2.5044166-01 | 2.4130808-01 | 2.3883125-01 | 2.0046014-01 | 1.3271368-01 | EAST |
| | 2.1064325-01 | 2.8242164-01 | 3.1164222-01 | 3.2902046-01 | 3.9320290-01 | WEST |
| 2 | 2.7823532-01 | 2.9548458-01 | 2.2841050-01 | 1.9833377-01 | 1.8090766-01 | EAST |
| | 1.3744075-01 | 1.8922463-01 | 2.7247856-01 | 3.7143976-01 | 4.5500123-01 | WEST |
| 3 | 3.4749953-01 | 2.8231489-01 | 2.4838248-01 | 2.7041632-01 | 3.4031444-01 | EAST |
| | 1.3487399-01 | 2.6420157-01 | 3.9429846-01 | 4.4656196-01 | 5.6919652-01 | WEST |
| 4 | 4.3433149-01 | 4.3272745-01 | 3.1343147-01 | 2.2531875-01 | 2.5431396-01 | EAST |
| | 2.0632935-01 | 2.3707239-01 | 2.2833791-01 | 2.8188775-01 | 3.5833683-01 | WEST |

COEFFICIENTS AND SLAB WIDTHS FOR ALL BEAMS WITH THE LOAD ON ALL FIVE LANES. AVG. E MODEL= 4.6583245+05 LB. PER SQ.IN.

LOAD POSITION      1

SECTION
VALUE        BEAM NUMBER
GAGED    [UNITS]    [FROM THE EAST

| | [EDGE WESTWARD] | LOAD ON LANE 1 | LOAD ON LANE 2 | LOAD ON LANE 3 | LOAD ON LANE 4 | LOAD ON LANE 5 |
|---|---|---|---|---|---|---|
| **1** | | | | | | |
| MOMENT COEFFICIENT X [CUBIC INCHES] | 1 | 9.7873454+05 | 6.2872464+05 | 4.6469115+05 | 3.3511977+05 | 2.6143629+05 |
| | 2 | 8.1737692+05 | 6.4790409-05 | 5.1517937+05 | 3.6554342+05 | 2.8665028+05 |
| | 3 | 6.2761684+05 | 6.1133696+05 | 5.6223947+05 | 4.2347713+05 | 3.3417189+05 |
| | 4 | 4.8055870+05 | 5.3440820+05 | 5.8839281+05 | 5.2141613+05 | 4.4884396+05 |
| | 5 | 3.3417189+05 | 4.2347713+05 | 5.6223947+05 | 6.1133696+05 | 6.2761684+05 |
| | 6 | 2.8665028+05 | 3.6554342+05 | 5.1517937+05 | 6.4790609+05 | 8.1737692+05 |
| | 7 | 2.6143629+05 | 3.3511977+05 | 4.6469115+05 | 6.2872464+05 | 9.7873454+05 |
| SLAB WIDTH [INCHES] | 1 | 4.2421883+00 | 4.0644918+00 | 3.9401096+00 | 4.1821633+00 | 4.4059897+00 |
| | 2 | 5.7225489+00 | 4.0867652+00 | 3.9714431+00 | 3.4819912+00 | 3.0492821+00 |
| | 3 | 3.3158723+00 | 3.6549951+00 | 2.8948661+00 | 2.6704872+00 | 2.0490034+00 |
| | 4 | 3.0803156+00 | 3.8694728+00 | 3.6220263+00 | 3.8898990+00 | 3.5663948+00 |
| | 5 | 2.0490034+00 | 2.6704872+00 | 2.8948661+00 | 3.6549951+00 | 3.3158723+00 |
| | 6 | 3.0492821+00 | 3.4819912+00 | 3.9714431+00 | 4.0867652+00 | 5.7225489+00 |
| | 7 | 4.4059897+00 | 4.1821633+00 | 3.9401096+00 | 4.0644918+00 | 4.2421883+00 |
| MOMENT COEFFICIENT Y [CUBIC INCHES] | 1 | 4.2198784+05 | 2.4114158+05 | 1.8074543+05 | 8.1731548-06 | -6.6512297-07 |
| | 2 | -2.349471+05 | 5.1280128-06 | 5.6886785-07 | -3.4832969-06 | -3.9607513-06 |
| | 3 | -6.5231378+05 | -2.5202694+05 | -8.4462980-06 | 1.5695427-06 | 9.1106426-06 |
| | 4 | -4.7259836+05 | -2.3601484+05 | 9.6885657-07 | 4.0976048-06 | 2.7258220+05 |
| | 5 | -9.1106426-06 | -1.5695427-06 | 8.4462980-06 | 2.5202694+05 | 6.5231378+05 |
| | 6 | 3.9607513-06 | 3.4832969-06 | -5.6886785-07 | -5.1280128-06 | 2.3494171+05 |
| | 7 | 6.6512297-07 | -8.1731548-06 | -1.8074543+05 | -2.4114158+05 | -4.2198784+05 |
| MIDWIDTH DEFLECTION COEFFICIENT [CU.IN. / LB.] | 1 | 2.7307031-08 | 2.0366250-08 | 1.4726250-08 | 1.0879375-08 | 7.8787500-09 |
| | 2 | 2.3049375-08 | 1.9789062-08 | 1.5613125-08 | 1.2342187-08 | 9.6074999-09 |
| | 3 | 2.0107500-08 | 1.9745156-08 | 1.7783125-08 | 1.5140156-08 | 1.2601875-08 |
| | 4 | 1.5603594-08 | 1.7239375-08 | 1.7555625-08 | 1.6925625-08 | 1.5348750-08 |
| | 5 | 1.2601875-08 | 1.5140156-08 | 1.7783125-08 | 1.9745156-08 | 2.0107500-08 |
| | 6 | 9.6074999-09 | 1.2342187-08 | 1.5613125-08 | 1.9789062-08 | 2.3049375-08 |
| | 7 | 7.8787500-09 | 1.0879375-08 | 1.4726250-08 | 2.0366250-08 | 2.7307031-08 |
| ROTATION COEFFICIENT [SQ.IN. / LB.] | 1 | -9.9841455-10 | -2.2251893-11 | 3.5046729-10 | 3.4212281-10 | 4.4726301-10 |
| | 2 | -1.0320027-09 | -9.2272532-11 | 4.1759588-10 | 5.7370650-10 | 6.2890275-10 |
| | 3 | -1.2198930-09 | -4.1689897-10 | 2.4252899-10 | 6.1008584-10 | 7.8780106-10 |
| | 4 | -1.0442175-09 | -6.9623774-10 | 2.3931460-11 | 7.3881342-10 | 1.1386910-09 |
| | 5 | -7.8780106-10 | -6.1008584-10 | -2.4252899-10 | 4.1689897-10 | 1.2198930-09 |
| | 6 | -6.2890275-10 | -5.7370650-10 | -4.1759588-10 | 9.2272532-11 | 1.0320027-09 |
| | 7 | -4.4726301-10 | -3.4212281-10 | -3.5046729-10 | 2.2251893-11 | 9.9841455-10 |

REACTIONS, MOMENTS, AND SLAB WIDTHS IN A SECTION GAGED FOR THE LOAD ON THREE DIFFERENT LANES.  AVGEM=   4.6583245+05
                                                                                                LB PER SQ.IN.

            LOAD POSITION              1                                         SECTION GAGED              1

            NO. LONGITUDINAL SUM OF MOMENTS  NECESSARY EM TOTAL LAST ABS. PERCENTAGE OF  SUM OF MOMT. Y SQ. TRANSVERSE
LOAD ON LANE  REACTION [LB.]      ABOUT X     FOR EQUILIBRIUM MOMT. X COR.    TOTAL SLAB      [LB.IN.]     REACTION [LB.]
             NORTHWARD +       [LB.IN.]     [LB. / SQ.IN.]   [LB.IN.]        WIDTH    TOP CLOCKWISE +   EASTWARD +
             [USING THE AVERAGE EM]    [AFTER CORRECTION OF THE NORTH LONG. REACTION]    [USING THE AVERAGE EM]

     1    -1.5190820+01   1.7638957+02   4.0020943+05   1.3562967-01        103    =4.5777993+01  -1.6221826+00

     2    -8.9683069+00   1.6520823+02   4.2729572+05   3.2313954+00        104    =1.2028449+01  -4.2623846=01

     3    -1.3400940+01   1.7108222+02   4.1262482+05   6.4464454=05        101     0.0000000+00   0.0000000+00

            AVERAGE NECESSARY EM   =   4.1337655+05


       MIDWIDTH DEFLECTIONS AND ROTATIONS IN A SECTION GAGED FOR THE LOAD ON THREE DIFFERENT LANES


LOAD ON LANE     BEAM 1          BEAM 2          BEAM 3          BEAM 4          BEAM 5          BEAM 6          BEAM 7


                           DEFLECTIONS IN HUNDREDTHOUSANDTHS OF AN INCH

     1           1272            1074             937             727             587             448             367

     2            949             922             920             803             705             575             507

     3            686             727             828             818             828             727             686

                              ROTATIONS IN MILLIONTHS OF A RADIAN
                        [CLOCKWISE ROTATIONS LOOKING SOUTH ARE POSITIVE]

     1           -465            =481            =568            -486            =367            -293            -208

     2           -10             =43             =194            -324            =284            -267            -159

     3            163             195             113              11            =113            -195            -163

TENTHS OF MICROSTRAINS AND DEFLECTIONS IN HUNDREDTHOUSANDTHS OF AN INCH.  AVG, E MODEL=  4.6583245+05 LB; PER SQ.IN,

LOAD POSITION          1

| GAGE NUMBER | SECTION GAGED 2 | LOAD ON LANE 1 | LOAD ON LANE 2 | LOAD ON LANE 3 | LOAD ON LANE 4 | LOAD ON LANE 5 | TYPE |
|---|---|---|---|---|---|---|---|
| 1 | | 663 | 471 | 321 | 247 | 189 | BEAM STRAIN |
| 2 | | 239 | 150 | 116 | 99 | 83 | BEAM STRAIN |
| 3 | | 693 | 477 | 317 | 235 | 171 | BEAM STRAIN |
| 4 | | 252 | 170 | 104 | 73 | 56 | BEAM STRAIN |
| 5 | | 563 | 485 | 364 | 288 | 230 | BEAM STRAIN |
| 6 | | 202 | 183 | 146 | 118 | 89 | BEAM STRAIN |
| 7 | | 590 | 490 | 348 | 259 | 183 | BEAM STRAIN |
| 8 | | 210 | 153 | 111 | 74 | 45 | BEAM STRAIN |
| 9 | | 412 | 450 | 406 | 336 | 267 | BEAM STRAIN |
| 10 | | 134 | 156 | 146 | 130 | 100 | BEAM STRAIN |
| 11 | | 438 | 463 | 399 | 336 | 259 | BEAM STRAIN |
| 12 | | 190 | 201 | 155 | 98 | 51 | BEAM STRAIN |
| 13 | | 349 | 413 | 433 | 406 | 330 | BEAM STRAIN |
| 14 | | 84 | 142 | 168 | 170 | 132 | BEAM STRAIN |
| 15 | | 336 | 398 | 412 | 373 | 298 | BEAM STRAIN |
| 16 | | 123 | 160 | 150 | 127 | 86 | BEAM STRAIN |
| 17 | | 1232 | 875 | 614 | 445 | 313 | BM; DEFLECTION |
| 18 | | 1131 | 879 | 647 | 490 | 367 | BM; DEFLECTION |
| 19 | | 1130 | 922 | 695 | 532 | 406 | BM; DEFLECTION |
| 20 | | 1028 | 928 | 752 | 604 | 478 | BM; DEFLECTION |
| 21 | | 922 | 870 | 788 | 602 | 489 | BM; DEFLECTION |
| 22 | | 802 | 829 | 775 | 680 | 577 | BM; DEFLECTION |
| 23 | | 776 | 835 | 817 | 750 | 659 | BM; DEFLECTION |
| 24 | | 664 | 751 | 821 | 806 | 767 | BM; DEFLECTION |

DISTANCES IN INCHES FROM THE TOP FIBER TO THE NEUTRAL AXIS IN THE BEAMS GAGED.  AVG. EM =   4.6583245+05 LB; PER SQ.IN,

BEAM NUMBER
[FROM THE EAST
EDGE WESTWARD]                    [AFTER CORRECTION FROM THE EFFECTS OF ANY LONGITUDINAL REACTION]

| BEAM NUMBER | LOAD ON LANE 1 | LOAD ON LANE 2 | LOAD ON LANE 3 | LOAD ON LANE 4 | LOAD ON LANE 5 | BEAM WALL |
|---|---|---|---|---|---|---|
| 1 | 2.6049542=01 | 3.1628312=01 | 2.8788850=01 | 2.0373506=01 | 9.6243735=02 | EAST |
| | 2.5583577=01 | 2.8747126=01 | 3.4924567=01 | 3.7022368=01 | 3.2988251=01 | WEST |
| 2 | 2.6005393=01 | 2.5040279=01 | 2.0491624=01 | 1.8024761=01 | 2.0632371=01 | EAST |
| | 2.7035392=01 | 3.3290465=01 | 3.6355500=01 | 4.0935078=01 | 4.4006401=01 | WEST |
| 3 | 3.3545506=01 | 3.0525719=01 | 2.8815016=01 | 2.2865284=01 | 2.2304326=01 | EAST |
| | 1.1276067=01 | 1.2586248=01 | 2.3299063=01 | 3.9472601=01 | 5.0803891=01 | WEST |
| 4 | 4.5675026=01 | 3.1386658=01 | 2.3289028=01 | 1.6107663=01 | 1.8269598=01 | EAST |
| | 2.4887339=01 | 1.9631679=01 | 2.7933423=01 | 3.1542898=01 | 3.8362957=01 | WEST |

COEFFICIENTS AND SLAB WIDTHS FOR ALL BEAMS WITH THE LOAD ON ALL FIVE LANES, AVG. E MODEL=   4.6583245+05 LBS PER SQ.IN.

LOAD POSITION          1

| SECTION GAGED | VALUE [UNITS] | BEAM NUMBER [FROM THE EAST EDGE WESTWARD] | LOAD ON LANE 1 | LOAD ON LANE 2 | LOAD ON LANE 3 | LOAD ON LANE 4 | LOAD ON LANE 5 |
|---|---|---|---|---|---|---|---|
| 2 | | | | | | | |
| | MOMENT COEFFICIENT X [CUBIC INCHES] | | | | | | |
| | | 1 | 1.1147991=04 | 7.0467225=05 | 4.5913568=05 | 3.6125411=05 | 3.0087317=05 |
| | | 2 | 9.3663194=05 | 7.2432228=05 | 5.1699916=05 | 4.0415338=05 | 3.2119417=05 |
| | | 3 | 7.0310128=05 | 6.9878977=05 | 5.8870557=05 | 4.8761702=05 | 3.9199894=05 |
| | | 4 | 5.1976732=05 | 6.0673562=05 | 6.1681901=05 | 5.8693853=05 | 4.9515541=05 |
| | | 5 | 3.9199894=05 | 4.8761702=05 | 5.8870557=05 | 6.9878977=05 | 7.0310128=05 |
| | | 6 | 3.2119417=05 | 4.0415338=05 | 5.1699916=05 | 7.2432228=05 | 9.3663194=05 |
| | | 7 | 3.0087317=05 | 3.6125411=05 | 4.5913568=05 | 7.0467225=05 | 1.1147991=04 |
| | SLAB WIDTH [INCHES] | | | | | | |
| | | 1 | 3.9209296+00 | 3.1859064+00 | 3.3318553+00 | 3.9860987+00 | 4.9217066+00 |
| | | 2 | 3.7675597+00 | 3.7366557+00 | 3.9234103+00 | 3.5076963+00 | 2.8576186+00 |
| | | 3 | 5.9160723+00 | 4.1574564+00 | 3.7202780+00 | 3.1580737+00 | 2.5420519+00 |
| | | 4 | 3.4041387+00 | 4.2507731+00 | 3.7644988+00 | 3.9689105+00 | 3.6507750+00 |
| | | 5 | 2.5420519+00 | 3.1580737+00 | 3.7202780+00 | 4.1574564+00 | 5.9160723+00 |
| | | 6 | 2.8576186+00 | 3.5076963+00 | 3.9234103+00 | 3.7366557+00 | 3.7675597+00 |
| | | 7 | 4.9217066+00 | 3.9860987+00 | 3.3318553+00 | 3.1859064+00 | 3.9209296+00 |
| | MOMENT COEFFICIENT Y [CUBIC INCHES] | | | | | | |
| | | 1 | 5.2412198=05 | 4.9178986=05 | 2.6916015=05 | 9.8215015=06 | =4.7611788=06 |
| | | 2 | 1.0270338=05 | 3.4257021=05 | 1.2985910=05 | =1.2545072=06 | =1.0334765=05 |
| | | 3 | =1.3323484=05 | 2.4689768=05 | 8.2493127=06 | =7.1555645=07 | =1.5942578=06 |
| | | 4 | =6.1053101=05 | =1.5508463=05 | =1.5623714=05 | =1.3728873=05 | 1.4232112=06 |
| | | 5 | 1.5942578=06 | 7.1555645=07 | =8.2493127=06 | =2.4689768=05 | 1.3323484=05 |
| | | 6 | 1.0334765=05 | 1.2545072=06 | =1.2985910=05 | =3.4257021=05 | =1.0270338=05 |
| | | 7 | 4.7611788=06 | =9.8215015=06 | =2.6916015=05 | =4.9178986=05 | =5.2412198=05 |
| | MIDWIDTH DEFLECTION COEFFICIENT [CU.IN. / LB.] | | | | | | |
| | | 1 | 2.5363594=08 | 1.8826875=08 | 1.3526875=08 | 1.0039687=08 | 7.2974999=09 |
| | | 2 | 2.3164052=08 | 1.9856250=08 | 1.5527500=08 | 1.2183750=08 | 9.4912499=09 |
| | | 3 | 1.8508750=08 | 1.8236719=08 | 1.6771094=08 | 1.3765781=08 | 1.1450625=08 |
| | | 4 | 1.5454375=08 | 1.7026875=08 | 1.7576250=08 | 1.6703906=08 | 1.5300000=08 |
| | | 5 | 1.1450625=08 | 1.3765781=08 | 1.6771094=08 | 1.8236719=08 | 1.8508750=08 |
| | | 6 | 9.4912499=09 | 1.2183750=08 | 1.5527500=08 | 1.9856250=08 | 2.3164062=08 |
| | | 7 | 7.2974999=09 | 1.0039687=08 | 1.3526875=08 | 1.8826875=08 | 2.5363594=08 |
| | ROTATION COEFFICIENT [SQ.IN. / LB.] | | | | | | |
| | | 1 | =9.6754001=10 | 3.0874502=11 | 3.1319536=10 | 4.2473297=10 | 5.1401869=10 |
| | | 2 | =9.8210304=10 | 4.8505790=11 | 5.4750224=10 | 6.8911686=10 | 6.9580730=10 |
| | | 3 | =1.1541035=09 | =3.9766390=10 | =1.2697926=10 | 7.4974912=10 | 8.4132469=10 |
| | | 4 | =1.0657836=09 | =8.0392920=10 | 3.3392713=11 | 5.3637022=10 | 1.0284951=09 |
| | | 5 | =8.4132469=10 | =7.4974912=10 | 1.2697926=10 | 3.9766390=10 | 1.1541035=09 |
| | | 6 | =6.9580730=10 | =6.8911686=10 | =5.4750224=10 | =4.8505790=11 | 9.8210304=10 |
| | | 7 | =5.1401869=10 | =4.2473297=10 | =3.1319536=10 | =3.0874502=11 | 9.6754001=10 |

REACTIONS, MOMENTS, AND SLAB WIDTHS IN A SECTION GAGED FOR THE LOAD ON THREE DIFFERENT LANES.   AVGEM=   4.6583245+05
                                                                                                LBT PER SQ.IN.

LOAD POSITION          1                                         SECTION GAGED         2

| LOAD ON LANE | NO. LONGITUDINAL REACTION (LB.) NORTHWARD + (USING THE AVERAGE EM) | SUM OF MOMENTS ABOUT X [LB.IN.] | NECESSARY EM FOR EQUILIBRIUM [LB. / SQ.IN.] | TOTAL LAST ABS. MOMT. X COR. [LB.IN.] (AFTER CORRECTION OF THE NORTH LONG. REACTION) | PERCENTAGE OF TOTAL SLAB WIDTH | SUM OF MOMT. Y SO. [LB.IN.] TOP CLOCKWISE + (USING THE | TRANSVERSE REACTION (LB.) EASTWARD + AVERAGE EM) |
|---|---|---|---|---|---|---|---|
| 1 | -2.6542629+01 | 1.9976600+02 | 3.5052585+05 | 2.2040910=01 | 109 | 2.3273697+00 | 1.3134141=01 |
| 2 | -1.8283297+01 | 1.8575276+02 | 3.7696961+05 | 4.4290539=02 | 104 | 3.9486695+01 | 2.2283688+00 |
| 3 | -1.5080034+01 | 1.7452412+02 | 4.0122332+05 | 1.6139641=04 | 103 | =7.0000000+00 | -3.9503386=01 |

AVERAGE NECESSARY EM   =   3.7623959+05


MIDWIDTH DEFLECTIONS AND ROTATIONS IN A SECTION GAGED FOR THE LOAD ON THREE DIFFERENT LANES

| LOAD ON LANE | BEAM 1 | BEAM 2 | BEAM 3 | BEAM 4 | BEAM 5 | BEAM 6 | BEAM 7 |
|---|---|---|---|---|---|---|---|

DEFLECTIONS IN HUNDREDTHOUSANDTHS OF AN INCH

| LOAD ON LANE | BEAM 1 | BEAM 2 | BEAM 3 | BEAM 4 | BEAM 5 | BEAM 6 | BEAM 7 |
|---|---|---|---|---|---|---|---|
| 1 | 1182 | 1079 | 862 | 720 | 533 | 442 | 340 |
| 2 | 877 | 925 | 850 | 793 | 641 | 568 | 468 |
| 3 | 630 | 723 | 791 | 819 | 781 | 723 | 630 |

ROTATIONS IN MILLIONTHS OF A RADIAN
(CLOCKWISE ROTATIONS LOOKING SOUTH ARE POSITIVE)

| LOAD ON LANE | BEAM 1 | BEAM 2 | BEAM 3 | BEAM 4 | BEAM 5 | BEAM 6 | BEAM 7 |
|---|---|---|---|---|---|---|---|
| 1 | -451 | =457 | -538 | -496 | =392 | -324 | =239 |
| 2 | 14 | 23 | =185 | -374 | =349 | -321 | =198 |
| 3 | 146 | 255 | =59 | 16 | 59 | =255 | =146 |

MOMENT PERCENTAGES AND SLAB WIDTHS IN INCHES FOR ALL BEAMS AT ALL SECTIONS GAGED WITH THE LOAD ON THREE DIFFERENT LANES

MODEL LOAD = 1,7468717+01 LB.                                    AVG.E MODEL = 4.6583245+05 LB. PER SQ.IN.
                                        LOAD POSITION        1

| LOAD ON LANE | BEAM NUMBER [FROM THE EAST EDGE WESTWARD] | S E C T I O N 1 [NOMINAL MAXIMUM MOMENT] MOMENT %  | SLAB WIDTH | 2 [NOMINAL THIRD OF THE SPAN] MOMENT % | SLAB WIDTH | 3 [NOMINAL SIXTH OF THE SPAN] MOMENT % SLAB WIDTH |
|---|---|---|---|---|---|---|
| 1 | 1 | 2.5847690+01 | 4.2421883+00 | 2.5995894+01 | 3.9209296+00 | INSUFFICIENT GAGE RESPONSE |
|  | 2 | 2.1586349+01 | 5.7225489+00 | 2.1841232+01 | 3.7675597+00 | INSUFFICIENT GAGE RESPONSE |
|  | 3 | 1.6574919+01 | 3.3158723+00 | 1.6395553+01 | 5.9160723+00 | INSUFFICIENT GAGE RESPONSE |
|  | 4 | 1.2691217+01 | 3.0803156+00 | 1.2120405+01 | 3.4041387+00 | INSUFFICIENT GAGE RESPONSE |
|  | 5 | 8.8252443+00 | 2.0490034+00 | 9.1409864+00 | 2.5420519+00 | INSUFFICIENT GAGE RESPONSE |
|  | 6 | 7.5702321+00 | 3.0492821+00 | 7.4898967+00 | 2.8576186+00 | INSUFFICIENT GAGE RESPONSE |
|  | 7 | 6.9043484+00 | 4.4059897+00 | 7.0160332+00 | 4.9217066+00 | INSUFFICIENT GAGE RESPONSE |
|  | SUM ALL BEAMS | ONE HUNDRED | 2.5865200+01 | ONE HUNDRED | 2.7330077+01 |  |
| 2 | 1 | 1.7727950+01 | 4.0644918+00 | 1.7671834+01 | 3.1859064+00 | INSUFFICIENT GAGE RESPONSE |
|  | 2 | 1.8268804+01 | 4.0867652+00 | 1.8164620+01 | 3.7366557+00 | INSUFFICIENT GAGE RESPONSE |
|  | 3 | 1.7237676+01 | 3.6549951+00 | 1.7524313+01 | 4.1574564+00 | INSUFFICIENT GAGE RESPONSE |
|  | 4 | 1.5068540+01 | 3.8694728+00 | 1.5215771+01 | 4.2507731+00 | INSUFFICIENT GAGE RESPONSE |
|  | 5 | 1.1940651+01 | 2.6704872+00 | 1.2228504+01 | 3.1580737+00 | INSUFFICIENT GAGE RESPONSE |
|  | 6 | 1.0307113+01 | 3.4819912+00 | 1.0135395+01 | 3.5076963+00 | INSUFFICIENT GAGE RESPONSE |
|  | 7 | 9.4492666+00 | 4.1821633+00 | 9.0595634+00 | 3.9860987+00 | INSUFFICIENT GAGE RESPONSE |
|  | SUM ALL BEAMS | ONE HUNDRED | 2.6010367+01 | ONE HUNDRED | 2.5982660+01 |  |
| 3 | 1 | 1.2652876+01 | 3.9401096+00 | 1.2255057+01 | 3.3318553+00 | INSUFFICIENT GAGE RESPONSE |
|  | 2 | 1.4027598+01 | 3.9714431+00 | 1.3799525+01 | 3.9234103+00 | INSUFFICIENT GAGE RESPONSE |
|  | 3 | 1.5308978+01 | 2.8948661+00 | 1.5713482+01 | 3.7202780+00 | INSUFFICIENT GAGE RESPONSE |
|  | 4 | 1.6021096+01 | 3.6220263+00 | 1.6463874+01 | 3.7644988+00 | INSUFFICIENT GAGE RESPONSE |
|  | 5 | 1.5308978+01 | 2.8948661+00 | 1.5713482+01 | 3.7202780+00 | INSUFFICIENT GAGE RESPONSE |
|  | 6 | 1.4027598+01 | 3.9714431+00 | 1.3799525+01 | 3.9234103+00 | INSUFFICIENT GAGE RESPONSE |
|  | 7 | 1.2652876+01 | 3.9401096+00 | 1.2255057+01 | 3.3318553+00 | INSUFFICIENT GAGE RESPONSE |
|  | SUM ALL BEAMS | ONE HUNDRED | 2.5234864+01 | ONE HUNDRED | 2.5715586+01 |  |

BRIEF DESCRIPTION OF THIS BRIDGE MODEL [CODE IN CURB, PARPT, DIAPH, AND EXEND FREE, A ZERO MEANS NO AND A ONE MEANS YES]

| UNITS,. INCHES [SCALE = 1/16] | LENGTH OVERHANG BOTH ENDS | SPAN | SLAB WIDTH | BEAM BOTTOM AND SIDE WALLS | BEAM TOP WALL | CURB WIDTH | CURB THICKNESS | PARAPET WIDTH AND THICKNESS |
|---|---|---|---|---|---|---|---|---|
| 50 | 0.53 | 48.94 | 25 | 5/16 | 3/16 | 2 1/16 | 1/2 | 0.95 |

| NUMBER OF BEAMS | SLAB THICKNESS | CURB | PARAPET | DIAPHRAGMS | EXPANSION END FREE TRANSV.DIR. | PROTOTYPE LOAD [LB.] | AVG.E PROTOTYPE [LB. / SQ.IN.] |
|---|---|---|---|---|---|---|---|
| 7 | 5.0000000-01 | 0 | 0 | 0 | 0 | 72000 | 7.5000000+06 |

SPACINGS AND BEAM SIZES IN INCHES FOR THE EASTERN HALF OF THE CROSS SECTION

| SPACING EDGE TO CENTER | BEAM WIDTH AND DEPTH | SPACING CENTER TO CENTER | BEAM WIDTH AND DEPTH | SPACING CENTER TO CENTER | BEAM WIDTH AND DEPTH | SPACING CENTER TO CENTER | BEAM WIDTH AND DEPTH |
|---|---|---|---|---|---|---|---|
| 2.7800000+00 |  | 3.2400000+00 |  | 3.2400000+00 |  | 3.2400000+00 |  |
|  | 2.2470000+00 |  | 2.2420000+00 |  | 2.2420000+00 |  | 2.2460000+00 |
|  | 1.5190000+00 |  | 1.5130000+00 |  | 1.5060000+00 |  | 1.5000000+00 |

THE CROSS SECTIONAL AREA IS 2.4776500+01 SQ.IN., AND THE CENTROID IS 7.7708229-01 IN. BELOW THE TOP OF THE SLAB

```
TEST TO KNOW IF ALL THE DATA POINTS WERE READ
LABEL.. IF HOMEPHONE IS 8.678440+06, ALL THE DATA POINTS WERE READ.
HOMEPHONE  = 8.678440+06    IF HOMEPHONE IS NOT 8.678440+06, NOT ALL THE DATA POINTS WERE READ.

TYPE #END# STATEMENT EXECUTED.
CARDS REMAINING IN DECK ARE.-

MAR 23 68    06 49.9
```

## 13. FIGURES

It should be noted that Figs. 23 through 59 represent the behavior at the Section of Maximum Moment.
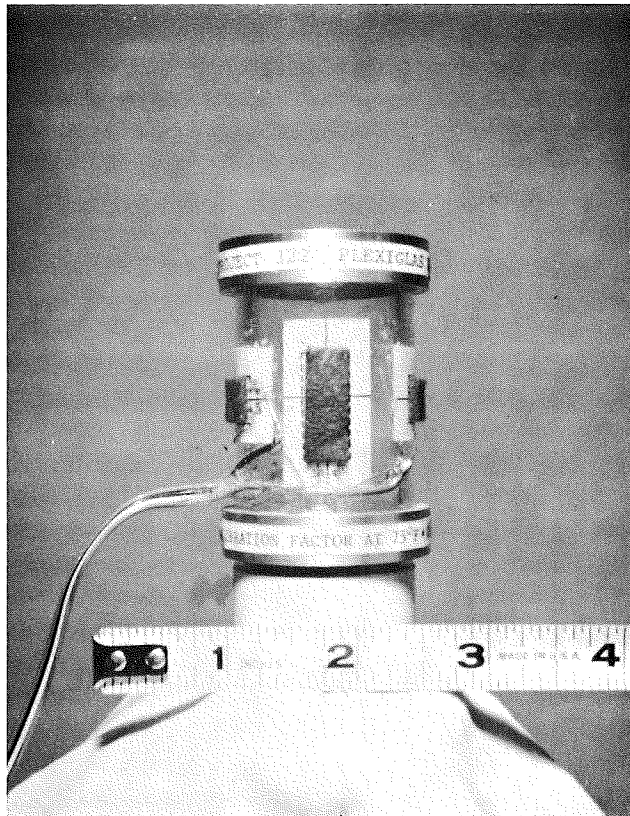
Fig. 1    Plexiglas Compensating Load Cell
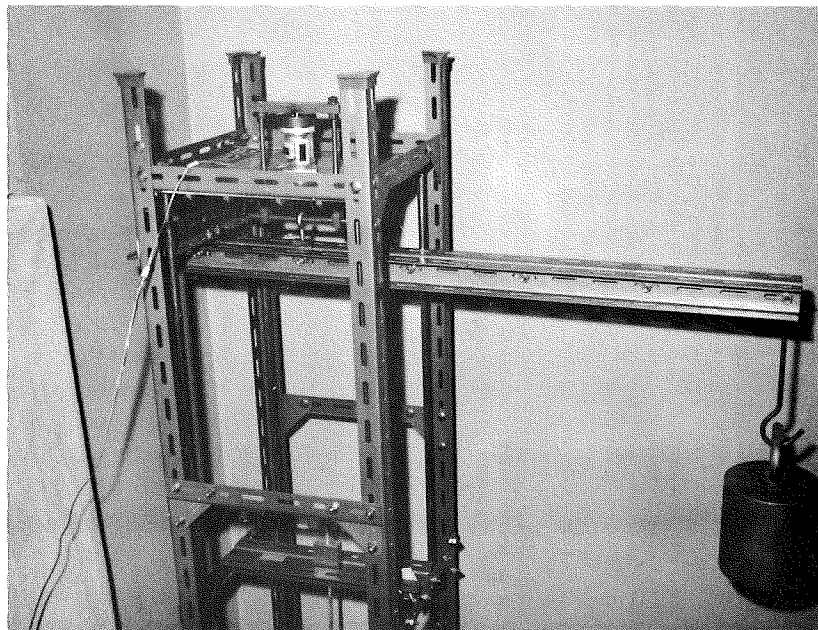


Fig. 2    Calibration of the Load Cell
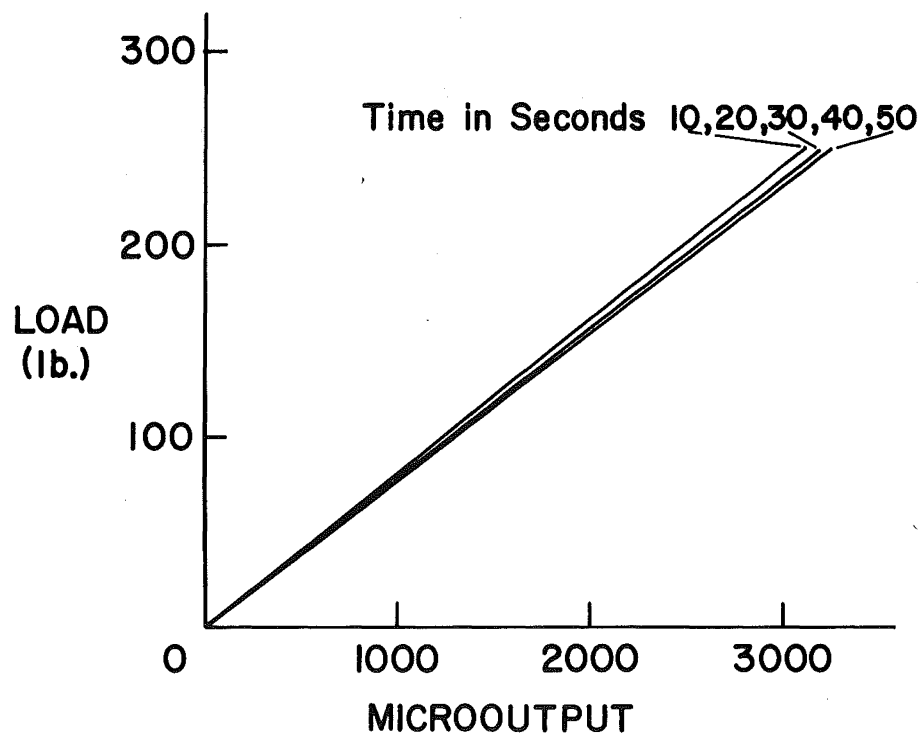
Fig. 3   Non-Instantaneous Calibration Factors
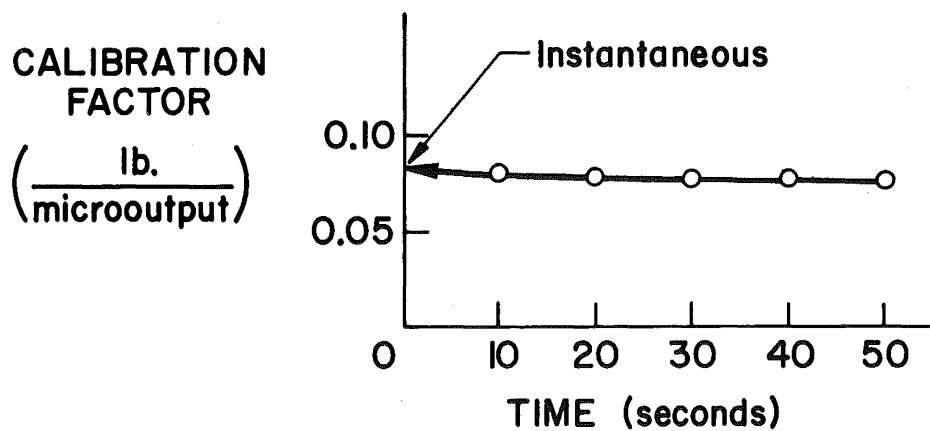


Fig. 4   Instantaneous Calibration Factor
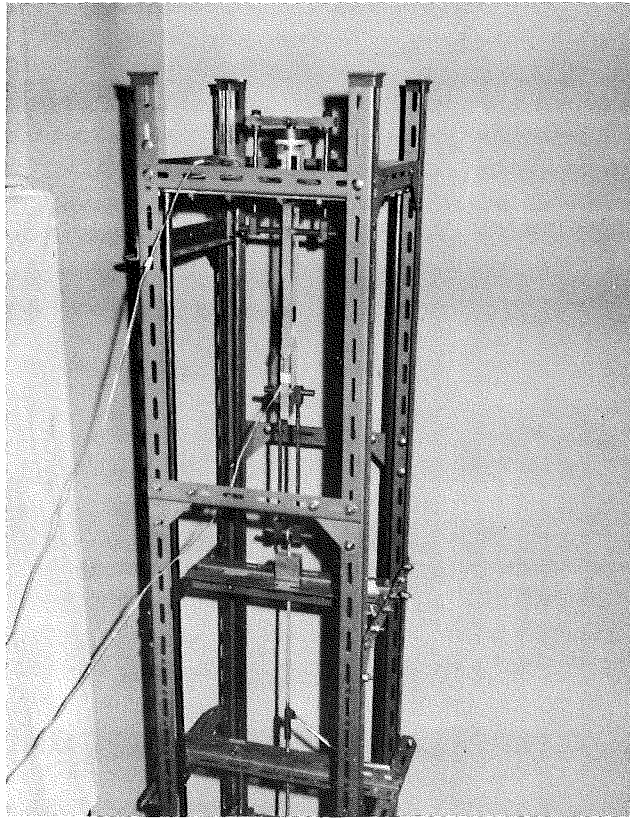
Fig. 5    Creep Compensated Tensile Test
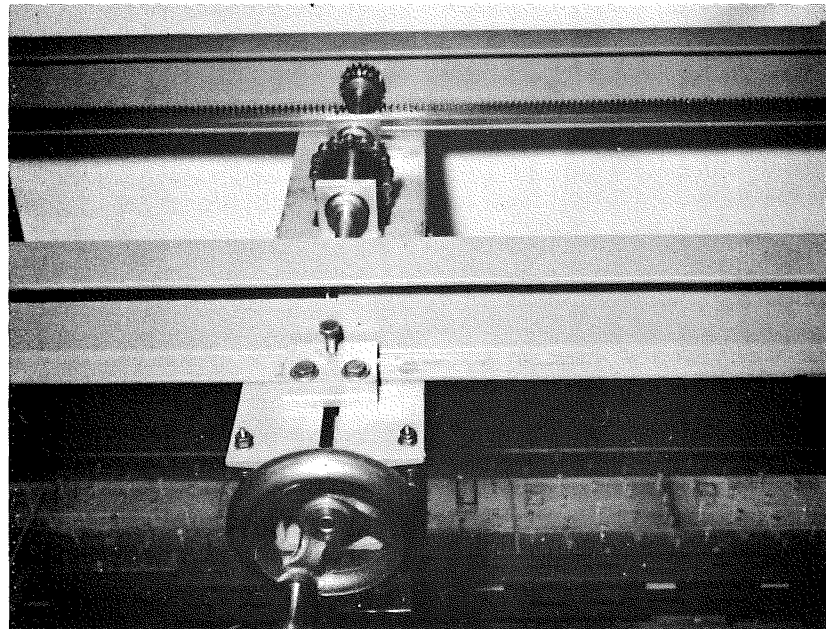


Fig. 6    Mechanism to Position the Load
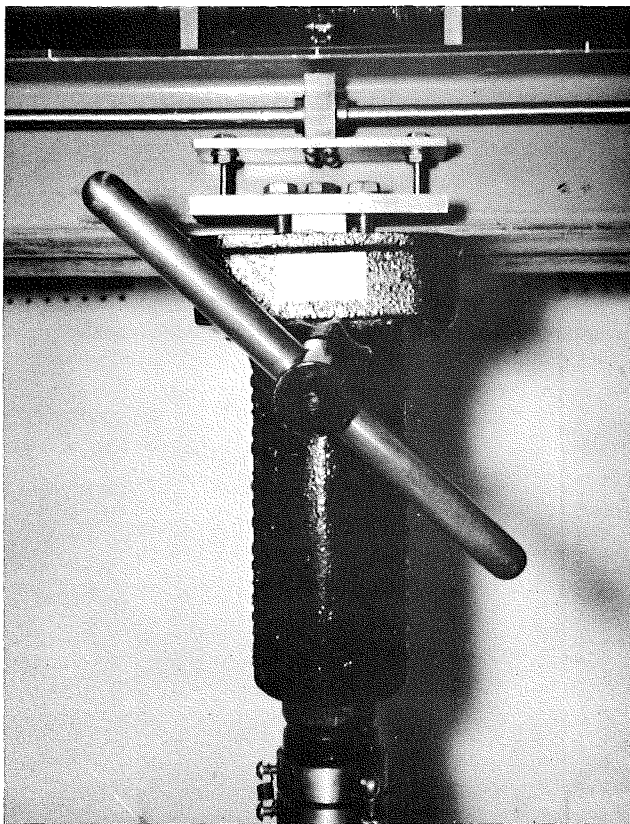
Fig. 7    Mechanical Jack Mounted
on Ball-Bushings
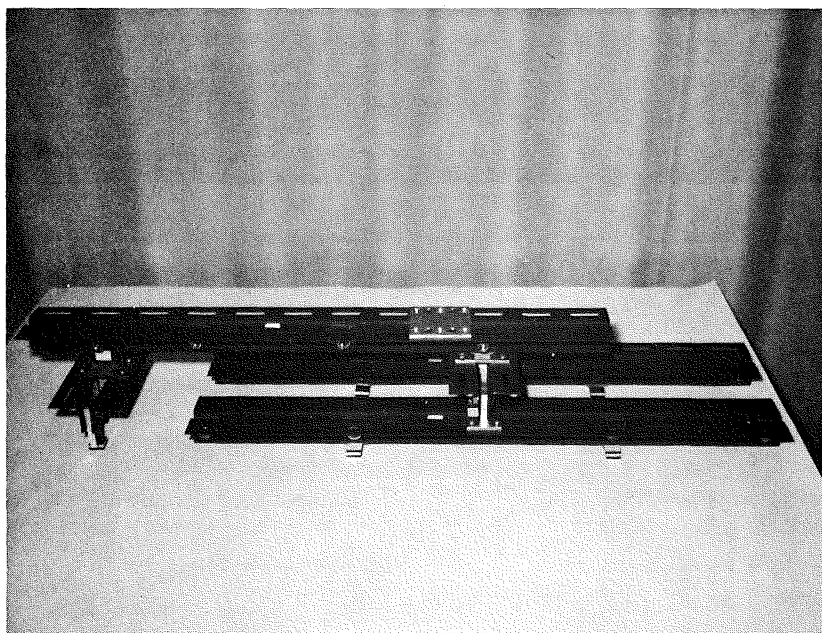


Fig. 8    Model Test Vehicle
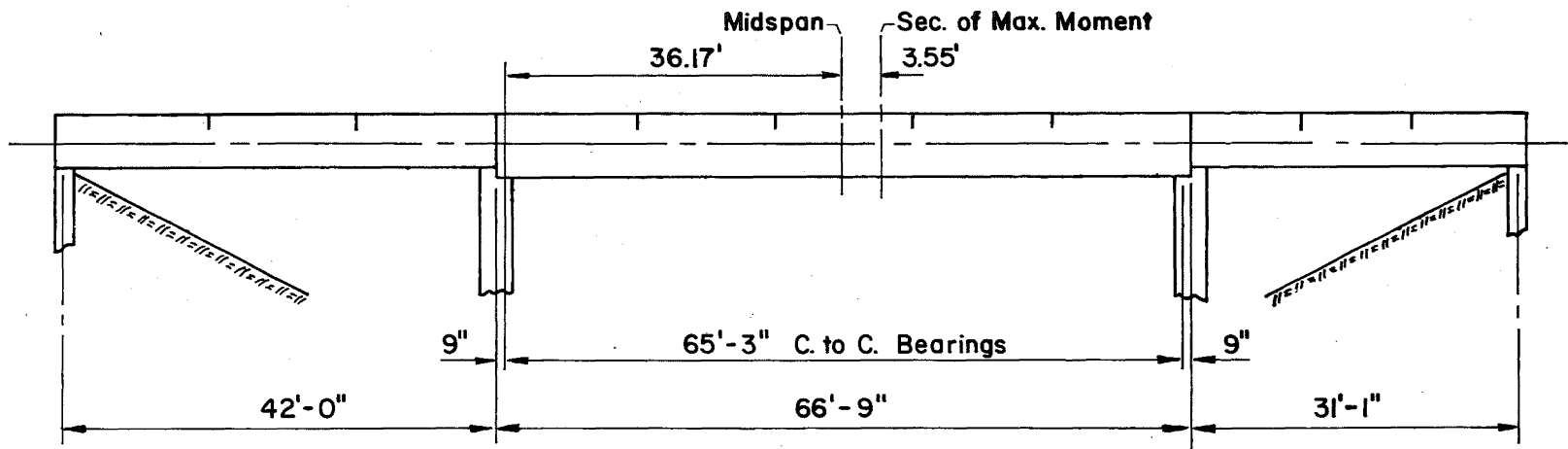
Fig. 9   Elevation of Berwick Bridge
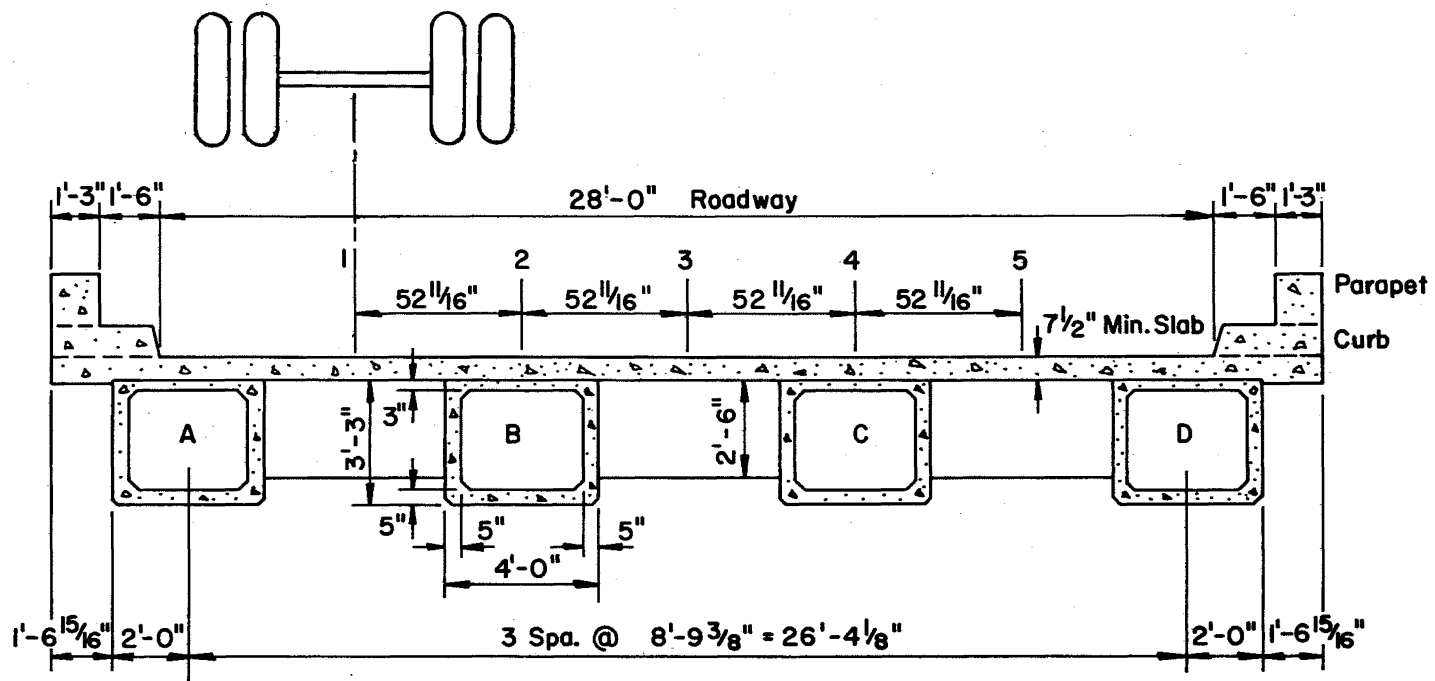
Fig. 10   Cross-Section of Berwick Bridge

- Longitudinal Gages
○ Transverse Gages
× Deflection Gages
▽ Diaphragm Gages

Fig. 11    Location of Gages

AXLE AND WHEEL SPACING

| FRONT | DRIVE | REAR |
|-------|-------|------|
| ↓ | ↓ | ↓ |
| 9.400k | 32.200k | 32.100k |
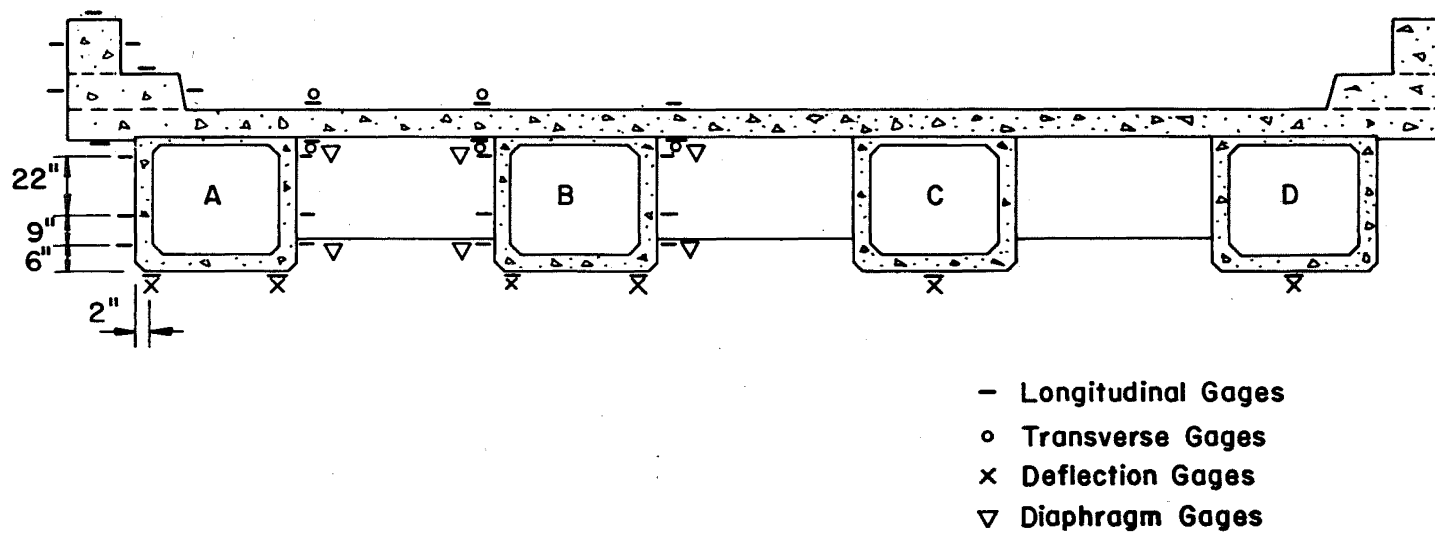
AXLE LOADS
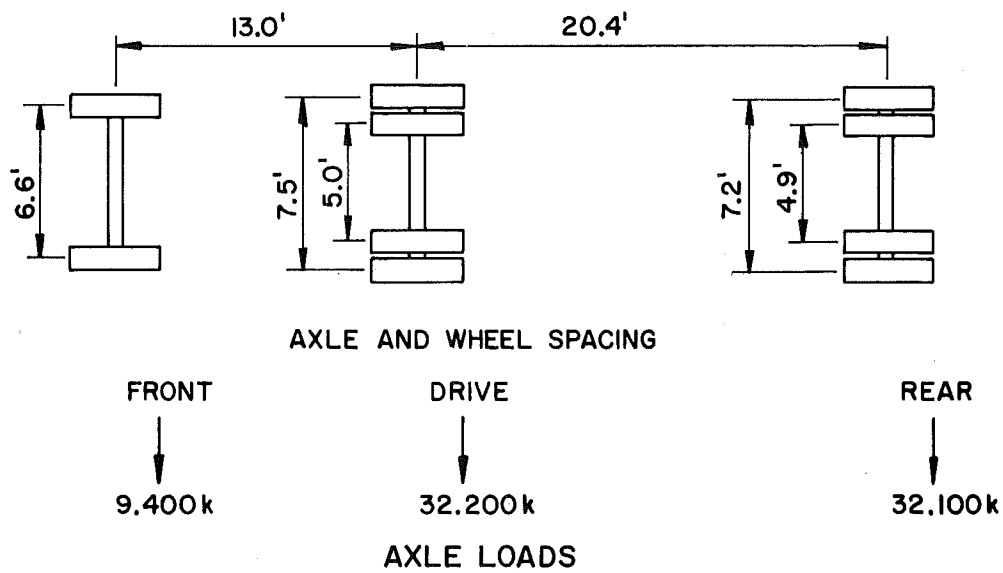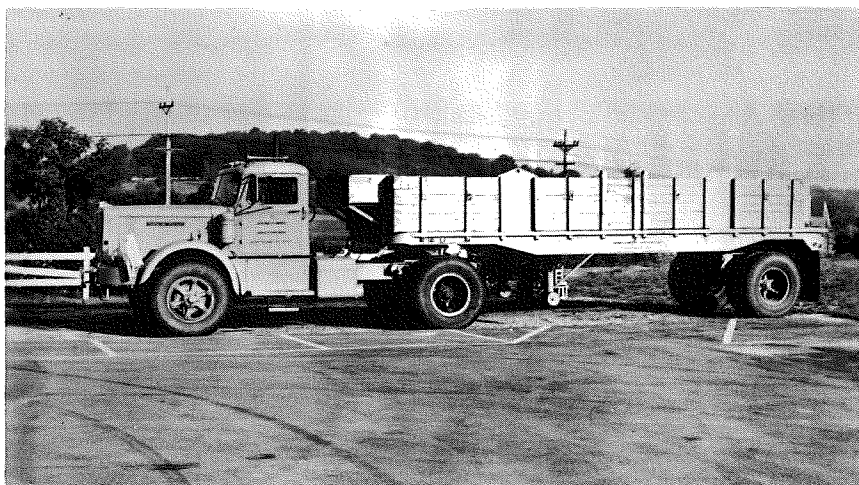
Fig. 12   Field Test Vehicle
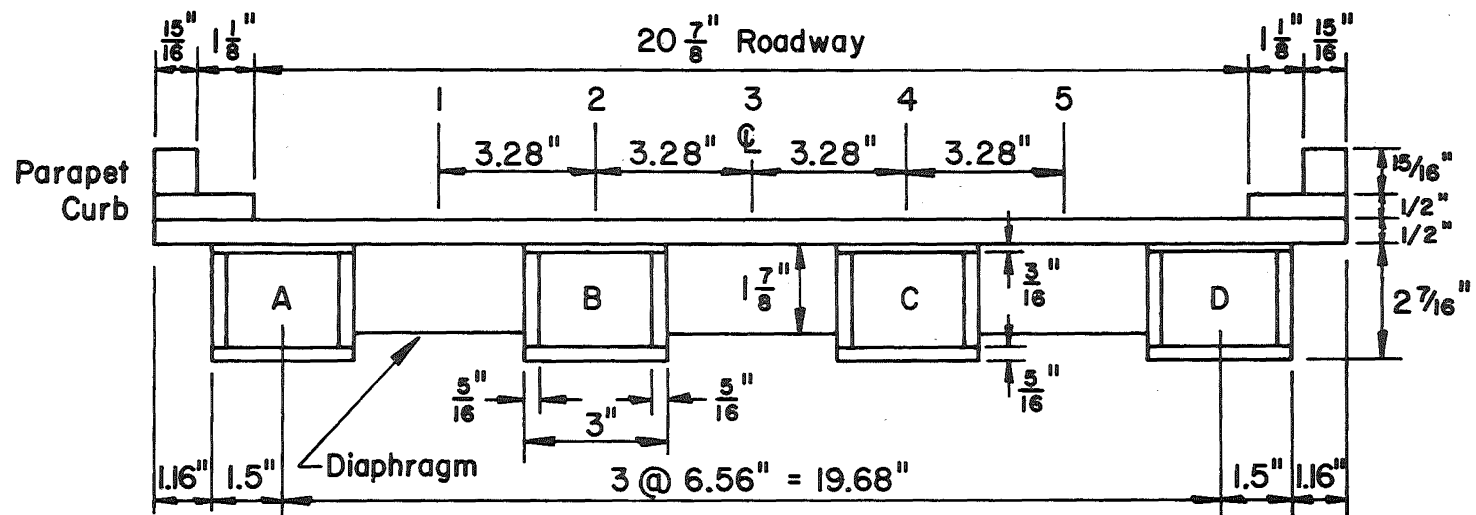
Fig. 13   Cross-Section of Pilot Model A1
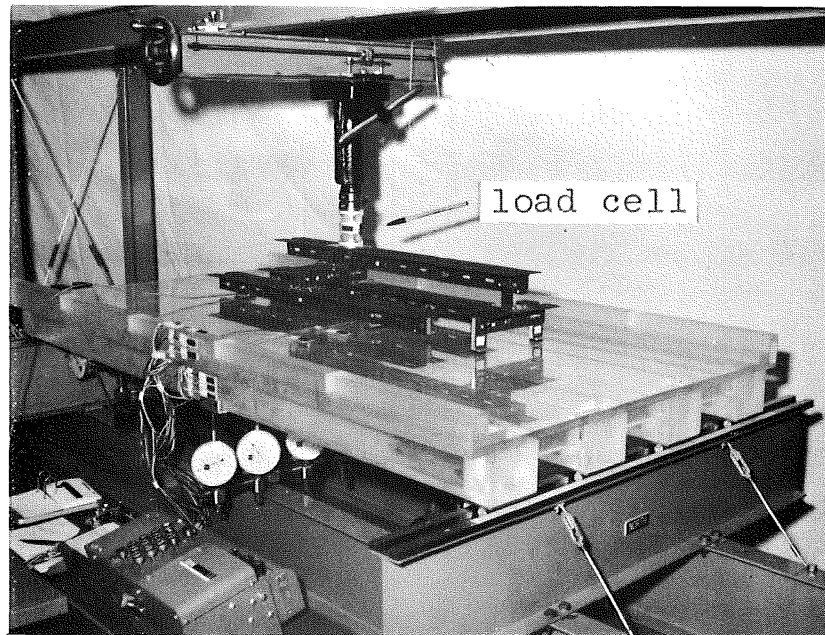
Fig. 14    Setup of Pilot Tests



Fig. 15    Torque Wrench
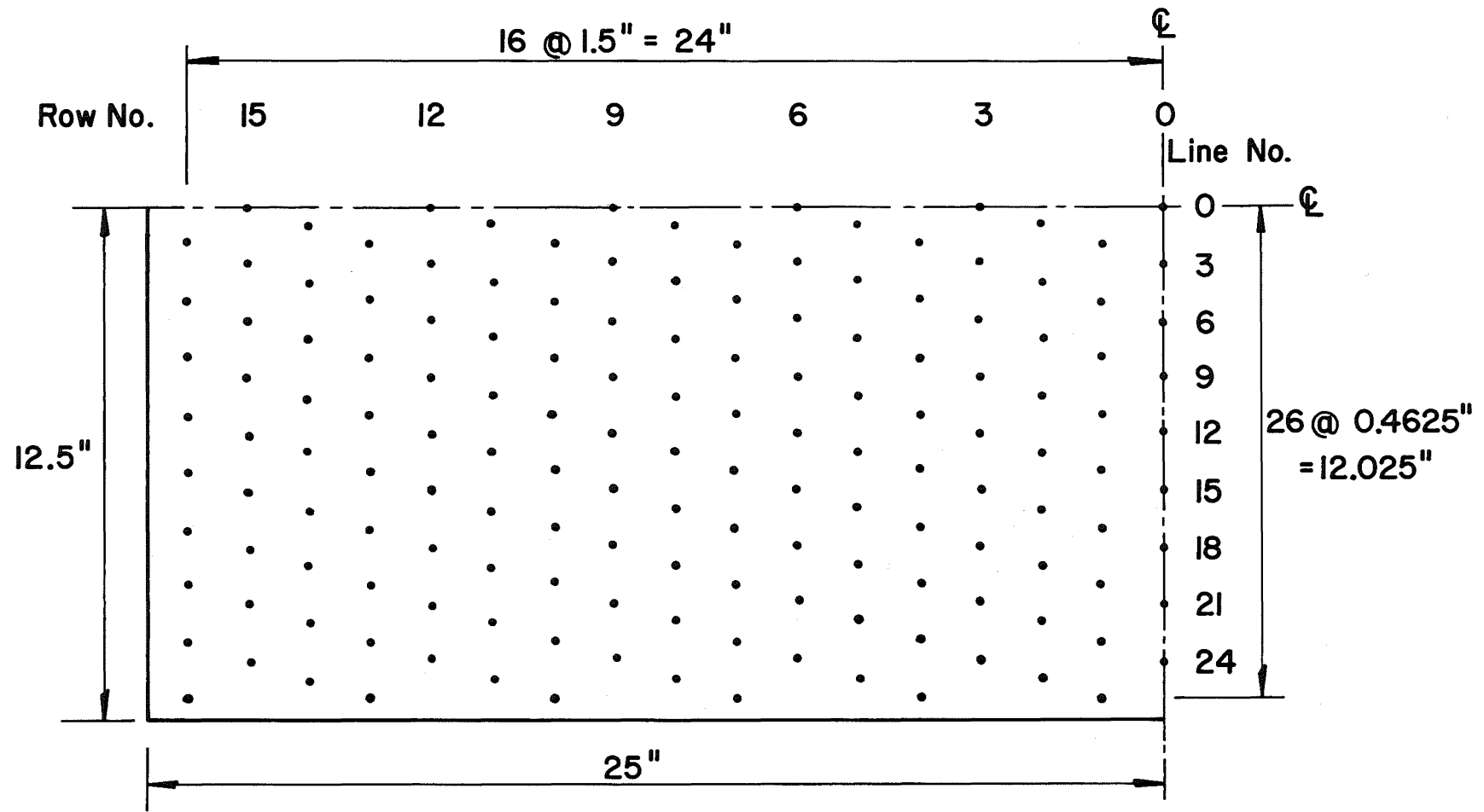
Fig. 16    Pattern of Slab Perforations - SE Quarter

No. 29 Holes

0.475"
0.95"
0.475"

0.35"    2 7/8"         3 1/2"          2 7/8"      0.35"

PLAN VIEW

0.95"

9.95"

ELEVATION
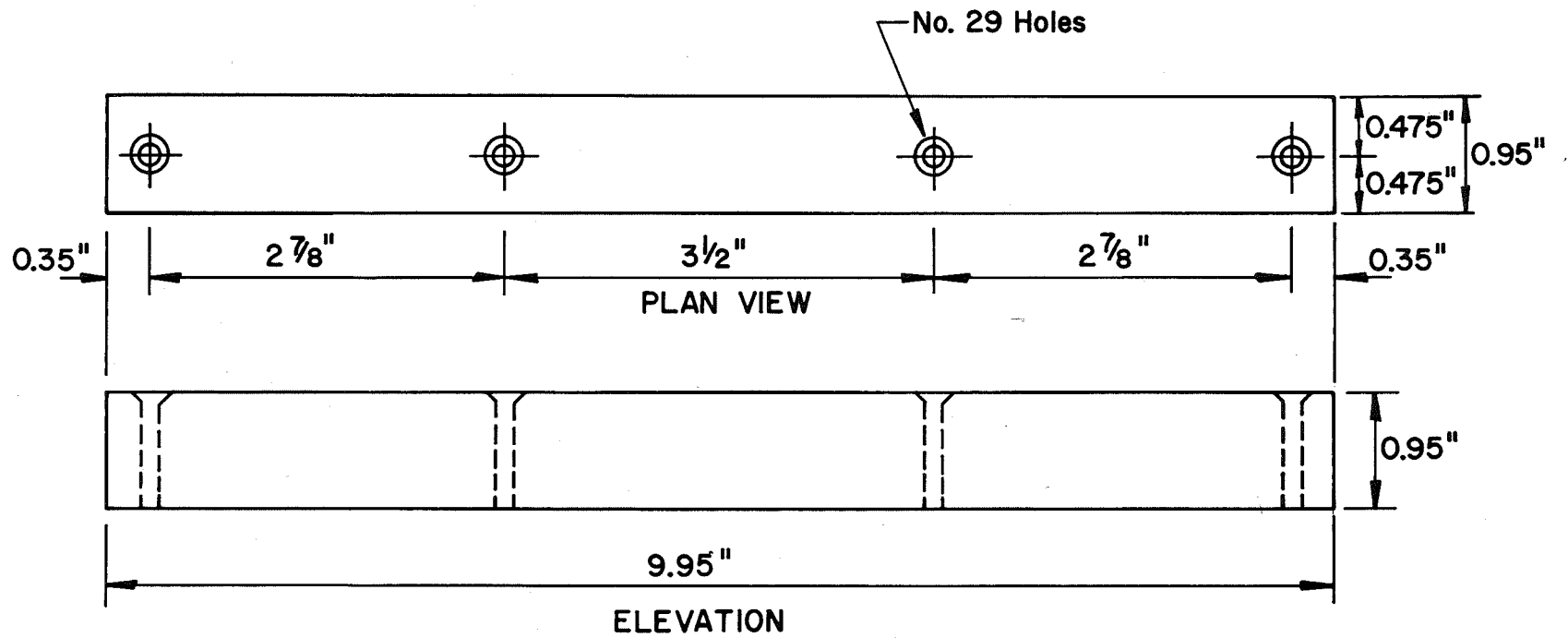
Fig. 17   Parapet Piece
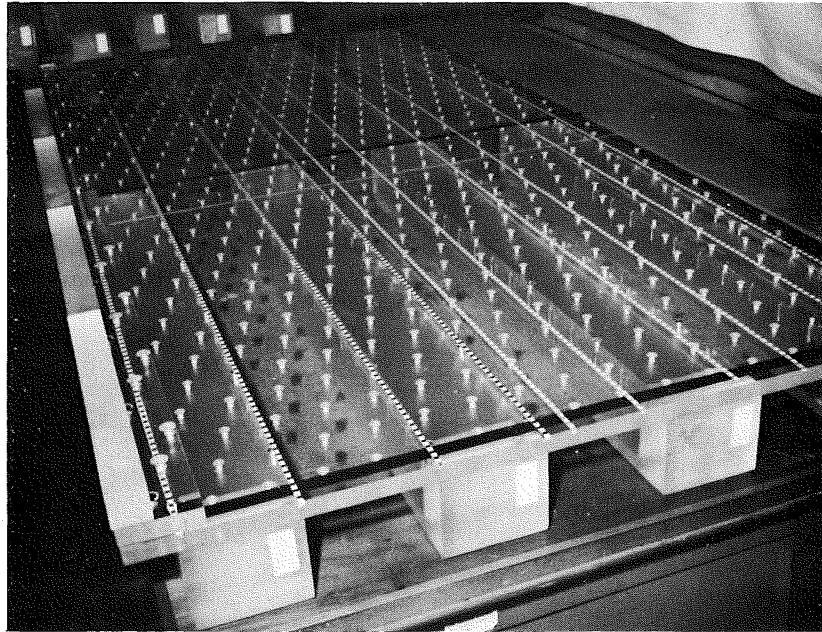
Fig. 18    Interchangeable Specimen Elements
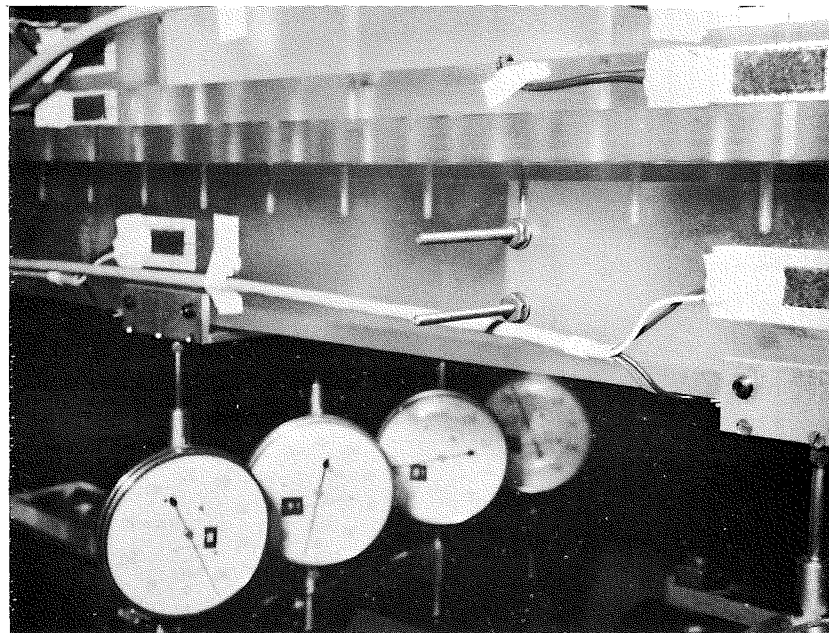


Fig. 19    Instrumentation at Midspan
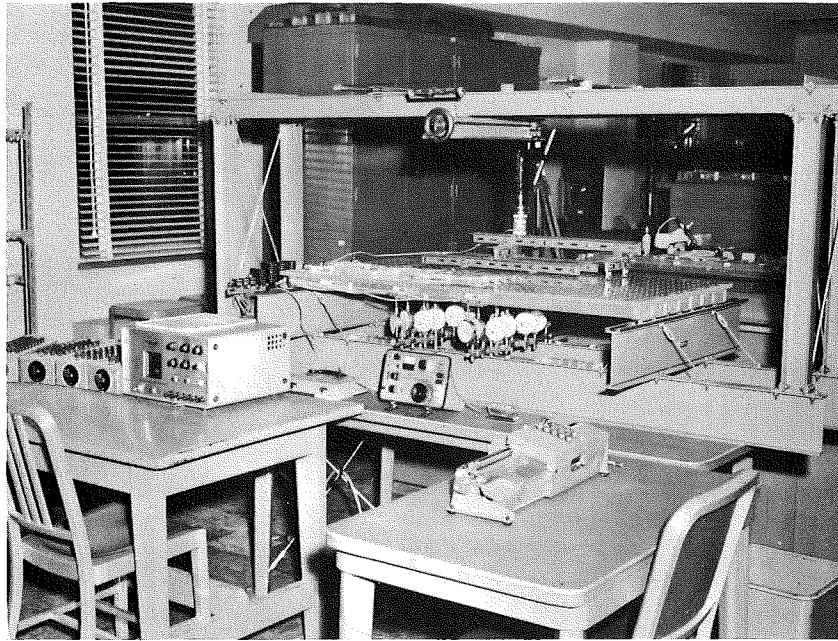
Fig. 20 General View of the Test Setup
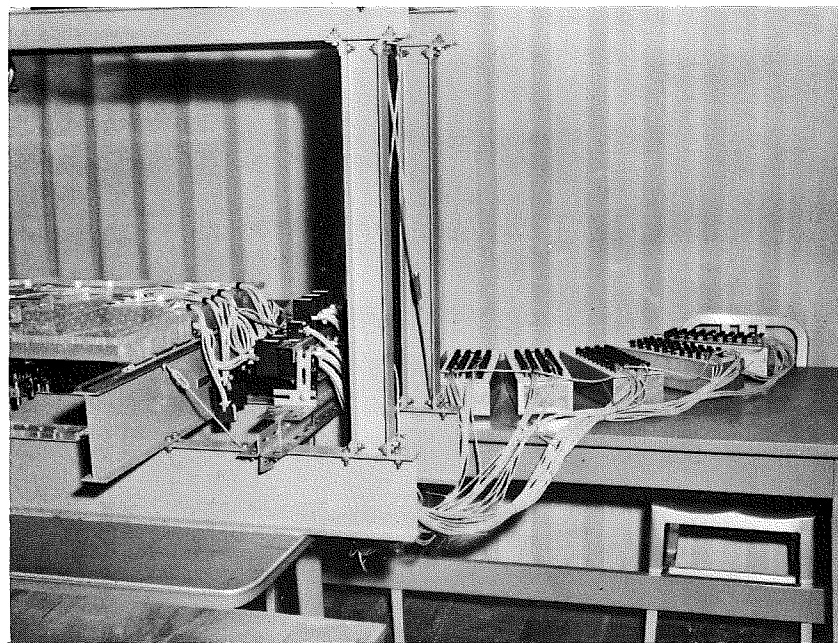


Fig. 21 Wiring from Connectors to Switching Boxes

Model Al and Prototype

Models Bl, B2, B3, and B4

Models B5, B6, B7, and B8

Models B9, BlO, Bll, and Bl2

Model Bl3

Model Bl4
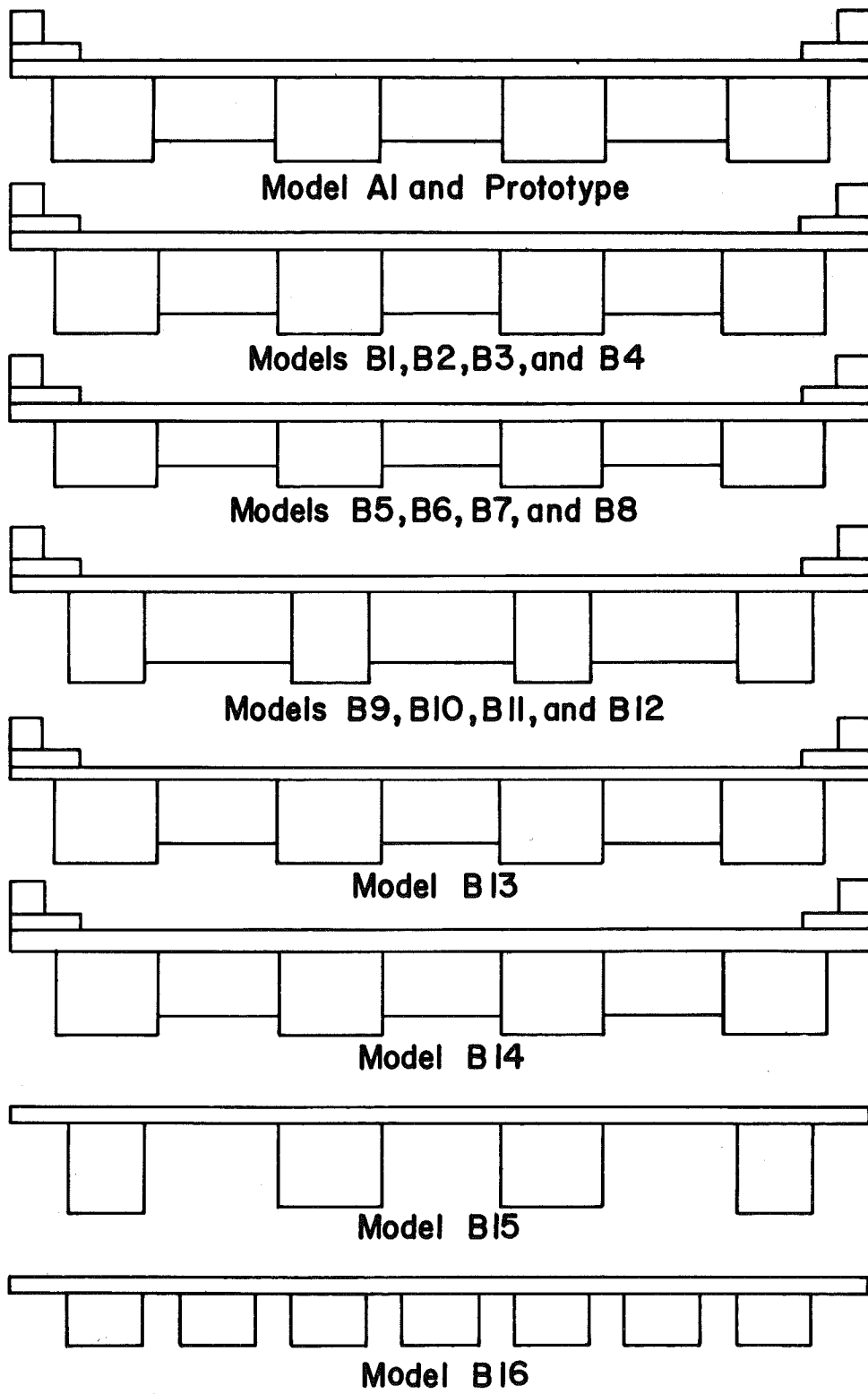
Model Bl5

Model Bl6

Fig. 22 Basic Cross-Sections Tested
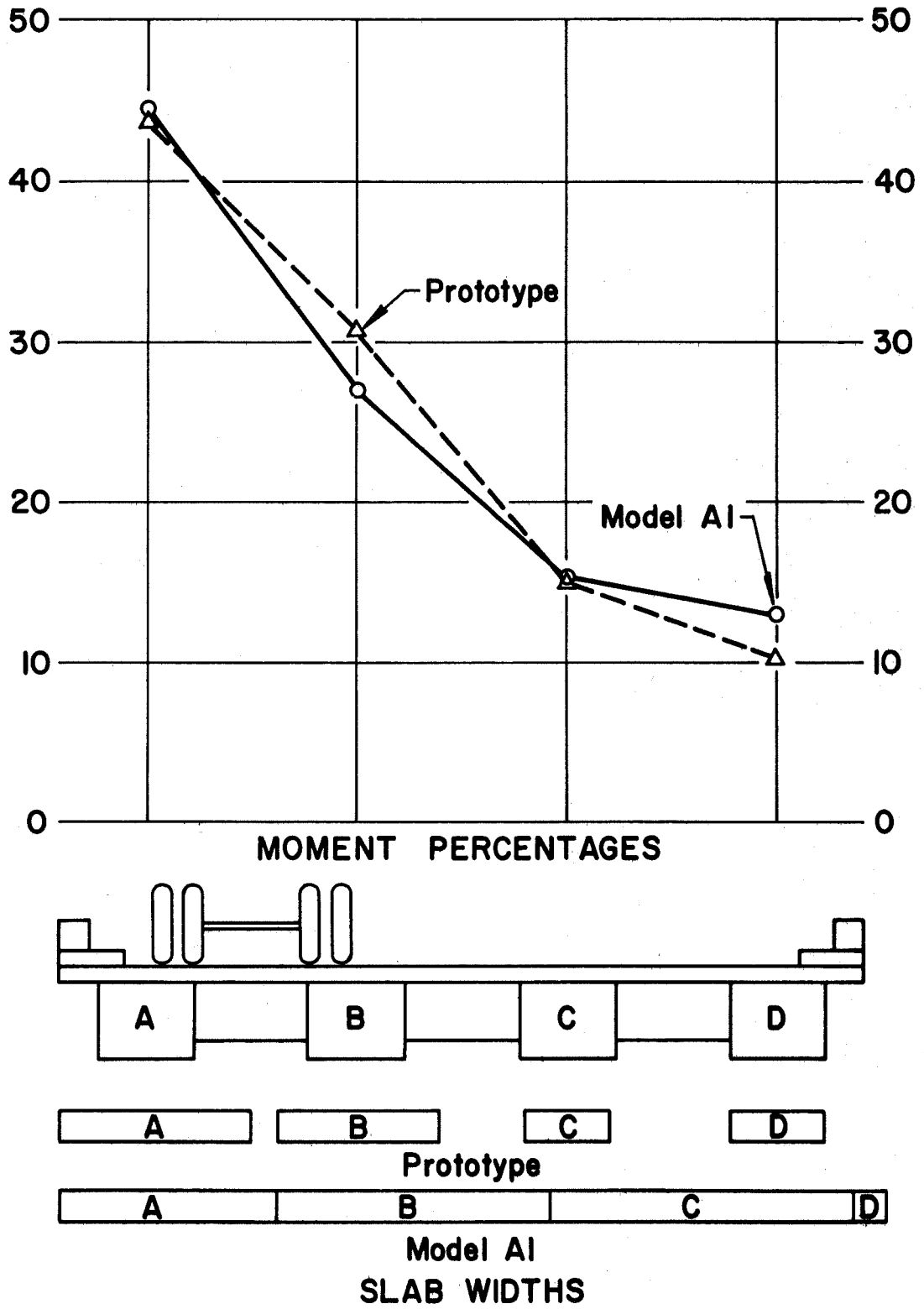
Fig. 23  Prototype and Model Al, Lane 1
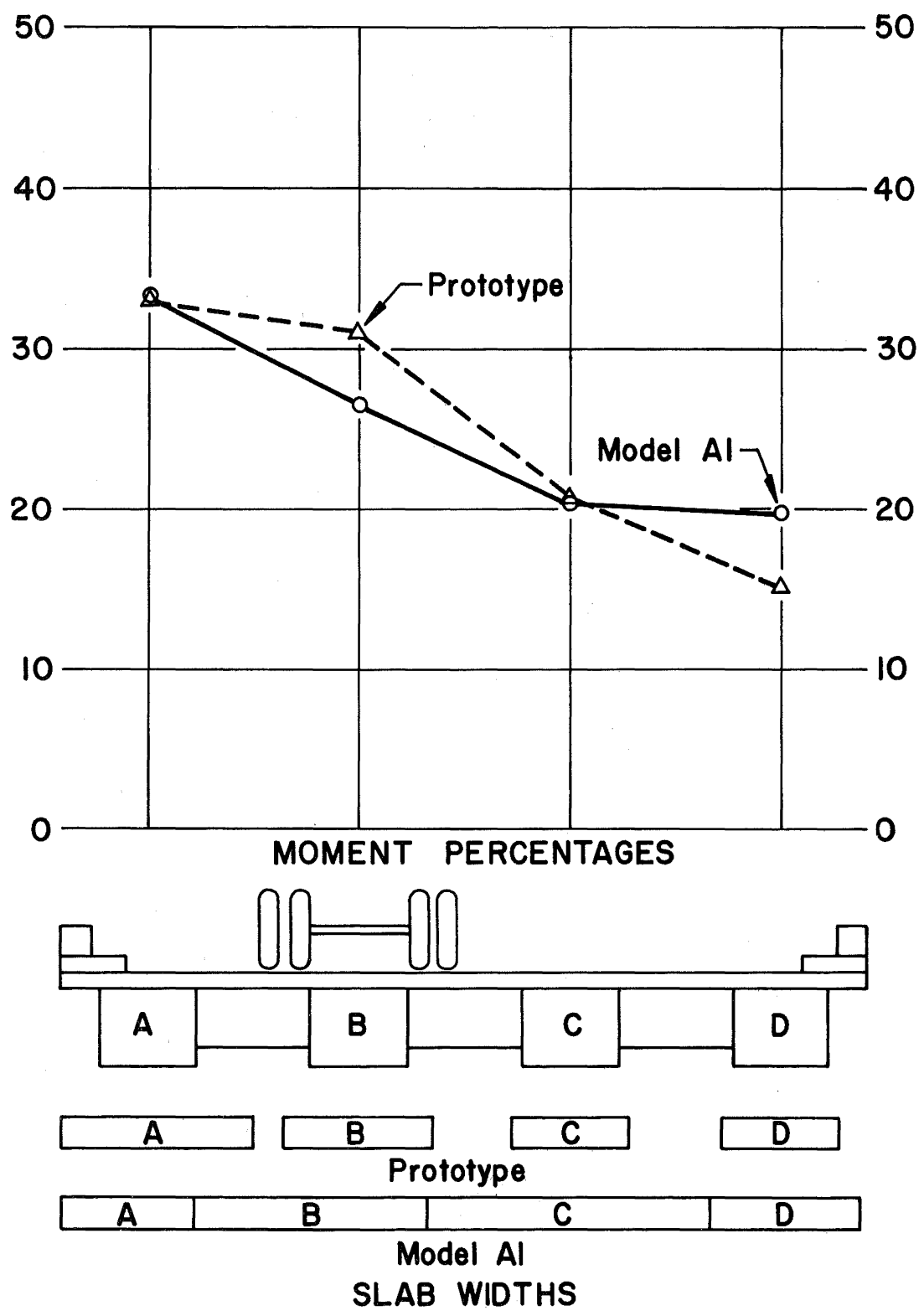
Fig. 24  Prototype and Model Al, Lane 2
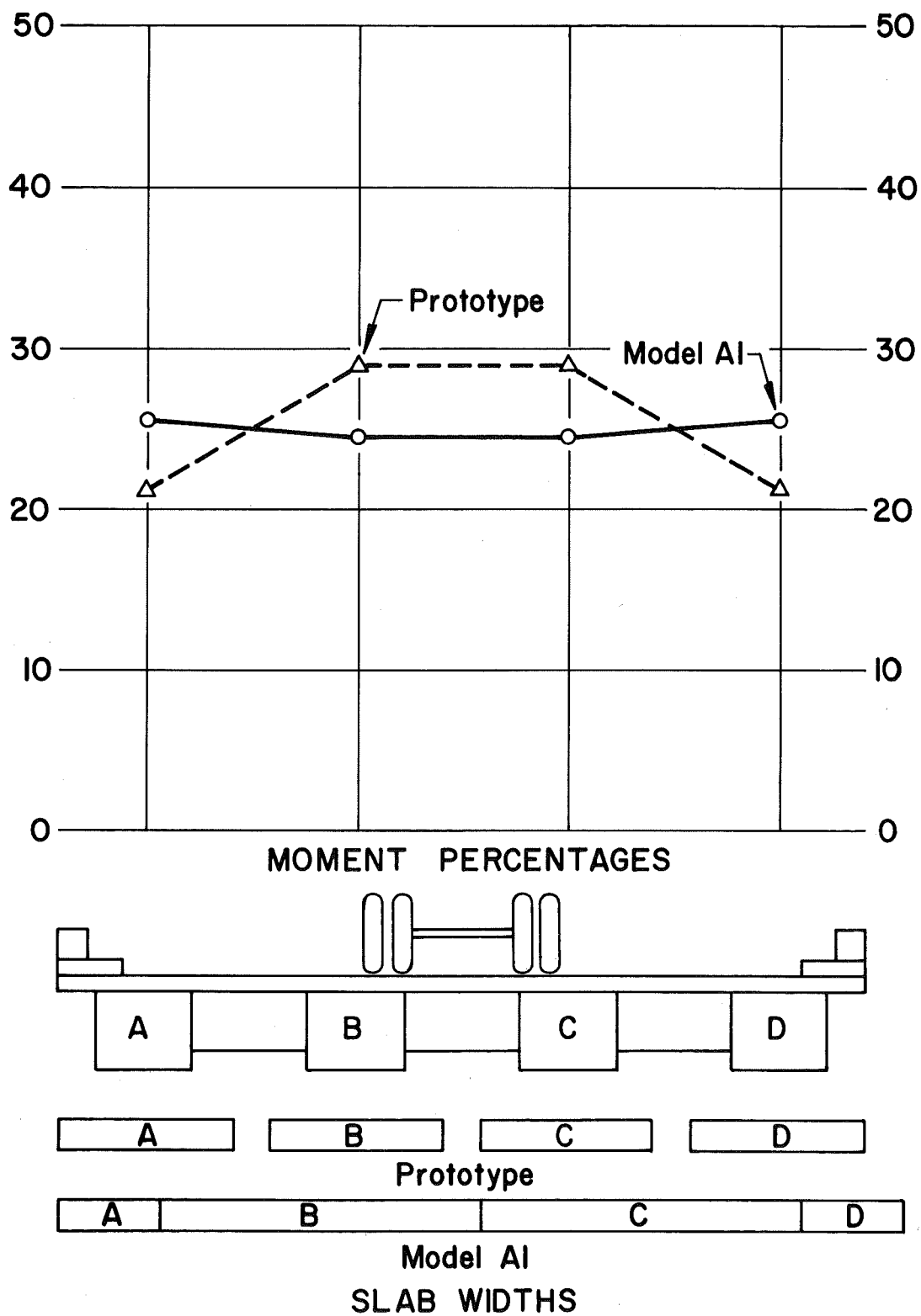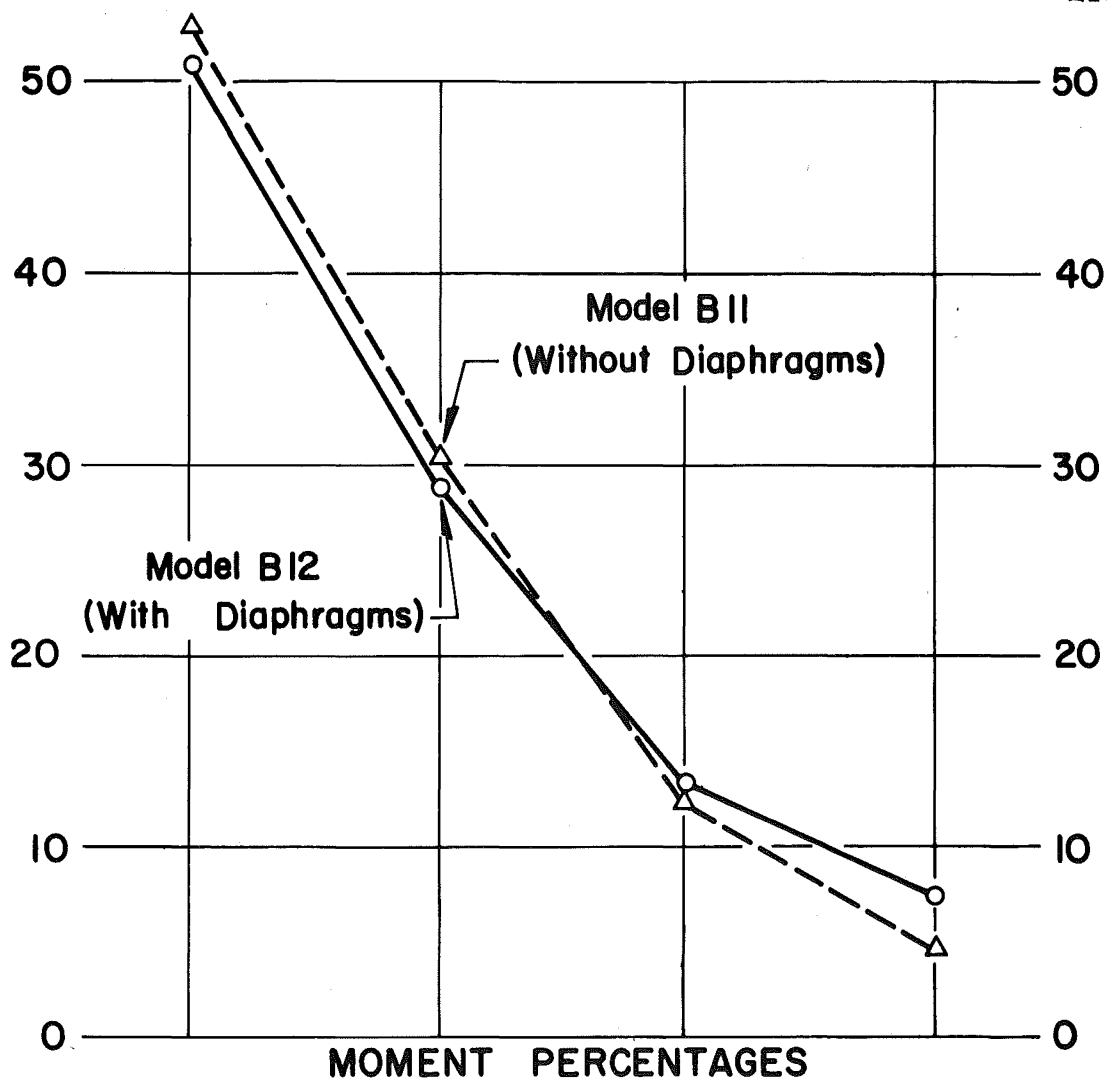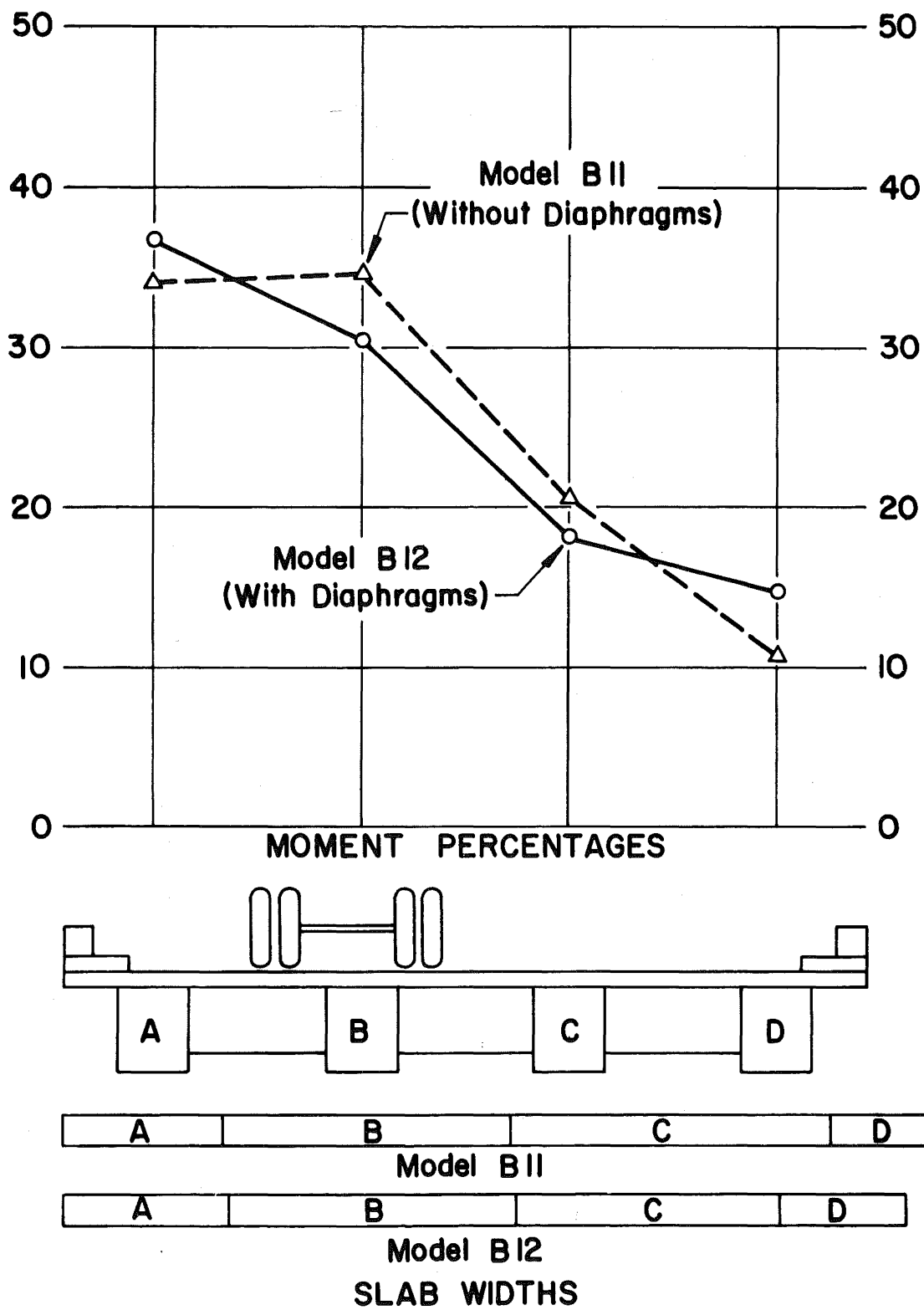
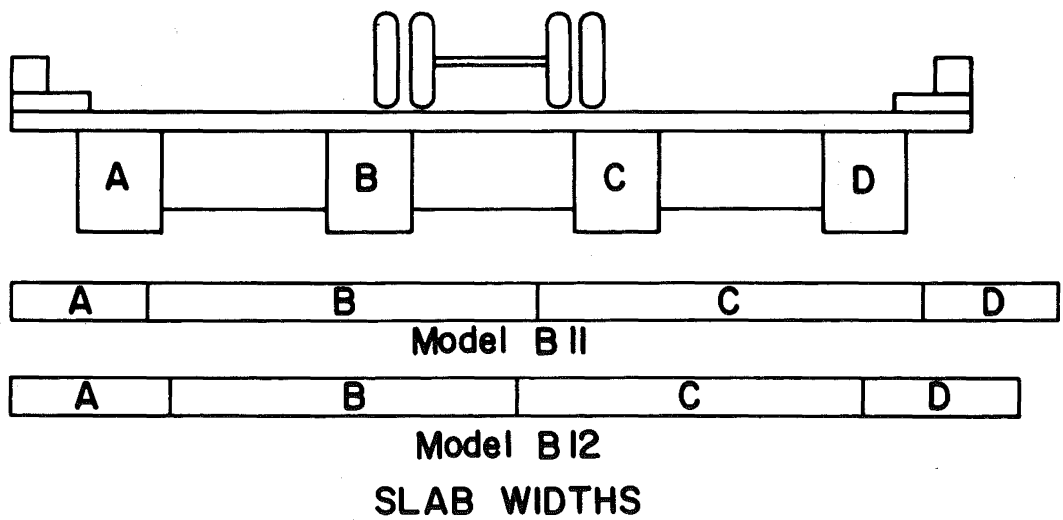Fig. 25    Prototype and Model Al, Lane 3
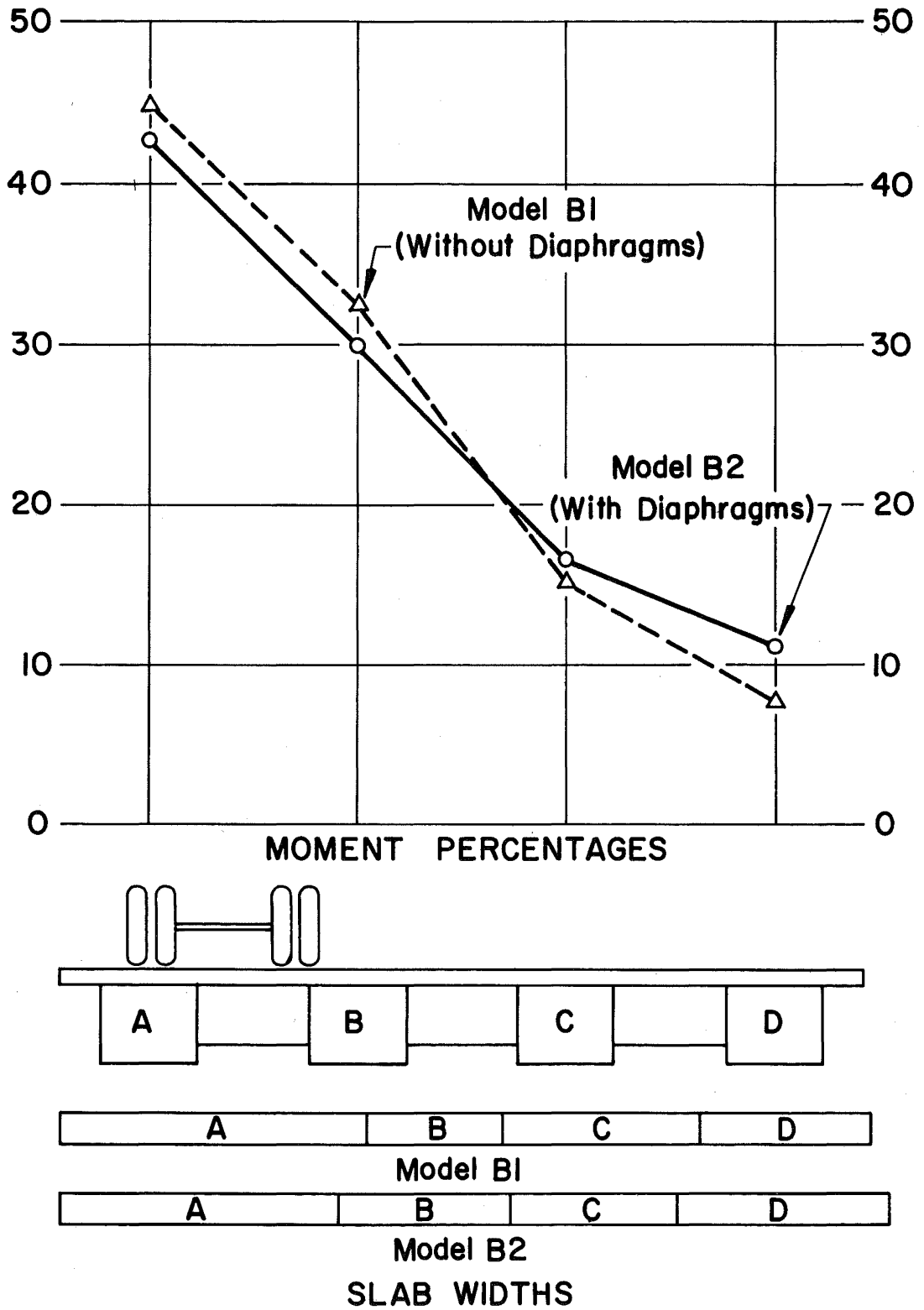
Fig. 26   Model B1 and Model B2, Lane 1
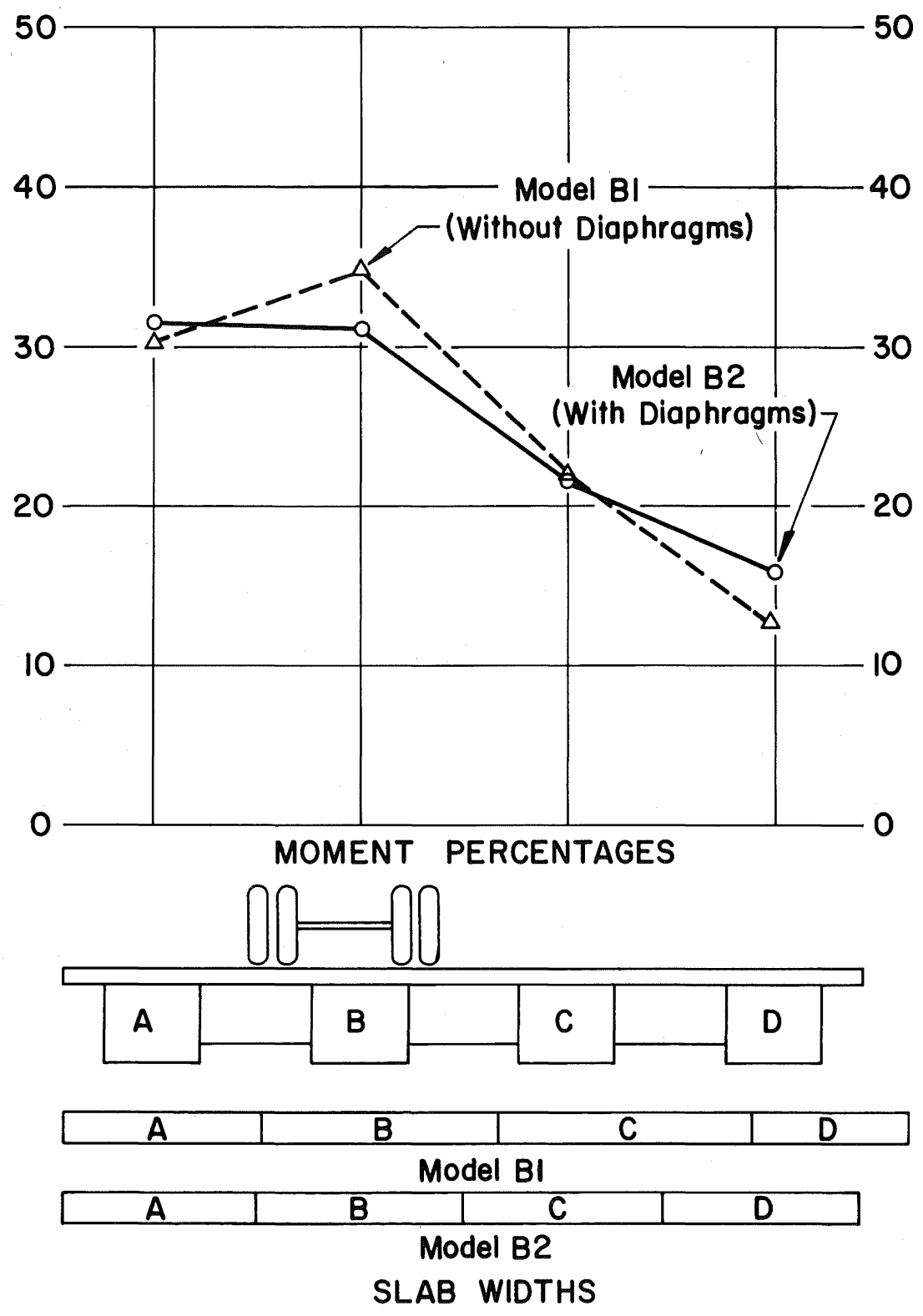
Fig. 27   Model B1 and Model B2, Lane 2
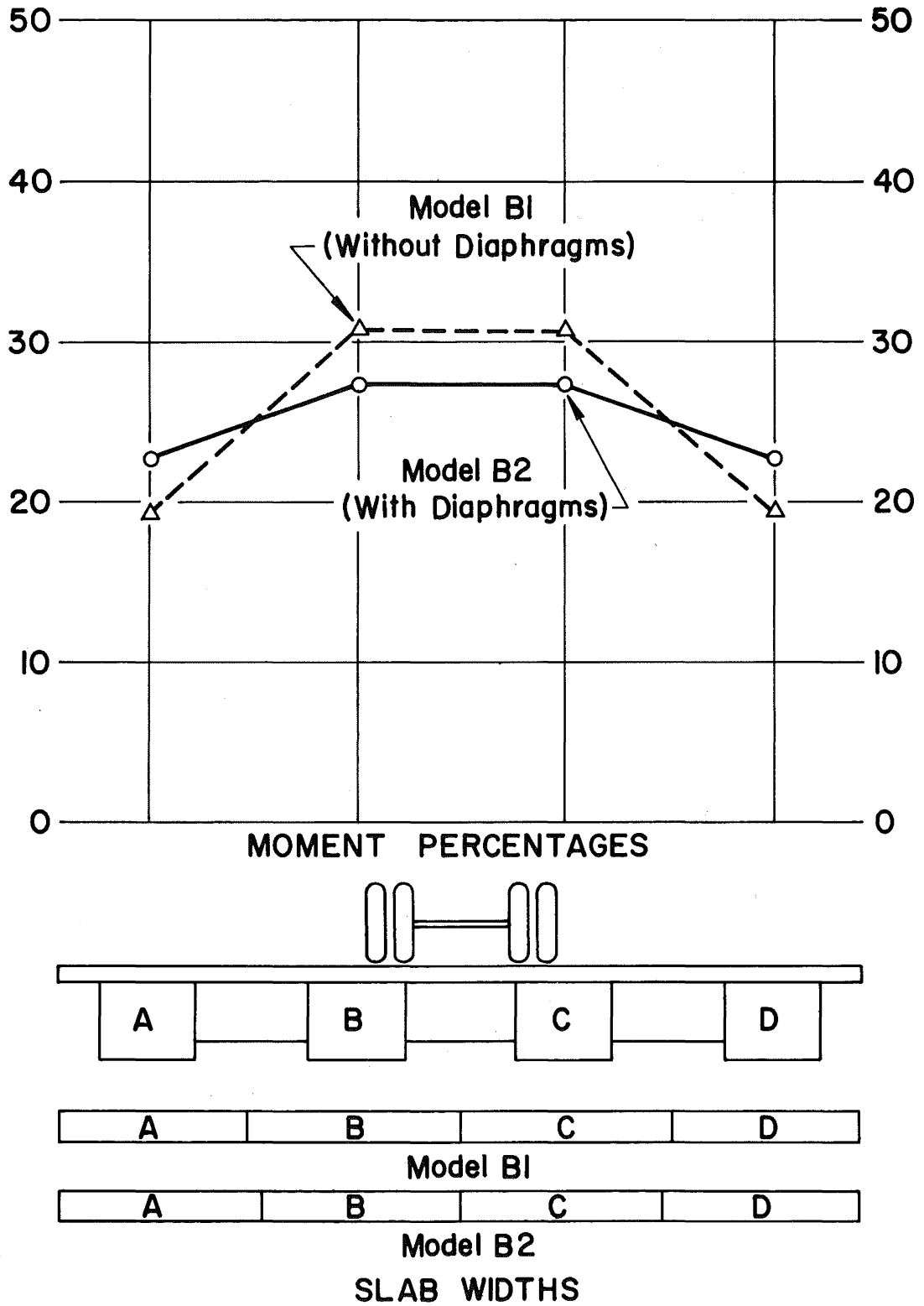
Fig. 28  Model B1 and Model B2, Lane 3
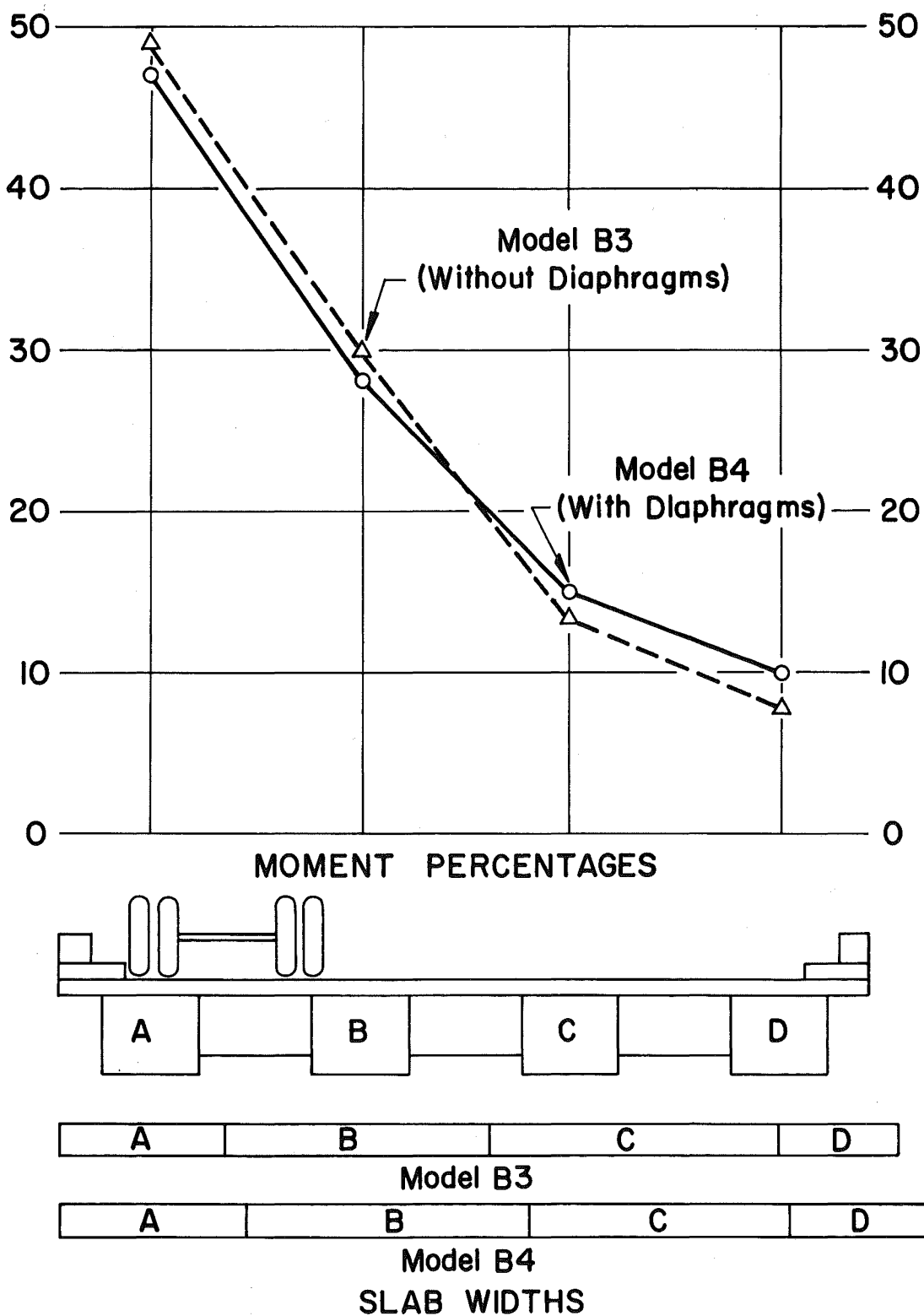
Fig. 29   Model B3 and Model B4, Lane 1
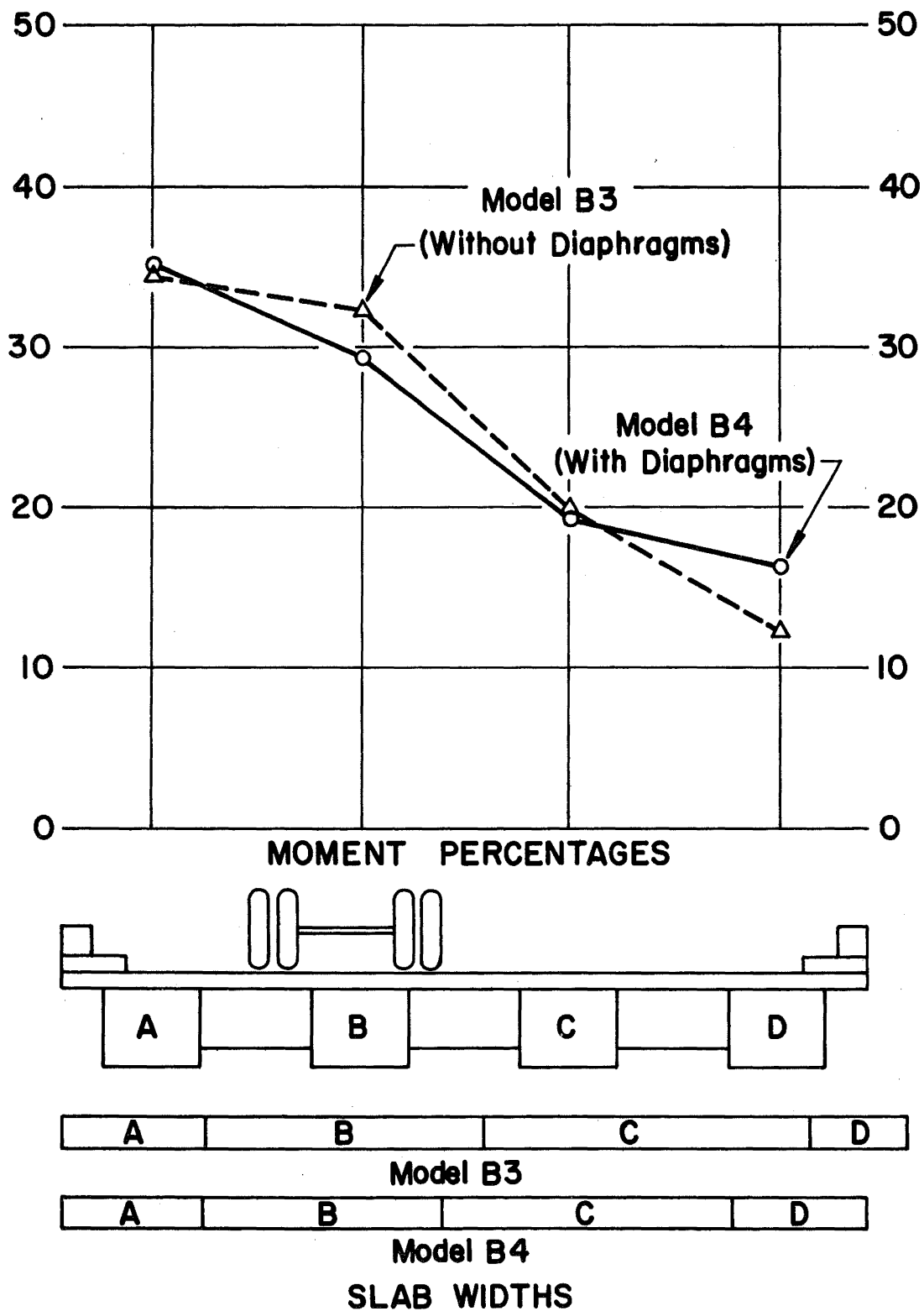
Fig. 30  Model B3 and Model B4, Lane 2
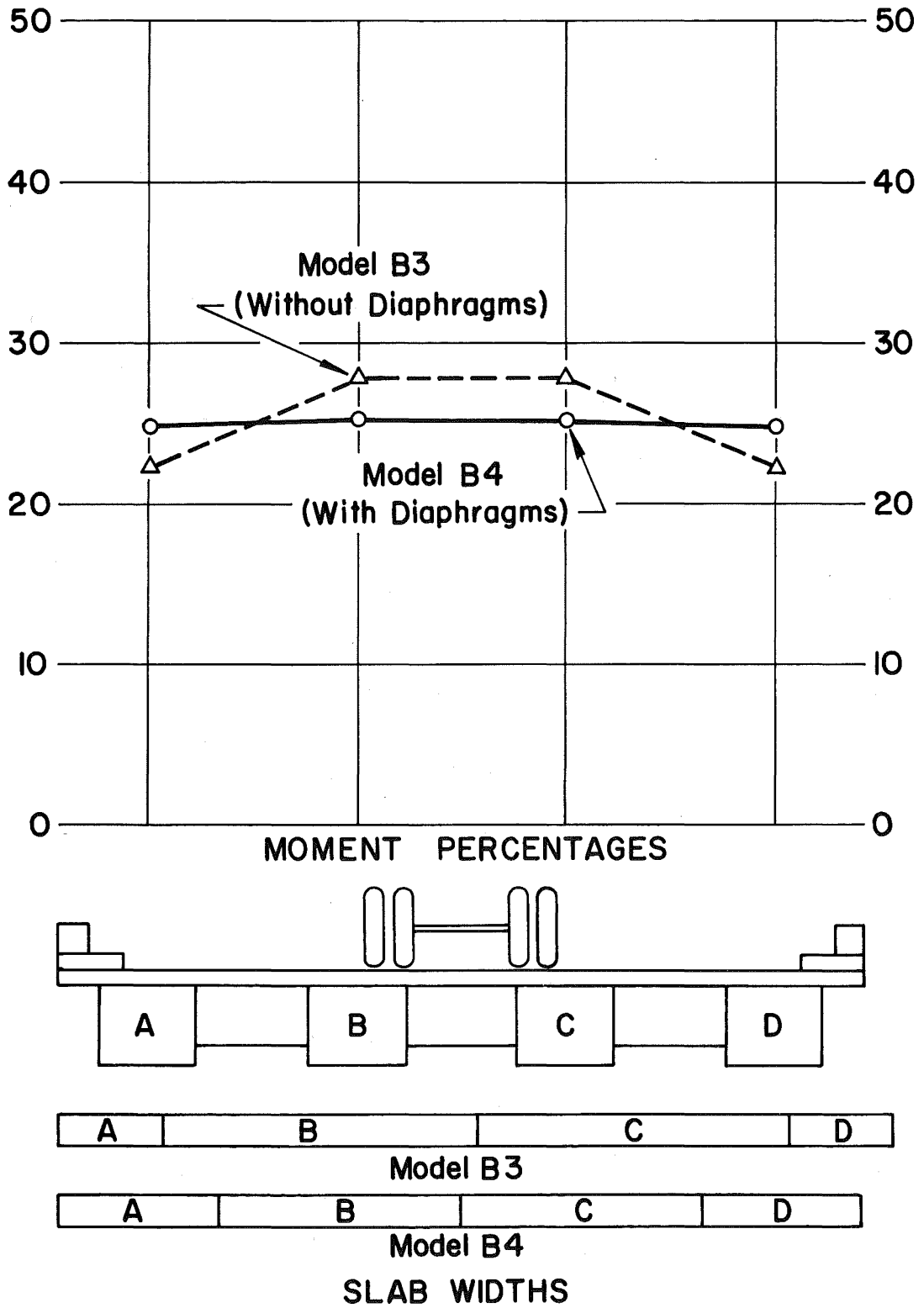
Fig. 31    Model B3 and Model B4, Lane 3
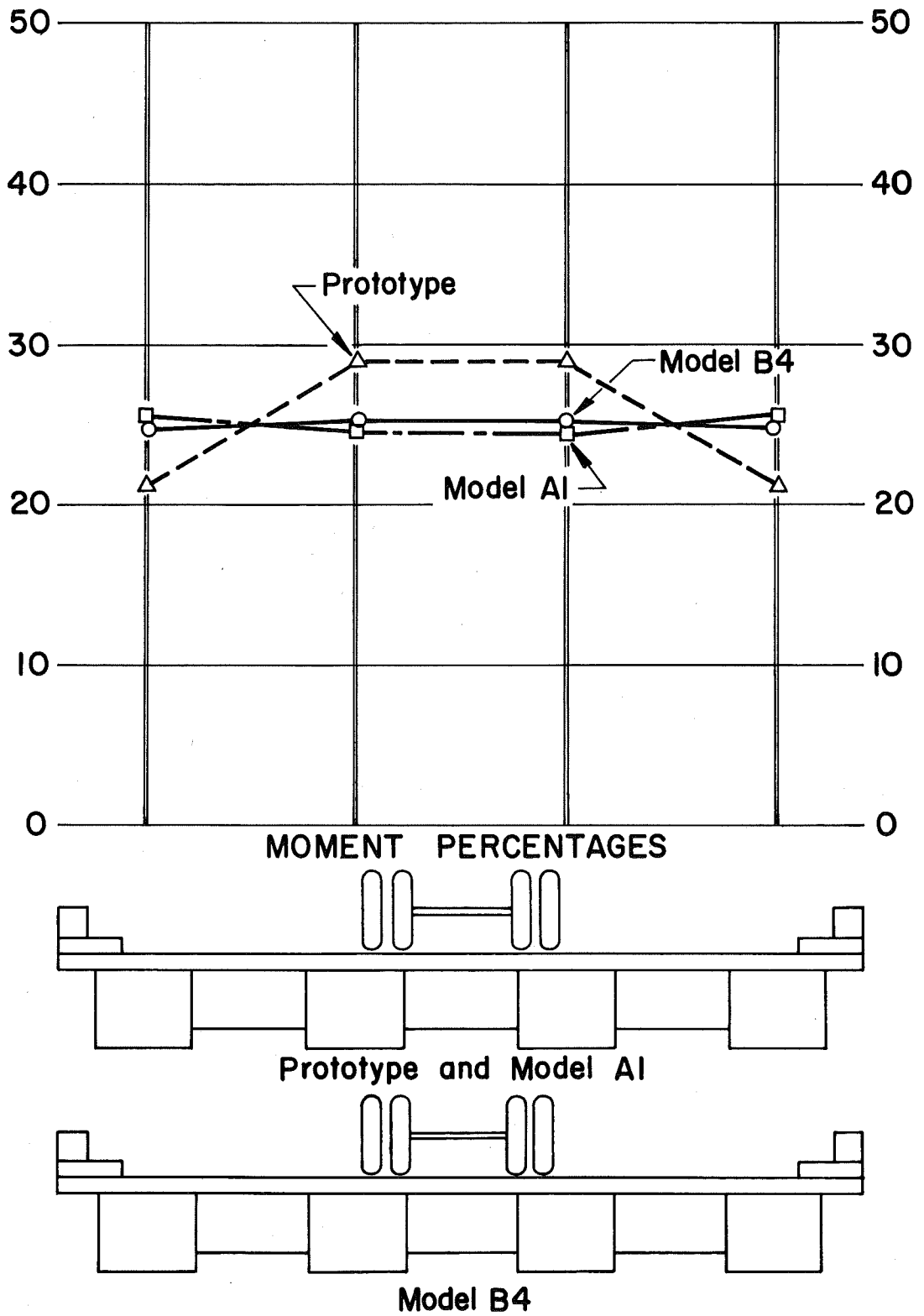
Fig. 32    Prototype, Model A1, and Model B4, Lane 3
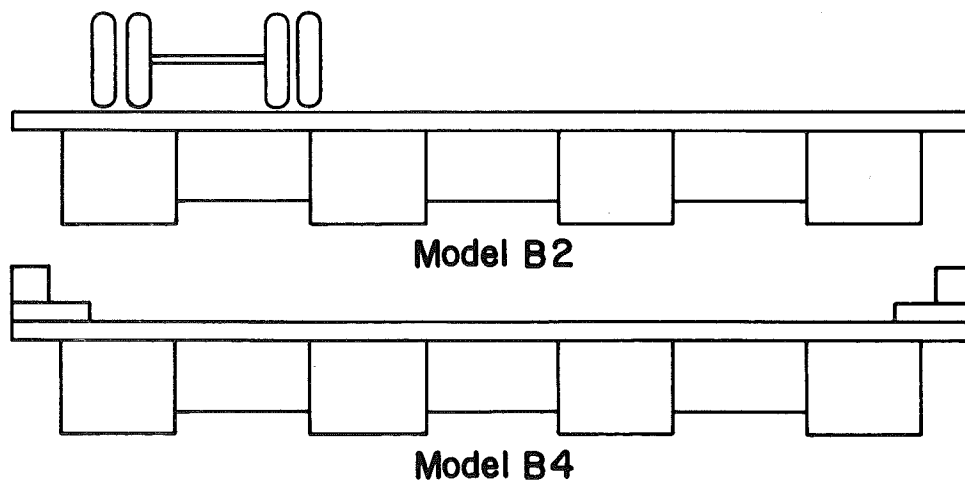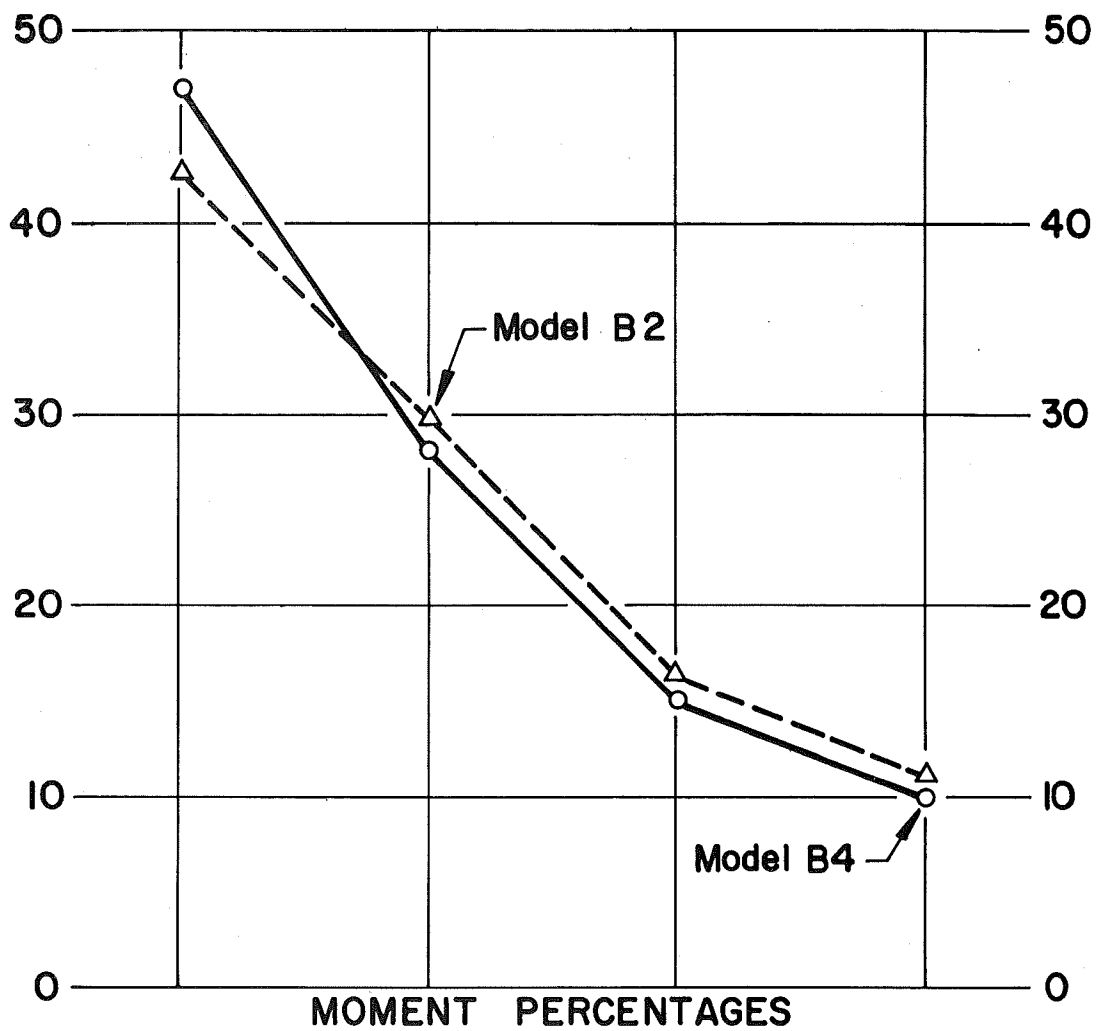
Fig. 33    Model B2 and Model B4, Lane 1
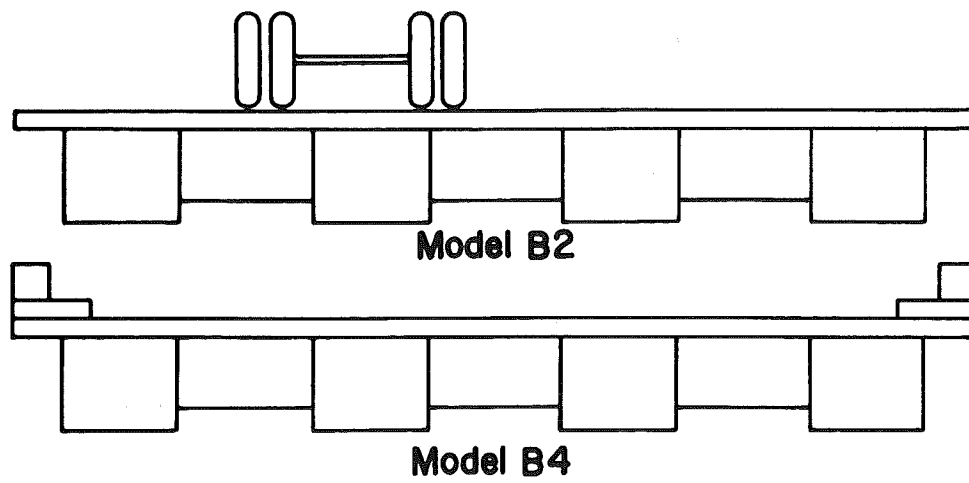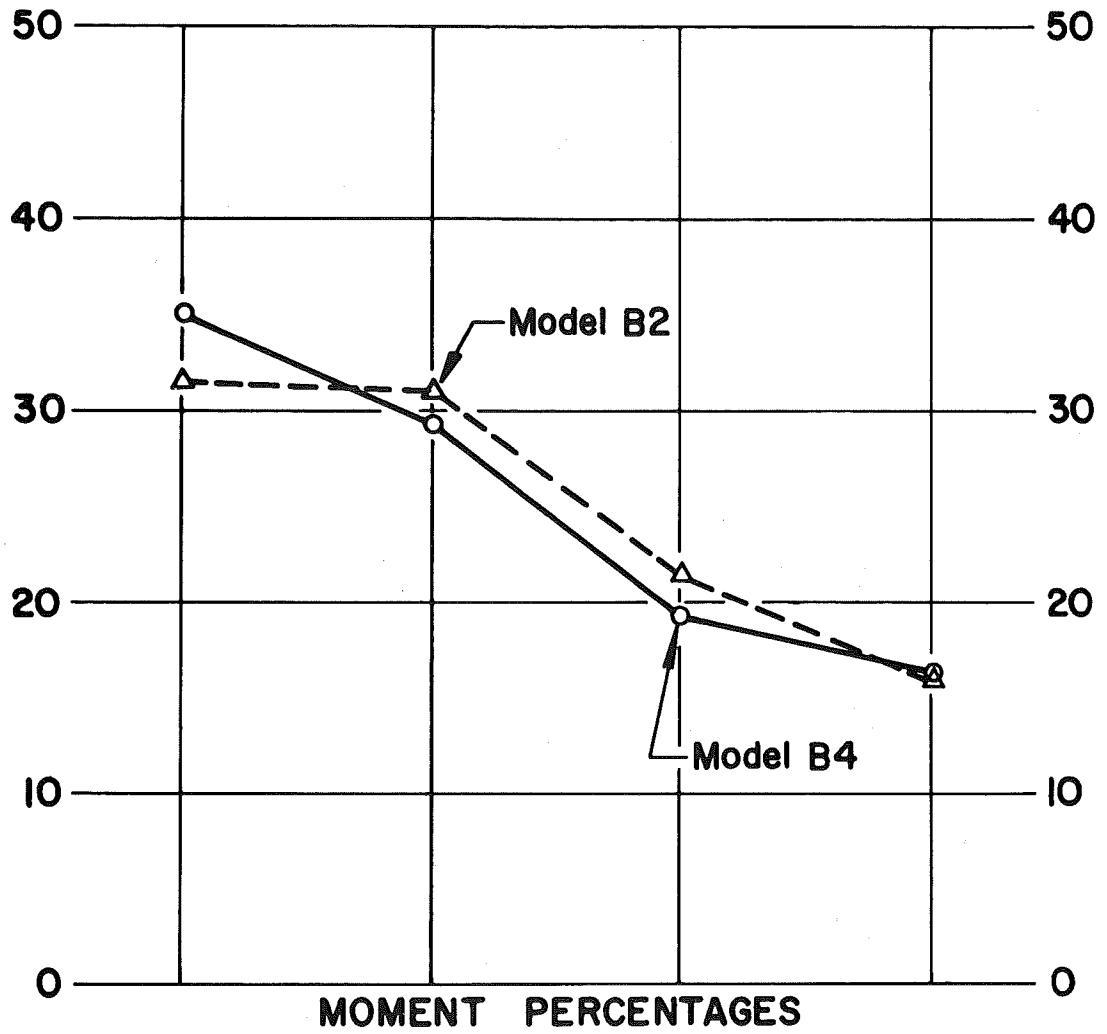
Fig. 34    Model B2 and Model B4, Lane 2
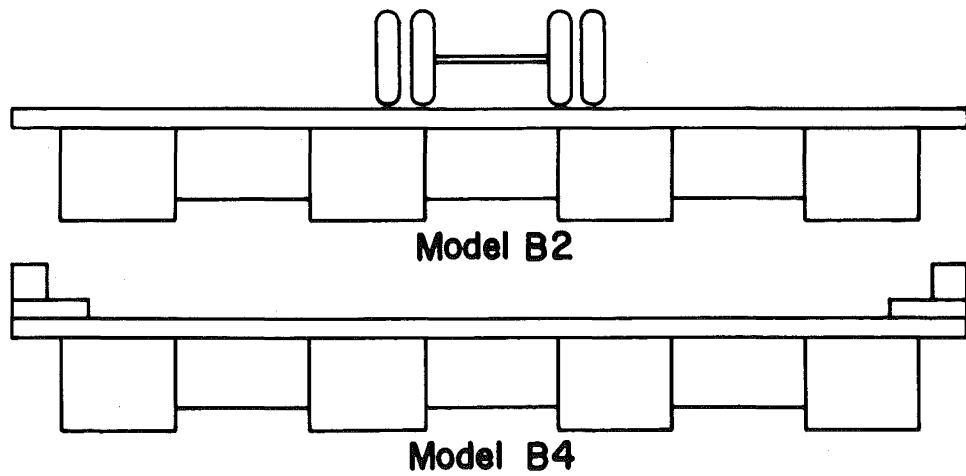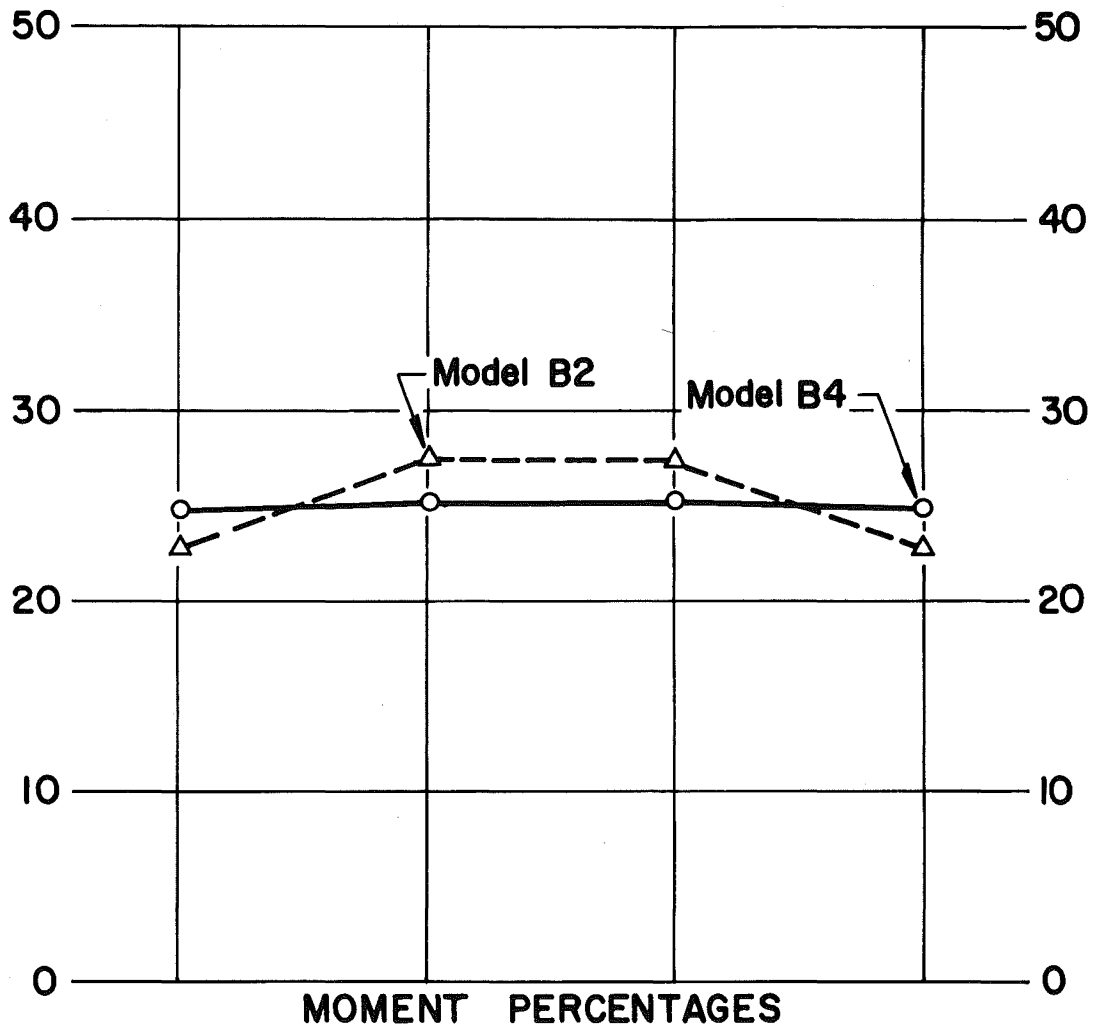
Fig. 35    Model B2 and Model B4, Lane 3
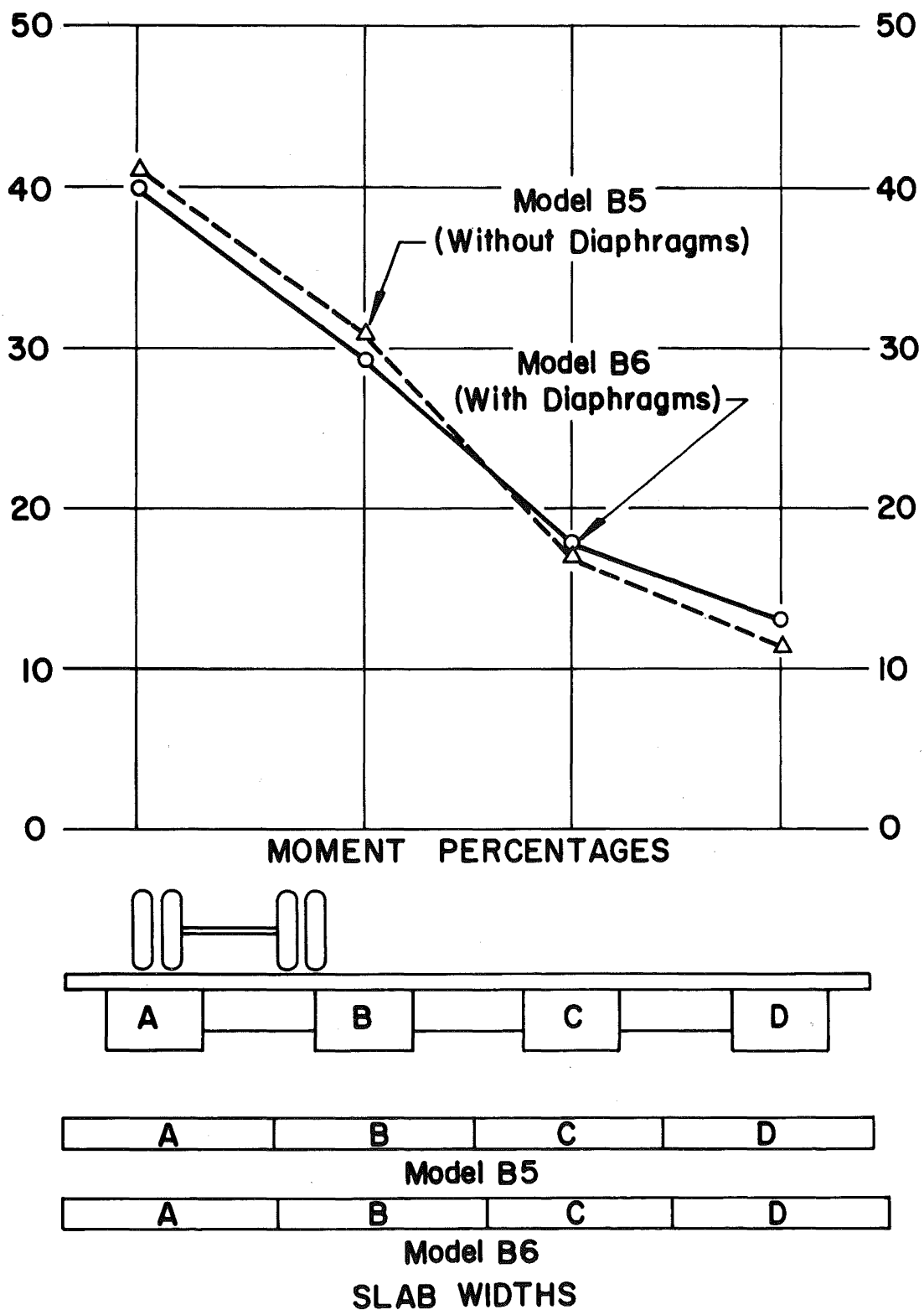
Fig. 36   Model B5 and Model B6, Lane 1
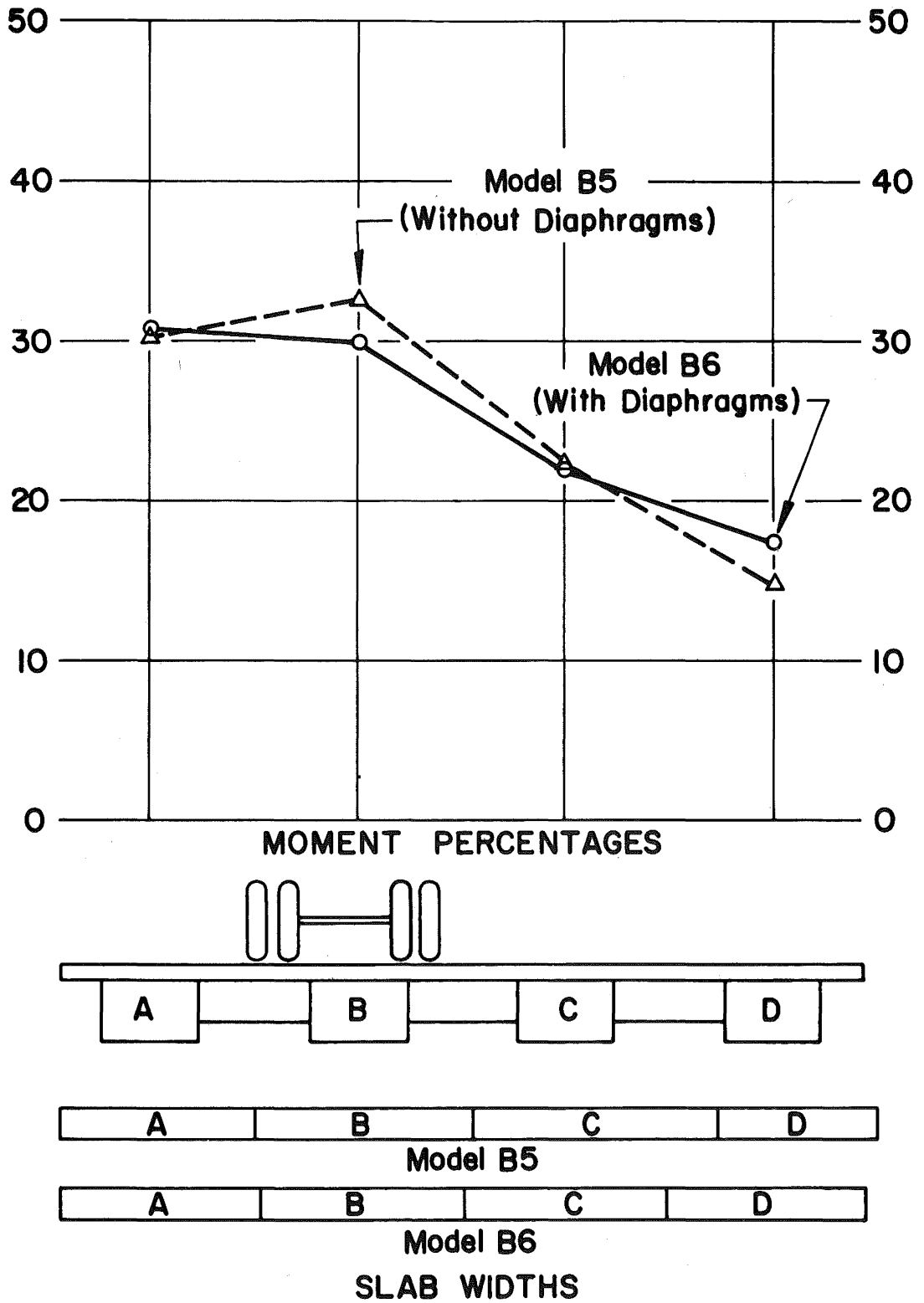
Fig. 37    Model B5 and Model B6, Lane 2
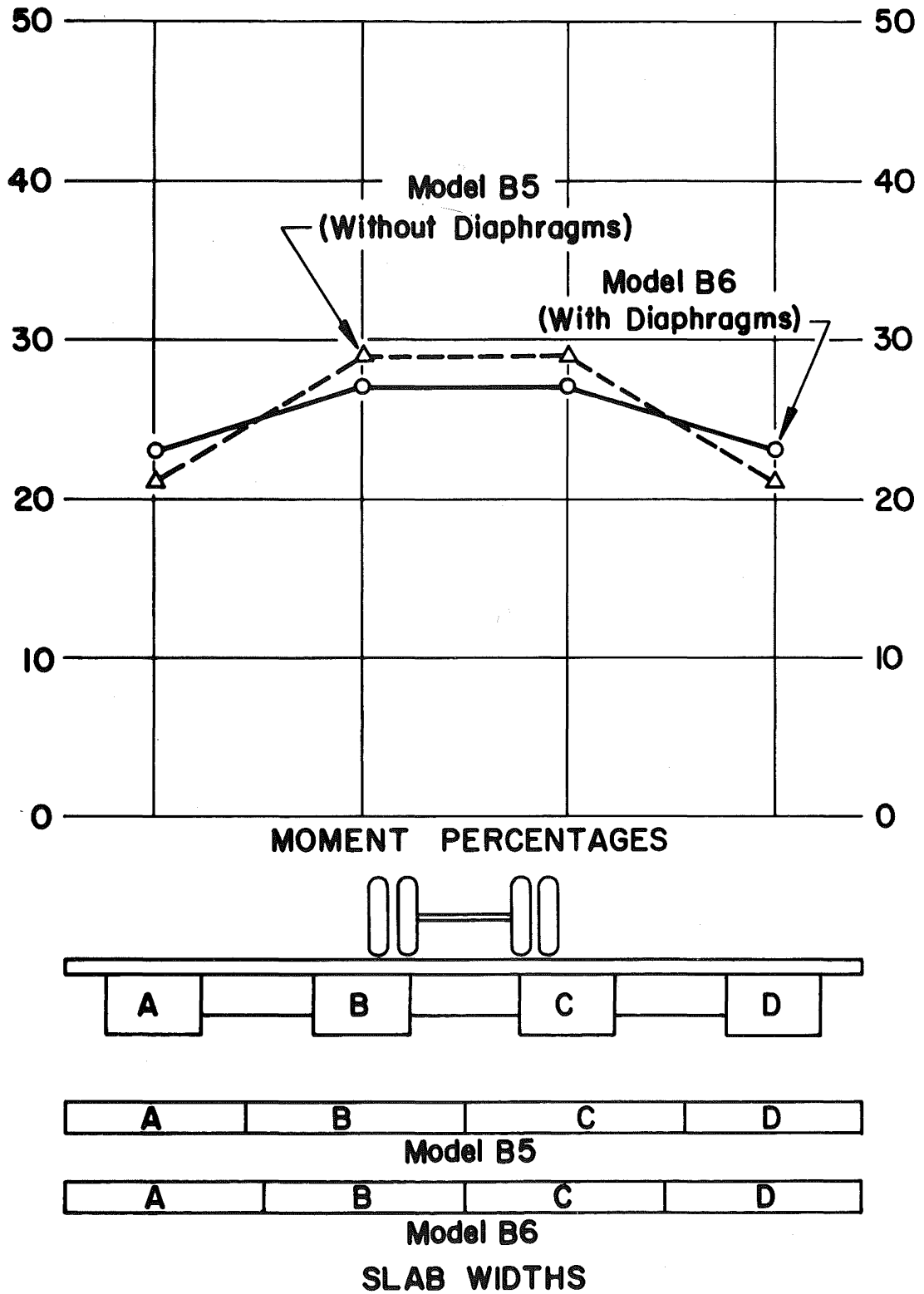
Fig. 38    Model B5 and Model B6, Lane 3
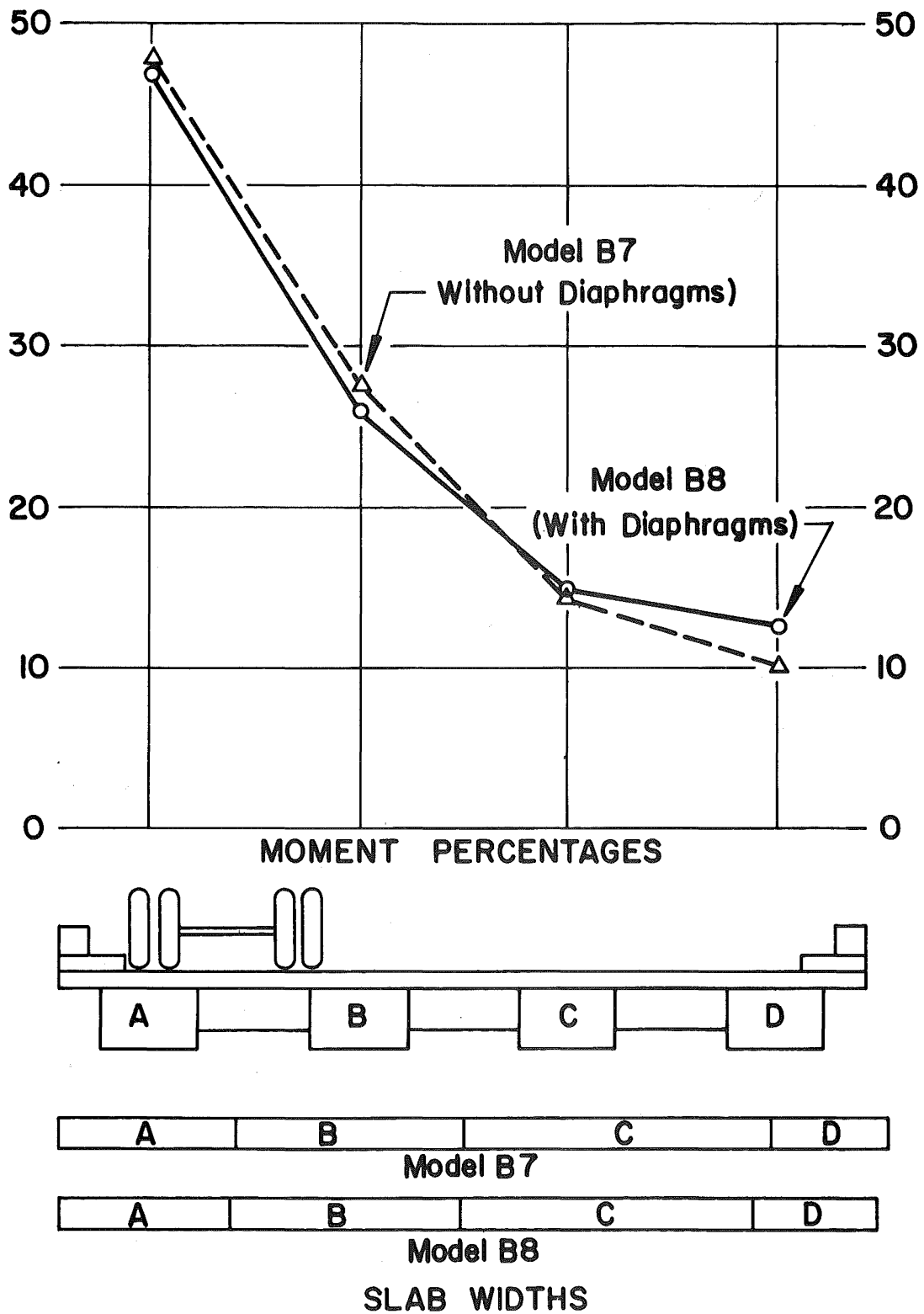
Fig. 39   Model B7 and Model B8, Lane 1
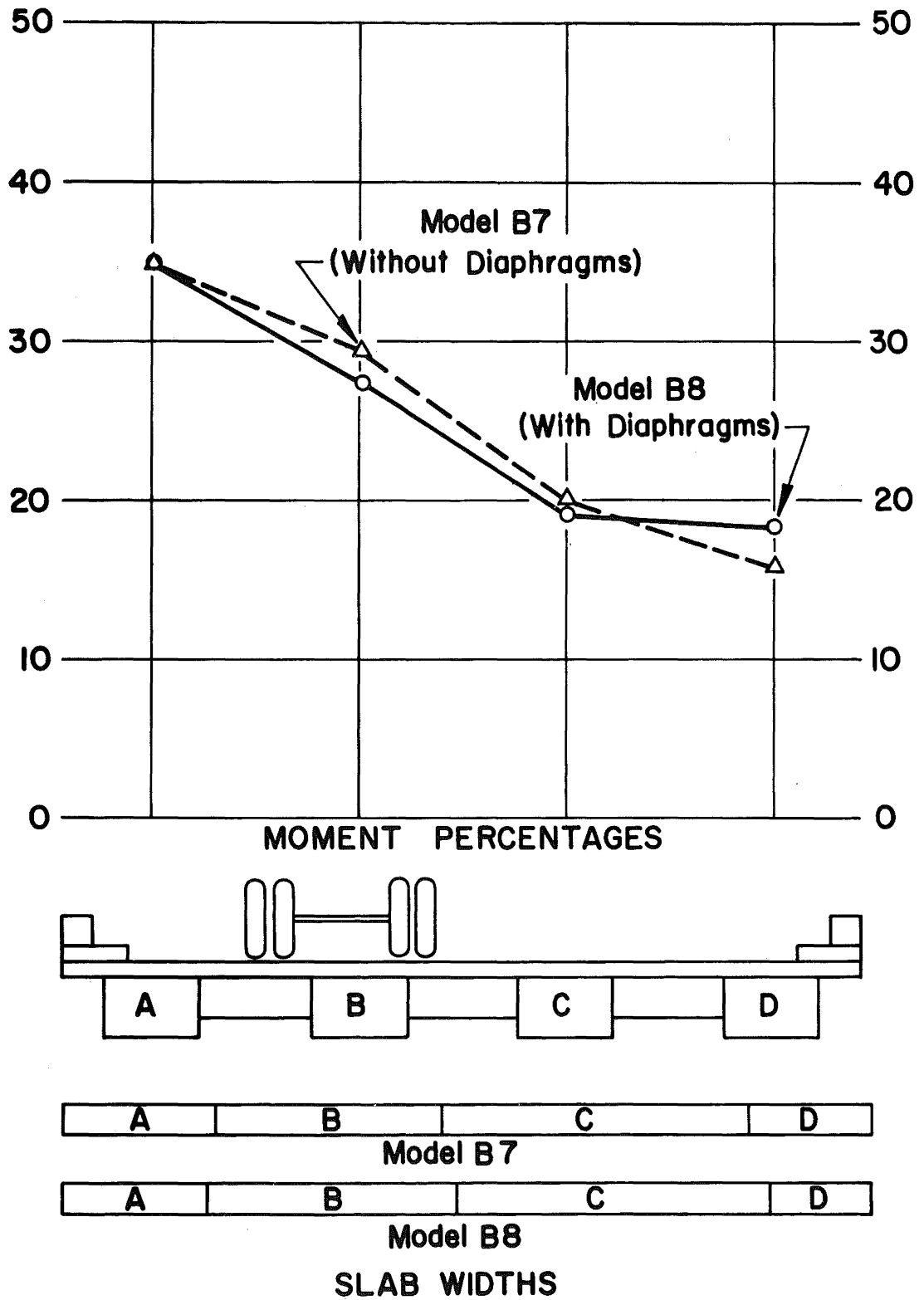
Fig. 40    Model B7 and Model B8, Lane 2
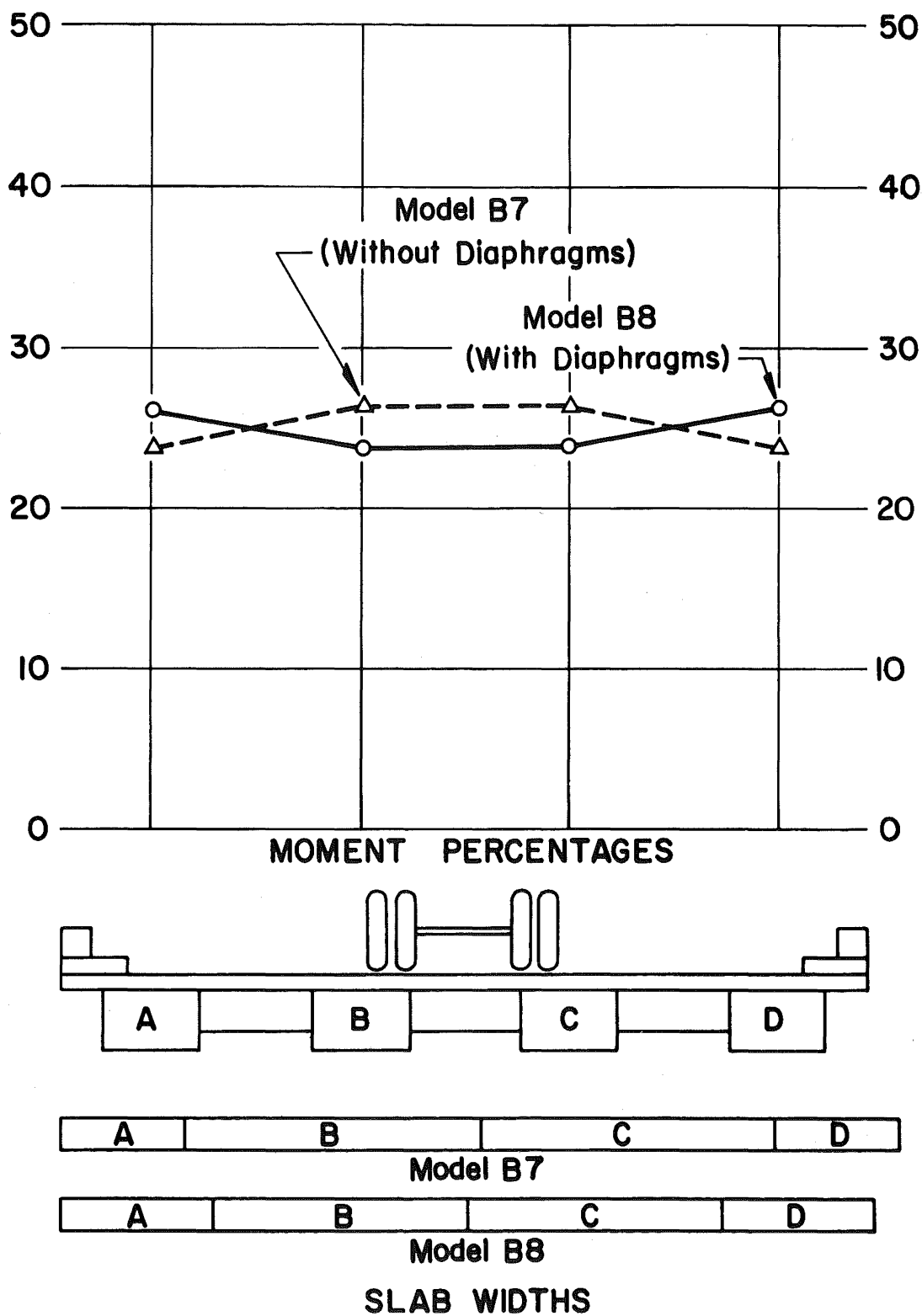
Fig. 41    Model B7 and Model B8, Lane 3
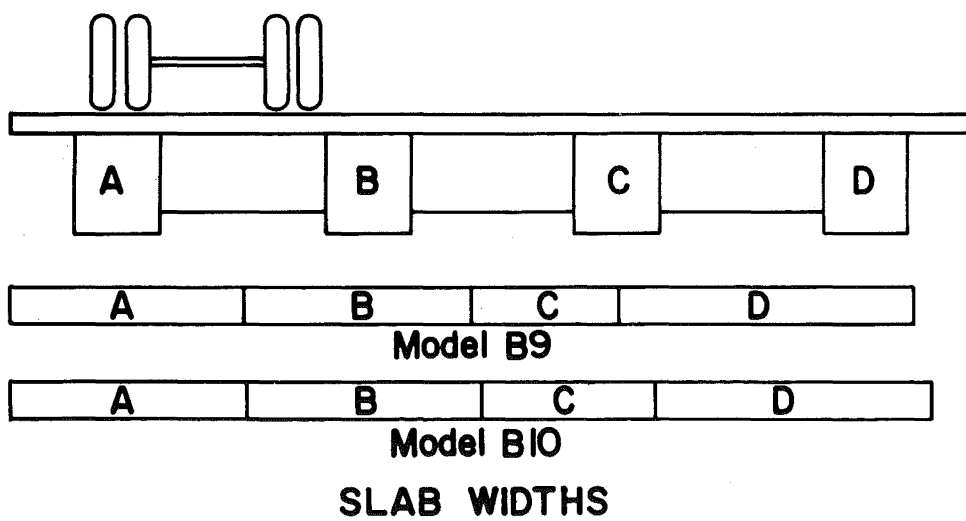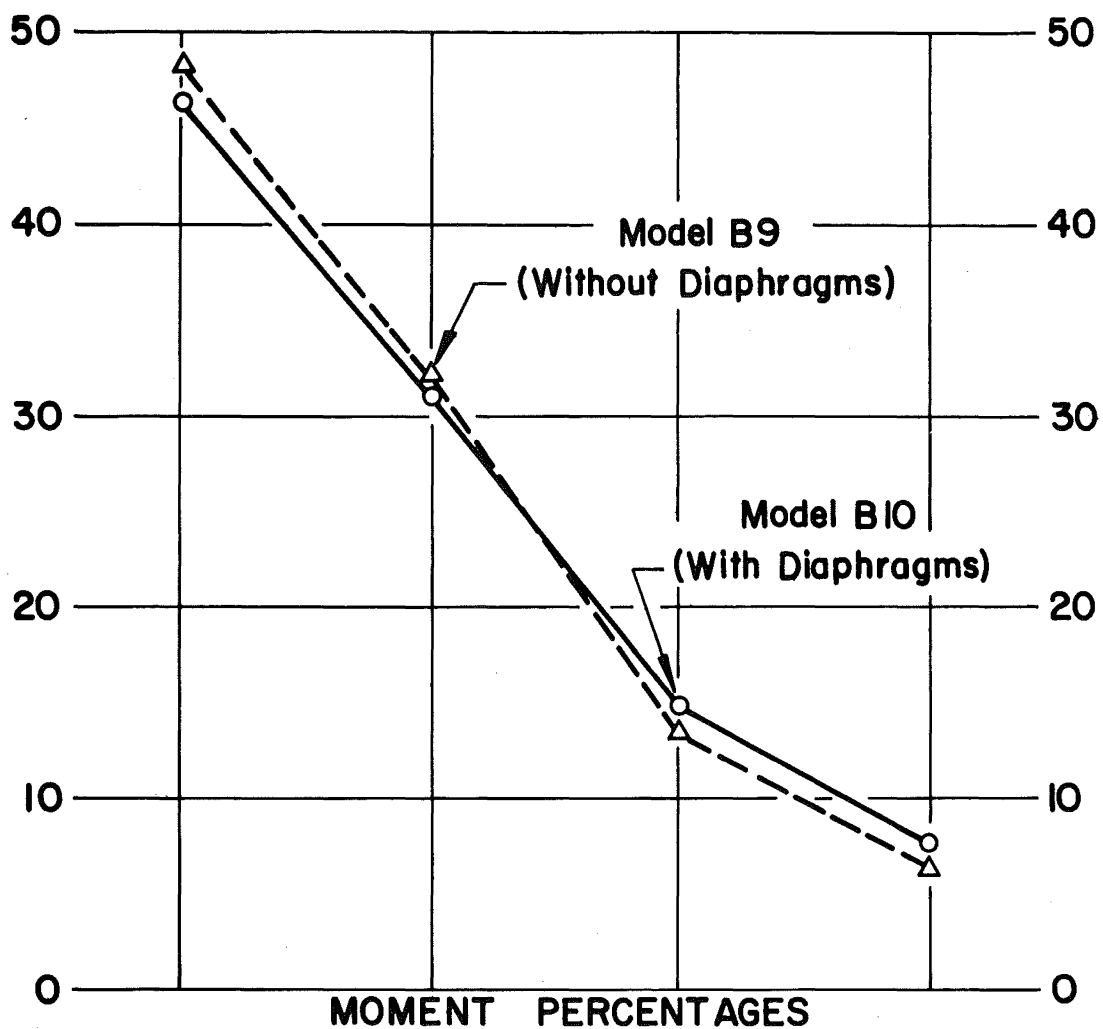
Fig. 42   Model B9 and Model B10, Lane 1
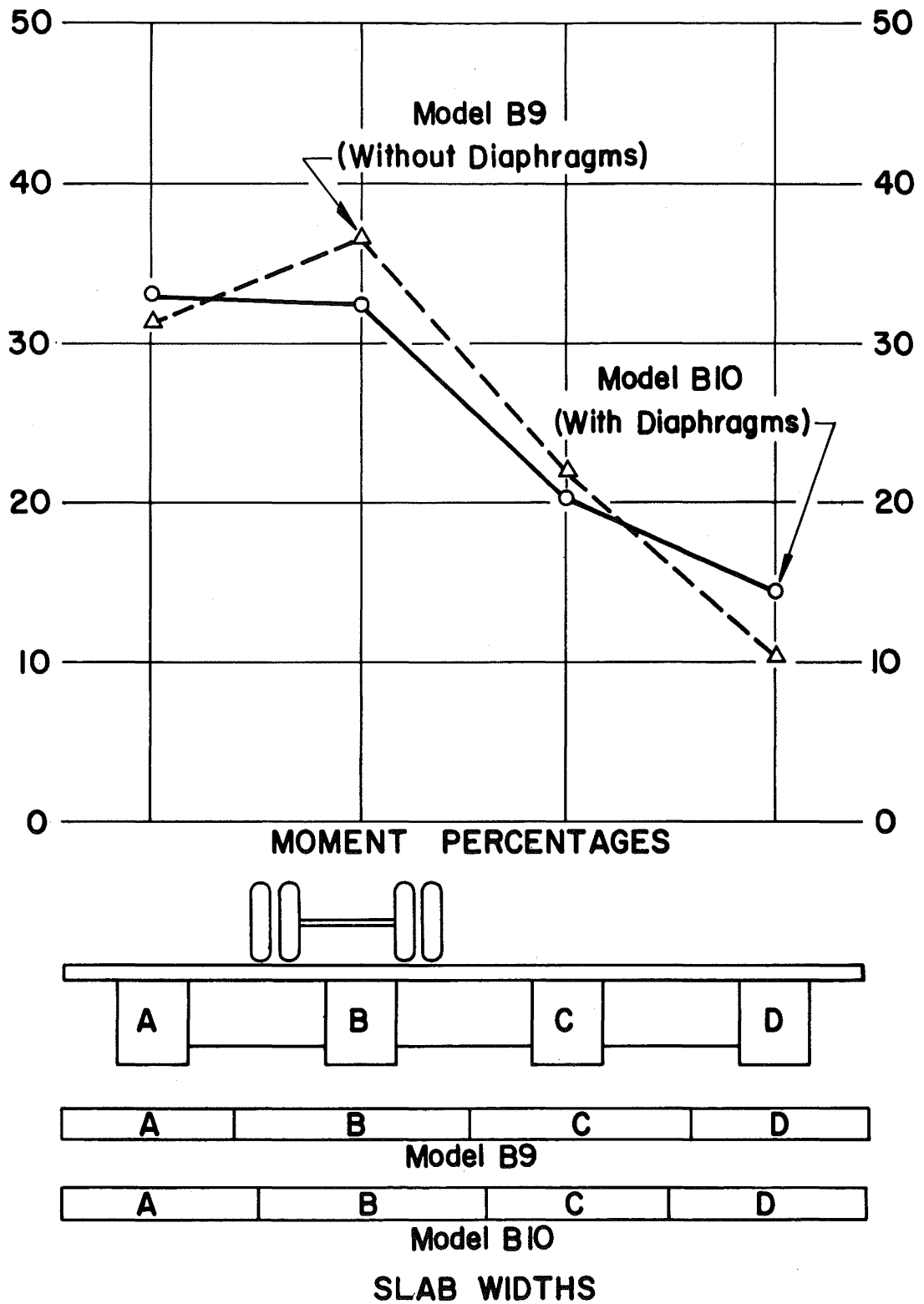
Fig. 43   Model B9 and Model B10, Lane 2
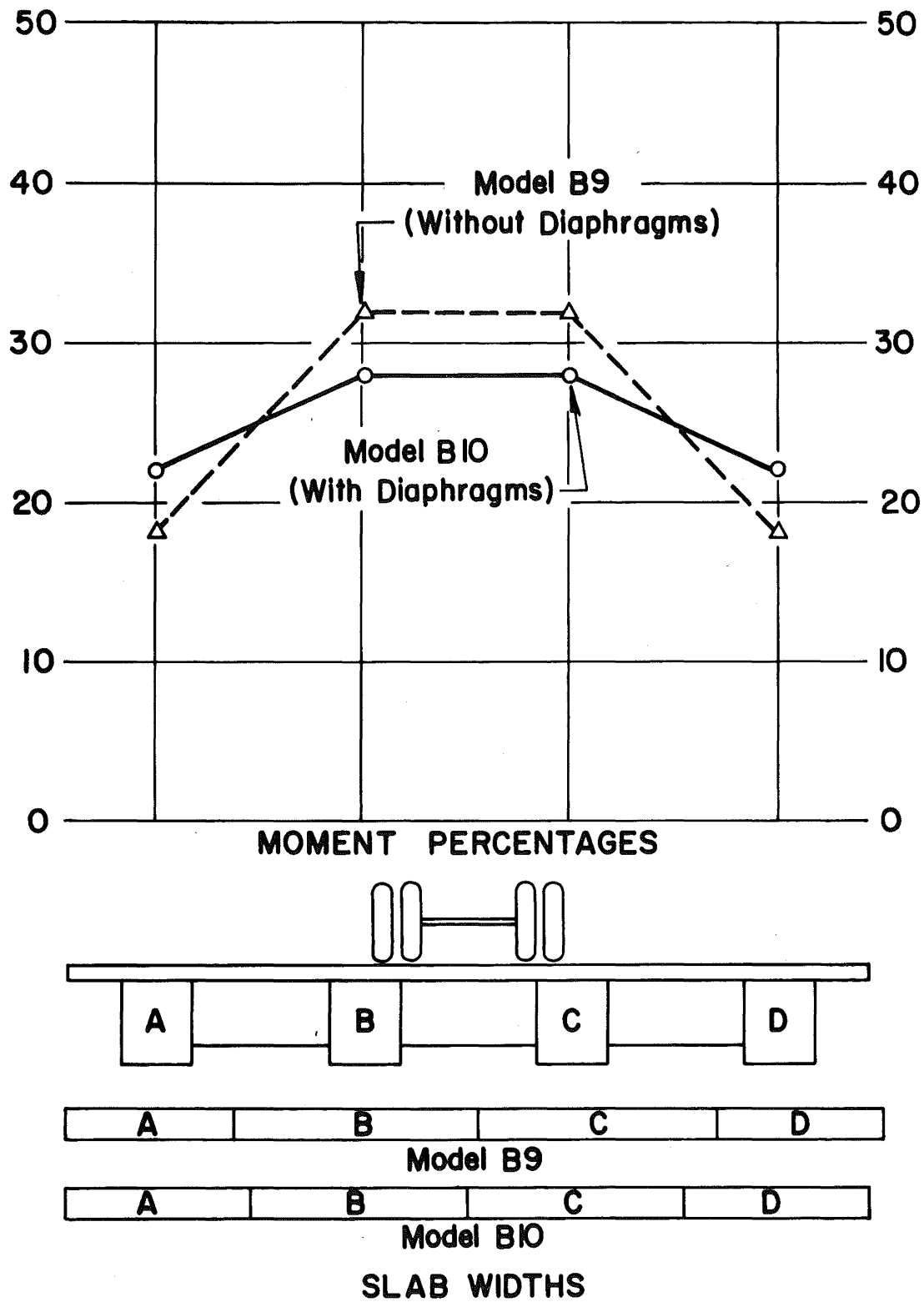
Fig. 44   Model B9 and Model B10, Lane 3
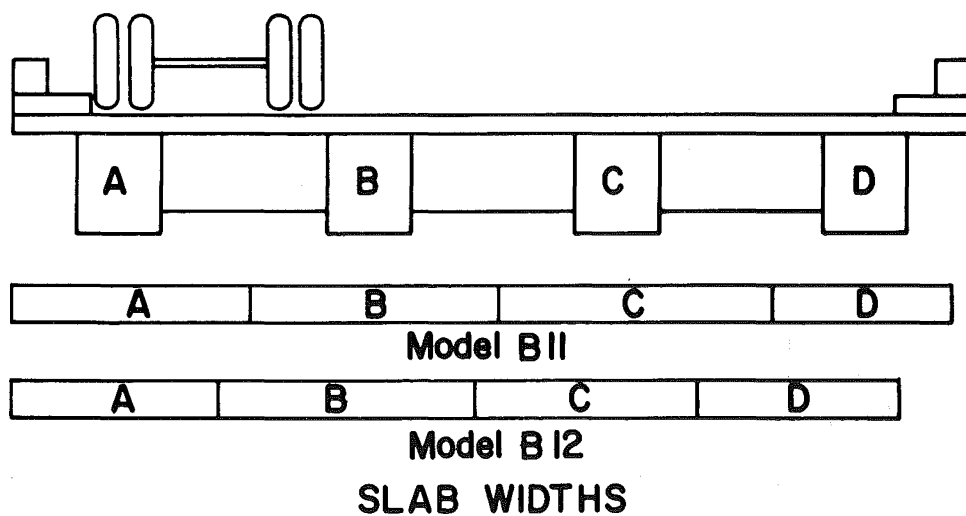
Fig. 45   Model B11 and Model B12, Lane 1

Fig. 46    Model B11 and Model B12, Lane 2
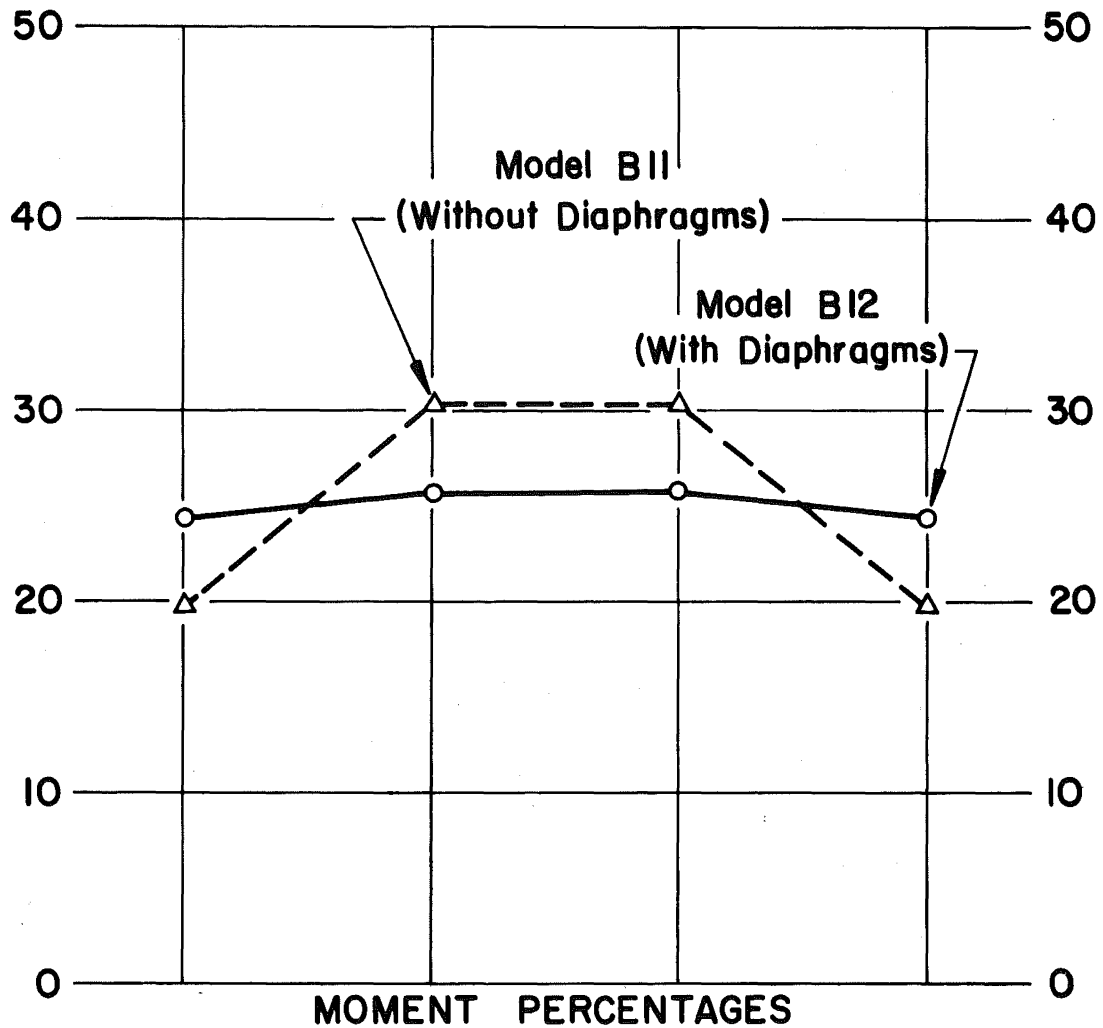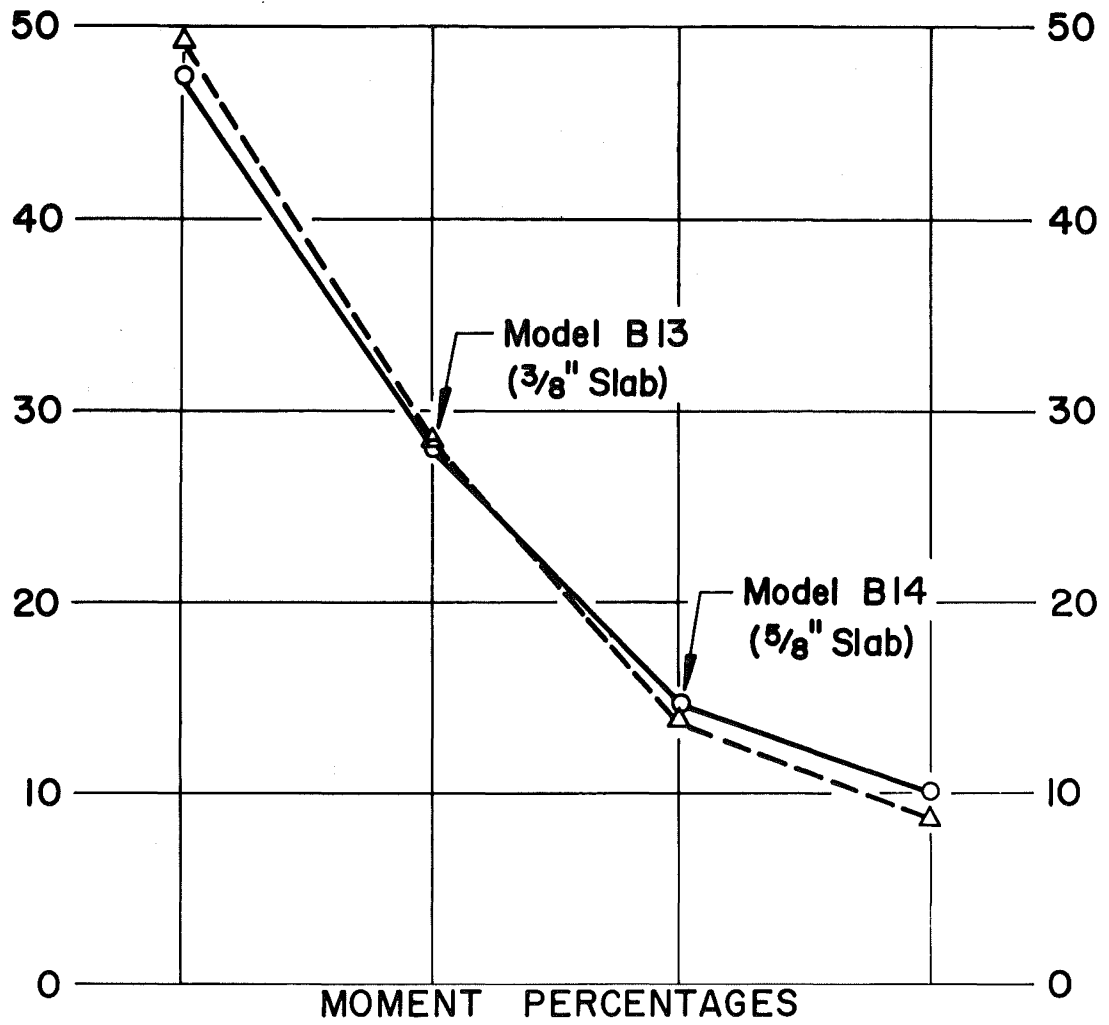
Fig. 47    Model B11 and Model B12, Lane 3
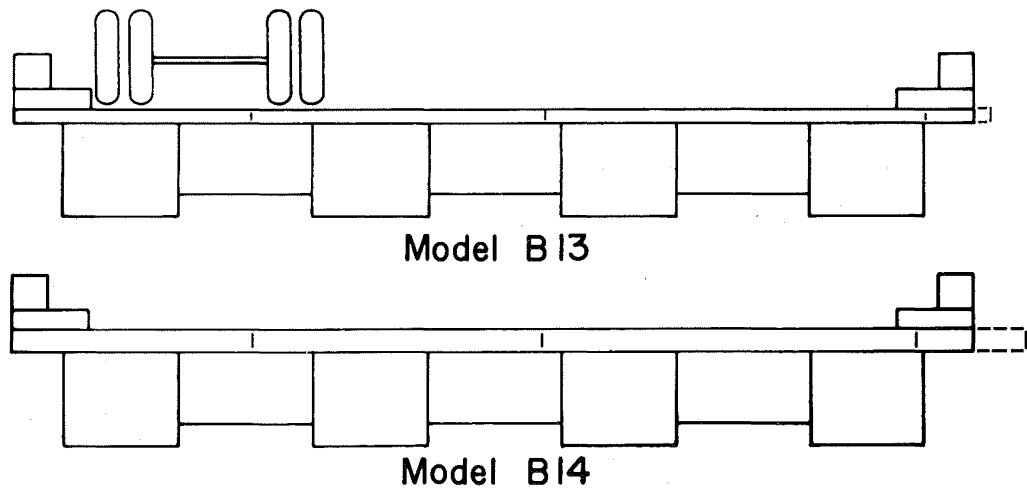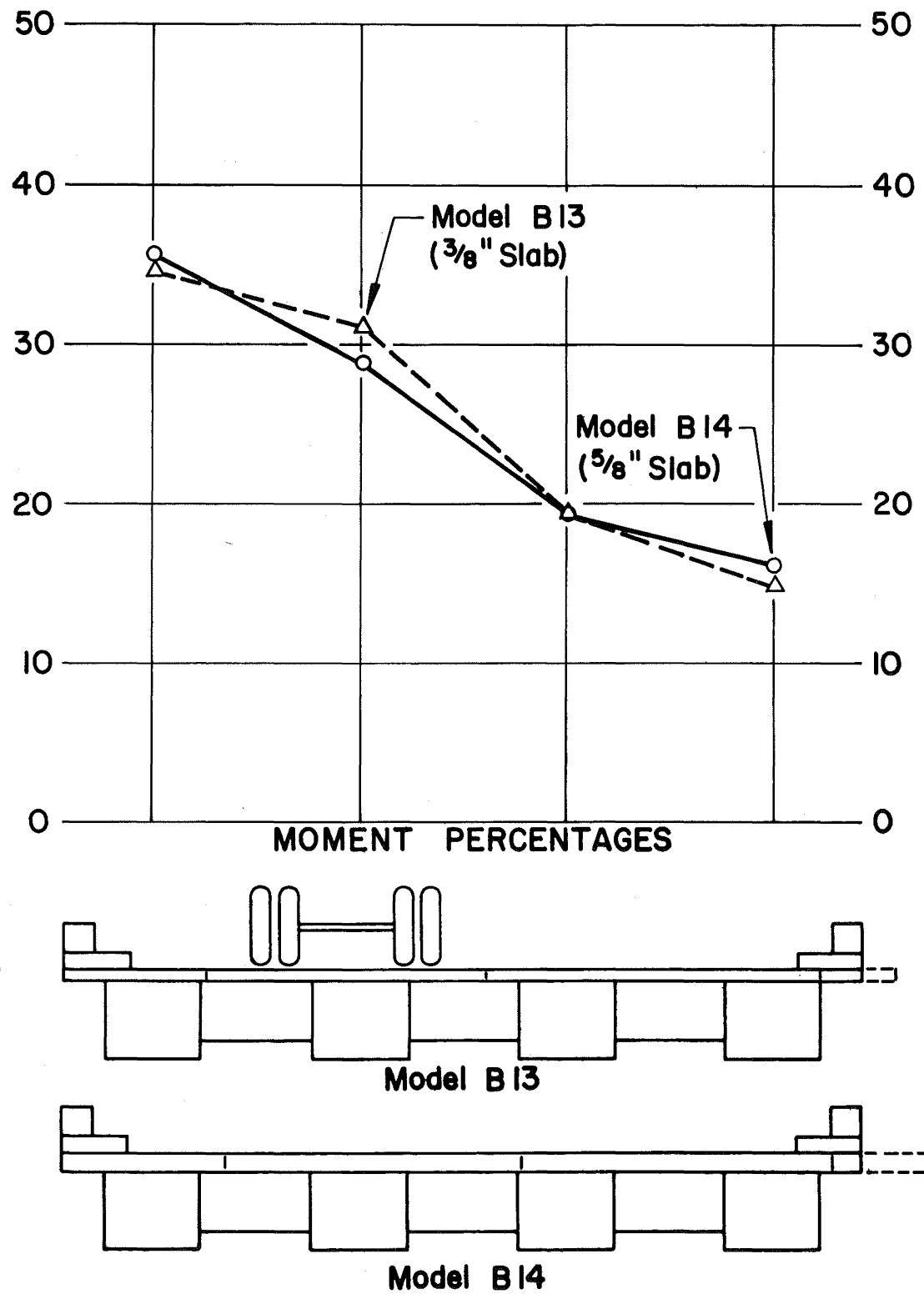
Fig. 48   Model B13 and Model B14, Lane 1

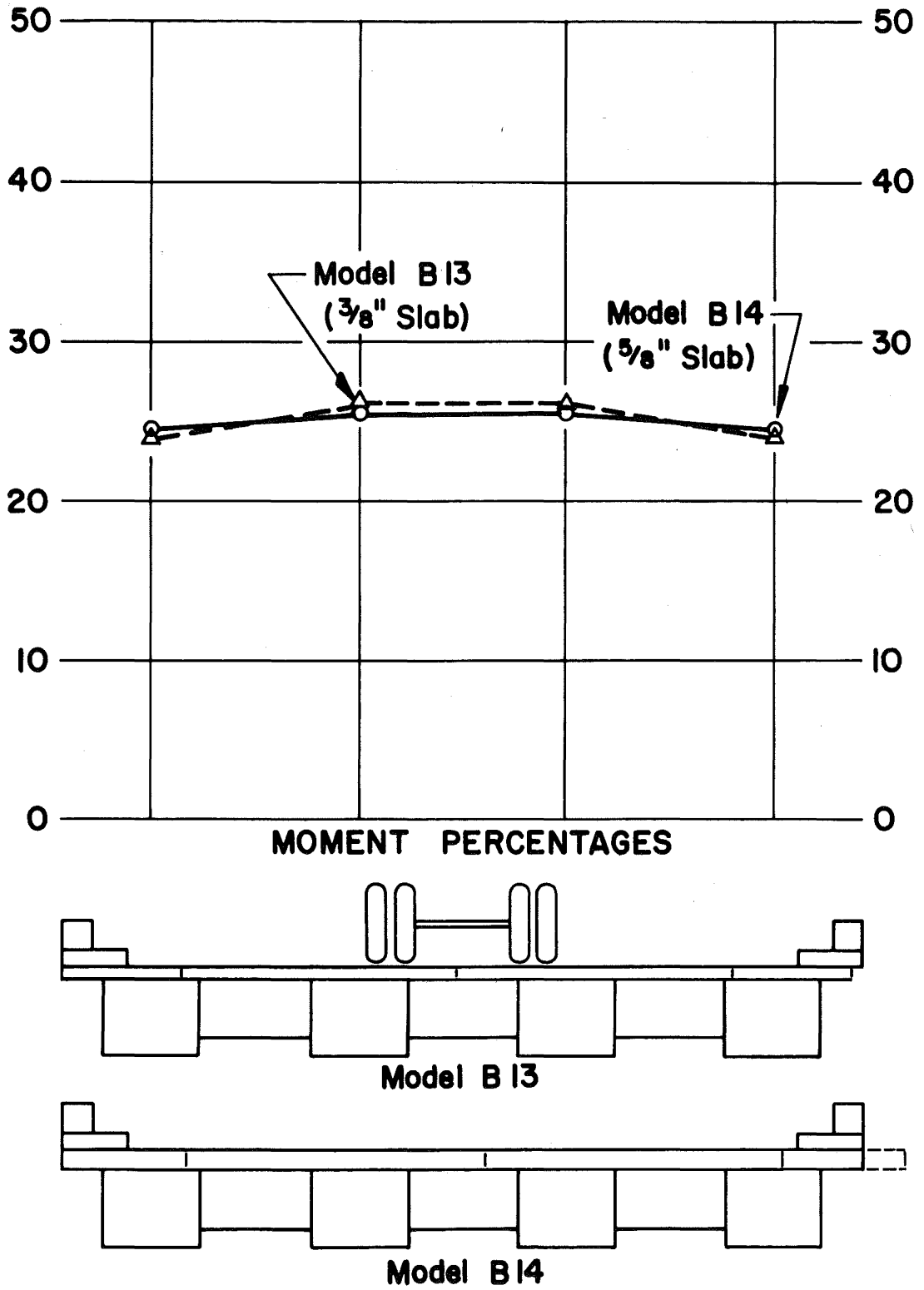Fig. 49    Model B13 and Model B14, Lane 2

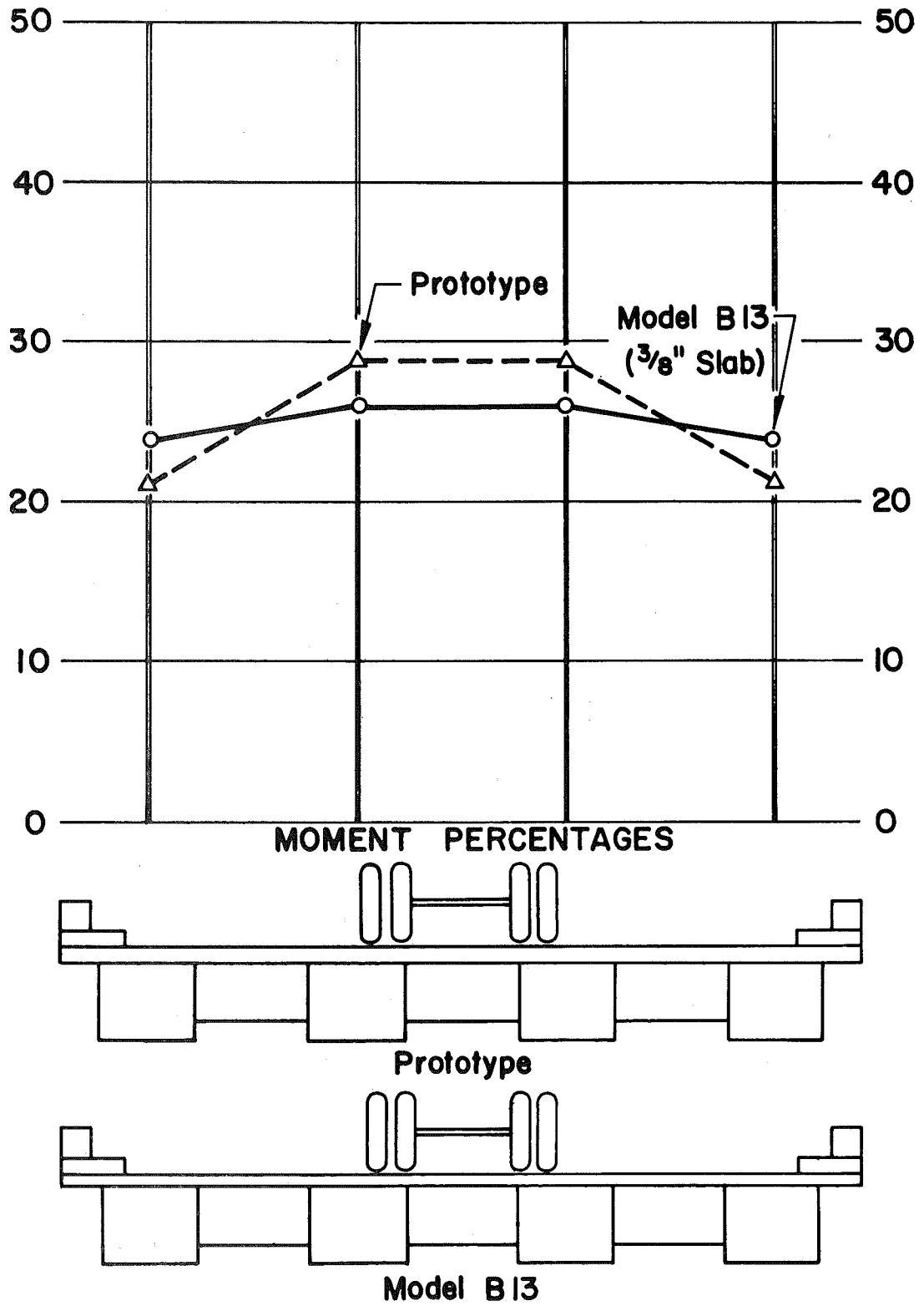Fig. 50    Model B13 and Model B14, Lane 3

134



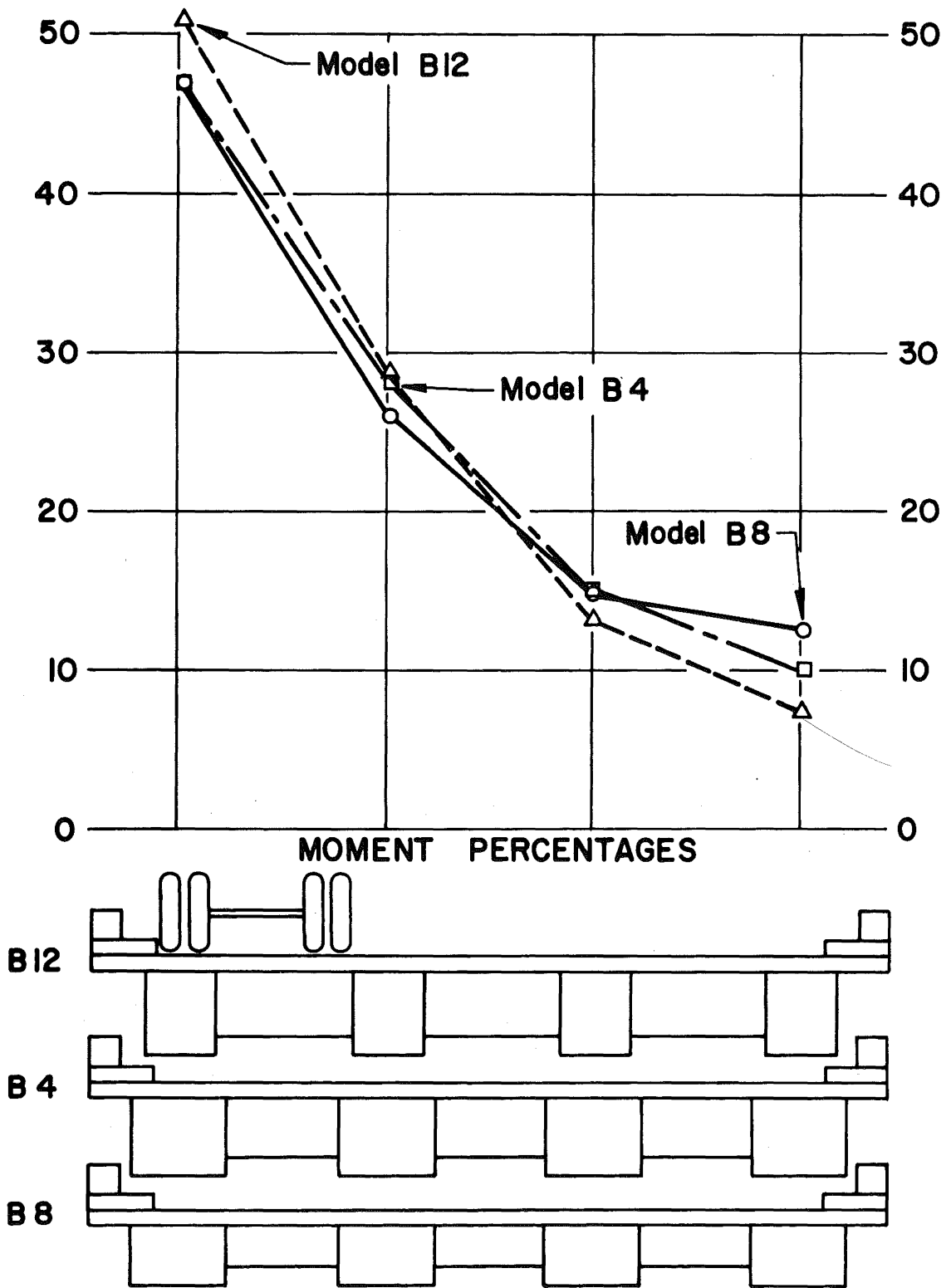Fig. 51　Prototype and Model B13, Lane 3

Fig. 52   Model B12, Model B4, and Model B8, Lane 1

Fig. 53    Model B12, Model B4, and Model B8, Lane 2
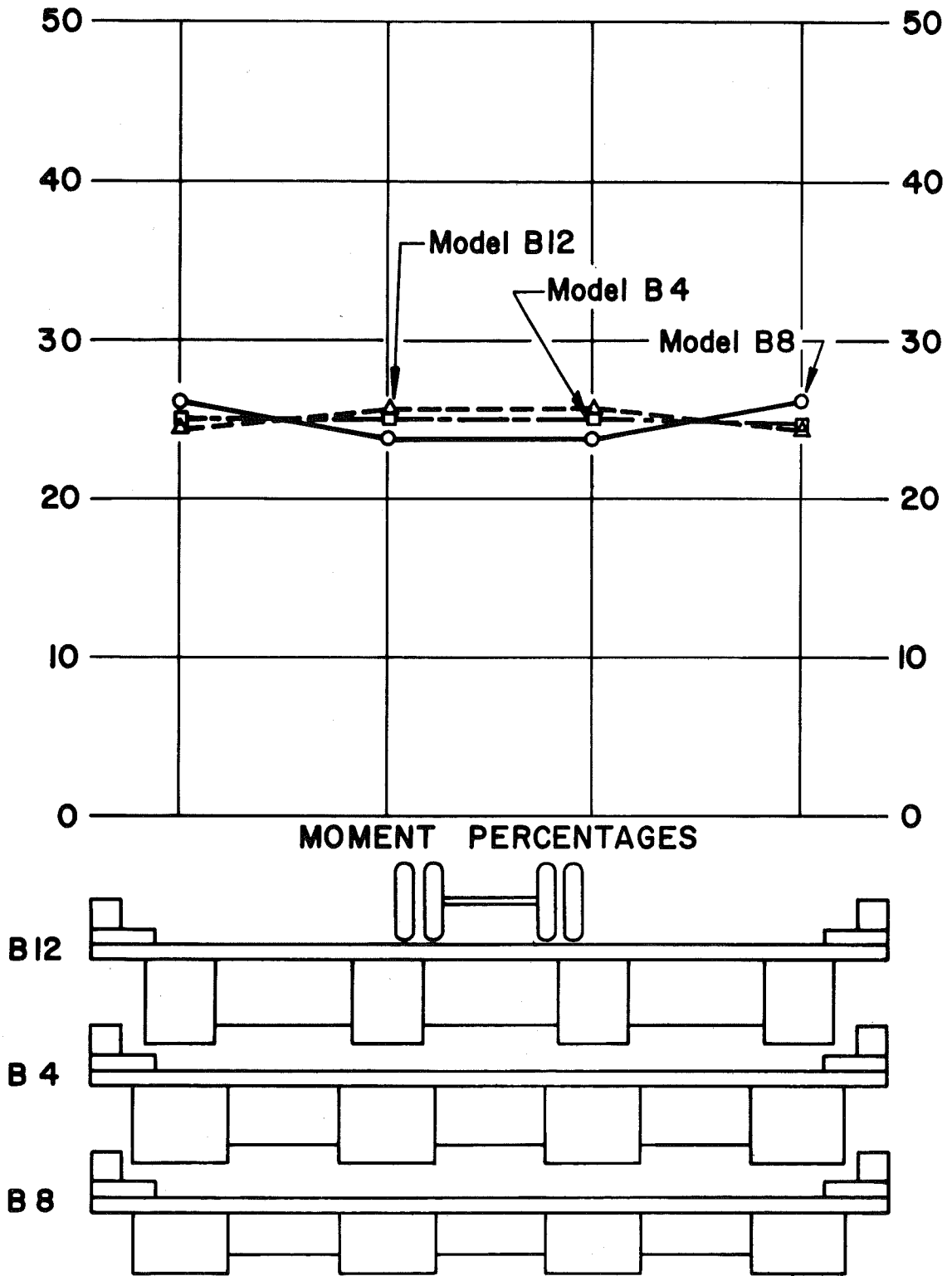
Fig. 54   Model B12, Model B4, and Model B8, Lane 3
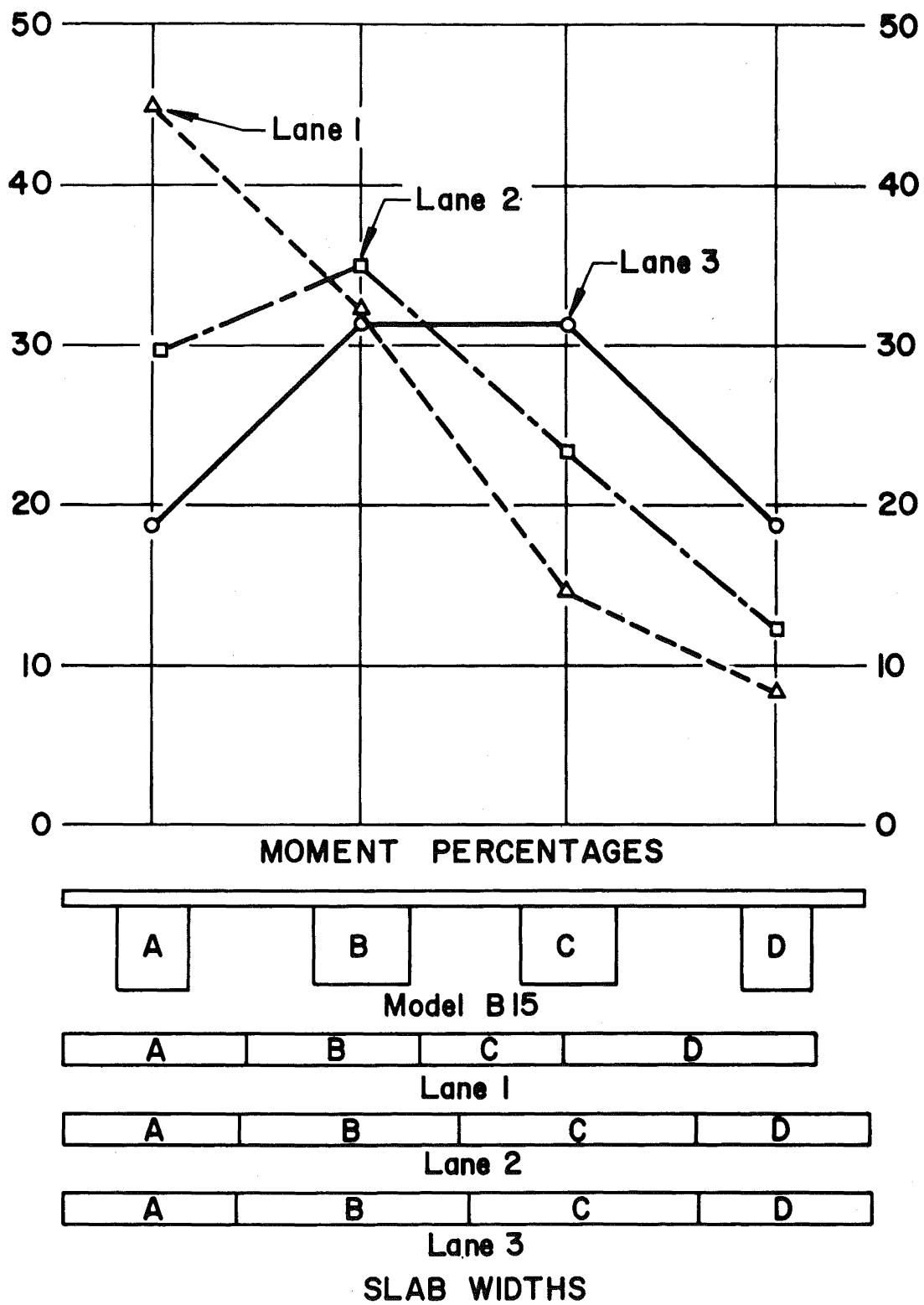
Fig. 55    Model B15, Lanes 1, 2, and 3

Fig. 56    Model B9, Model B1, and Model B15, Lane 1
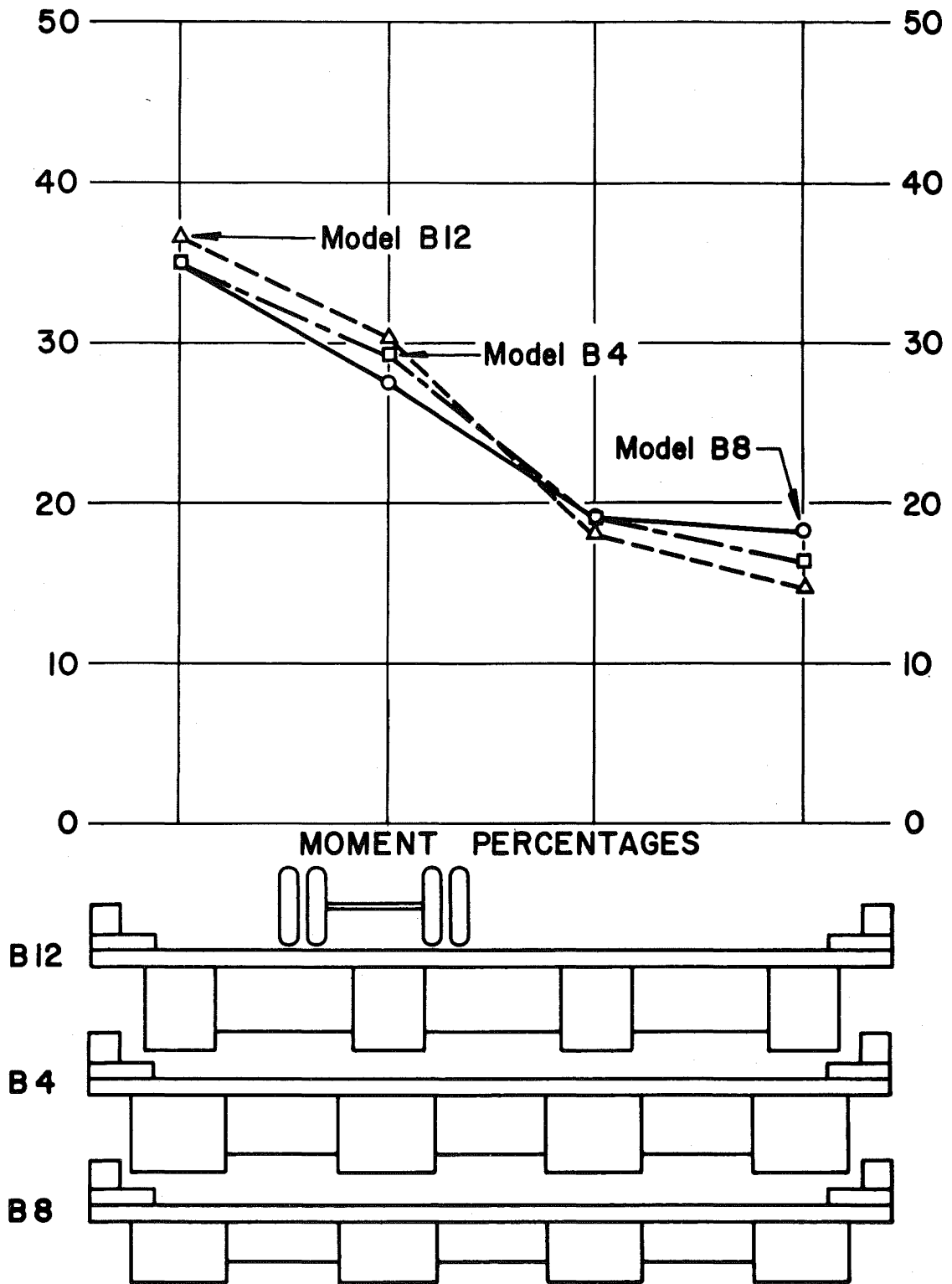
Fig. 57   Model B9, Model B1, and Model B15, Lane 2

Fig. 58    Model B9, Model B1, and Model B15, Lane 3
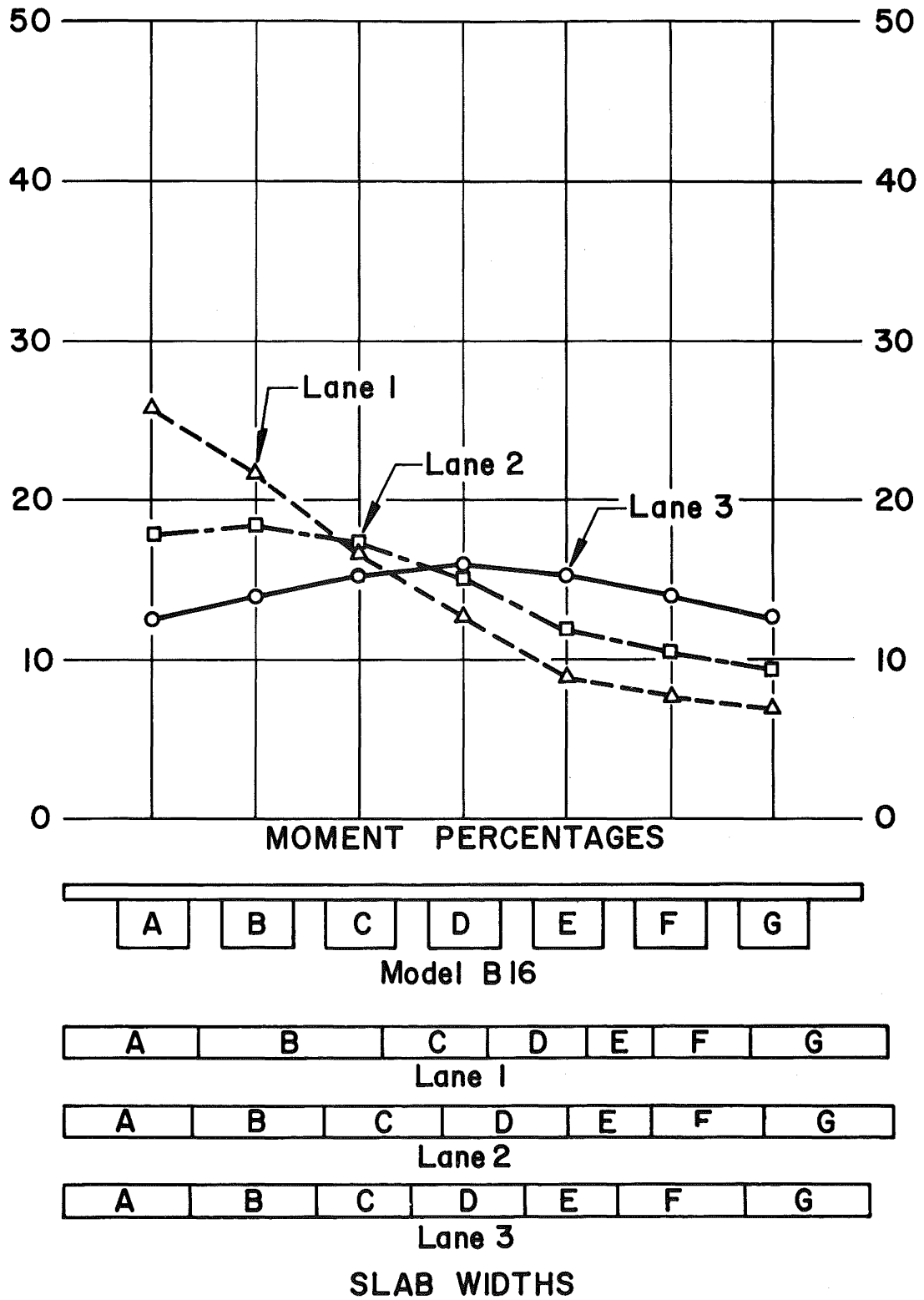
Fig. 59    Model B16, Lanes 1, 2, and 3

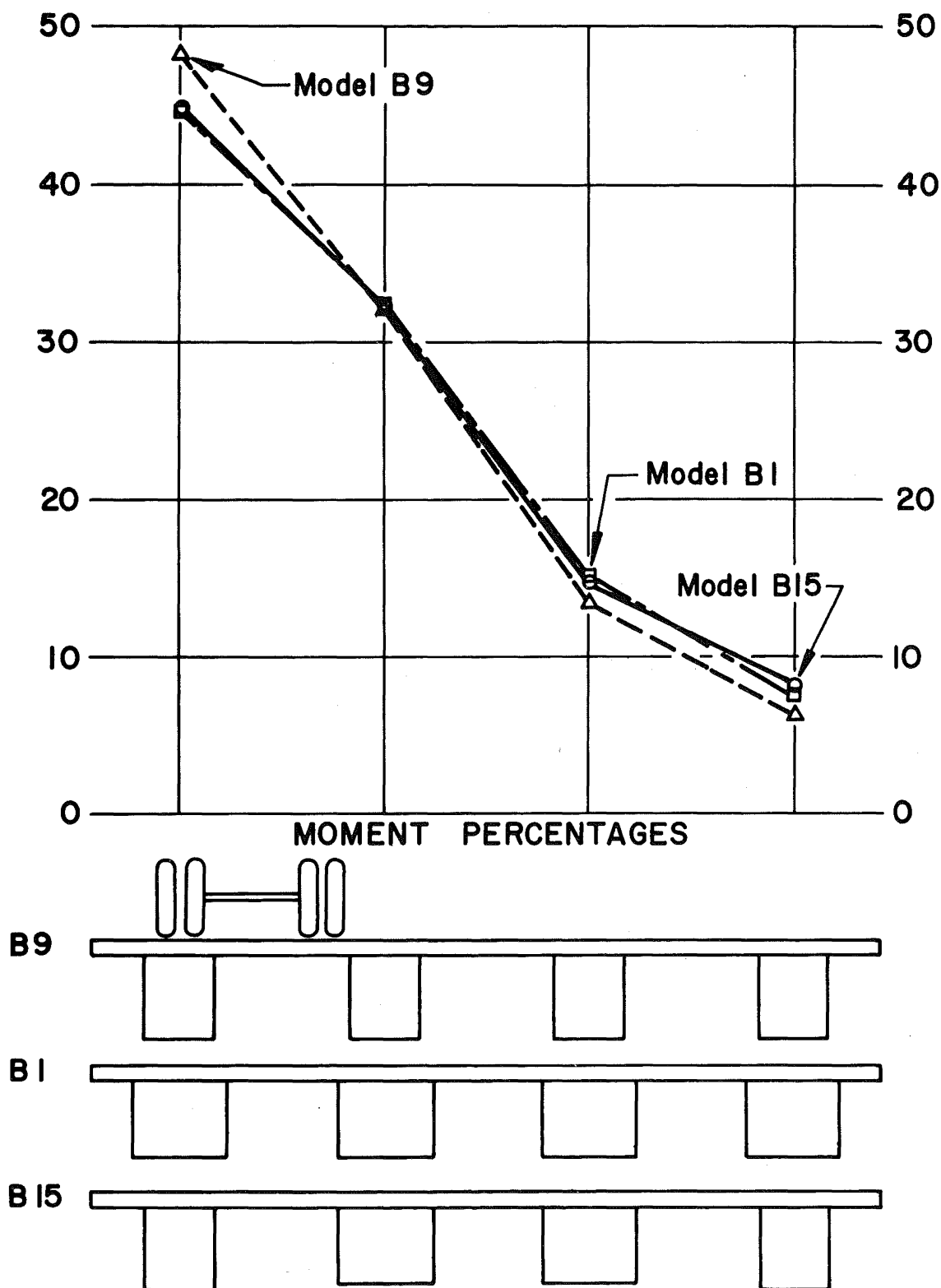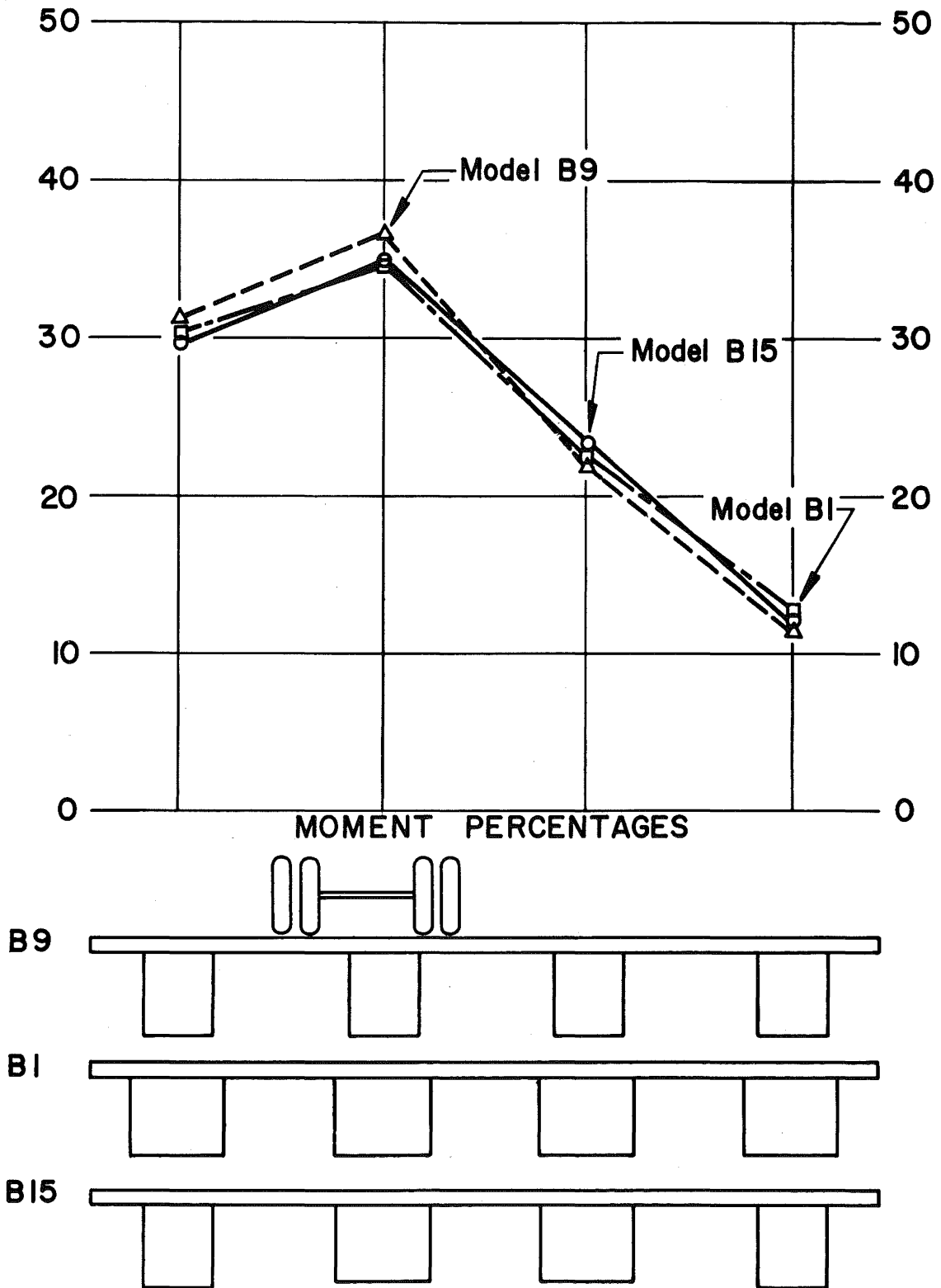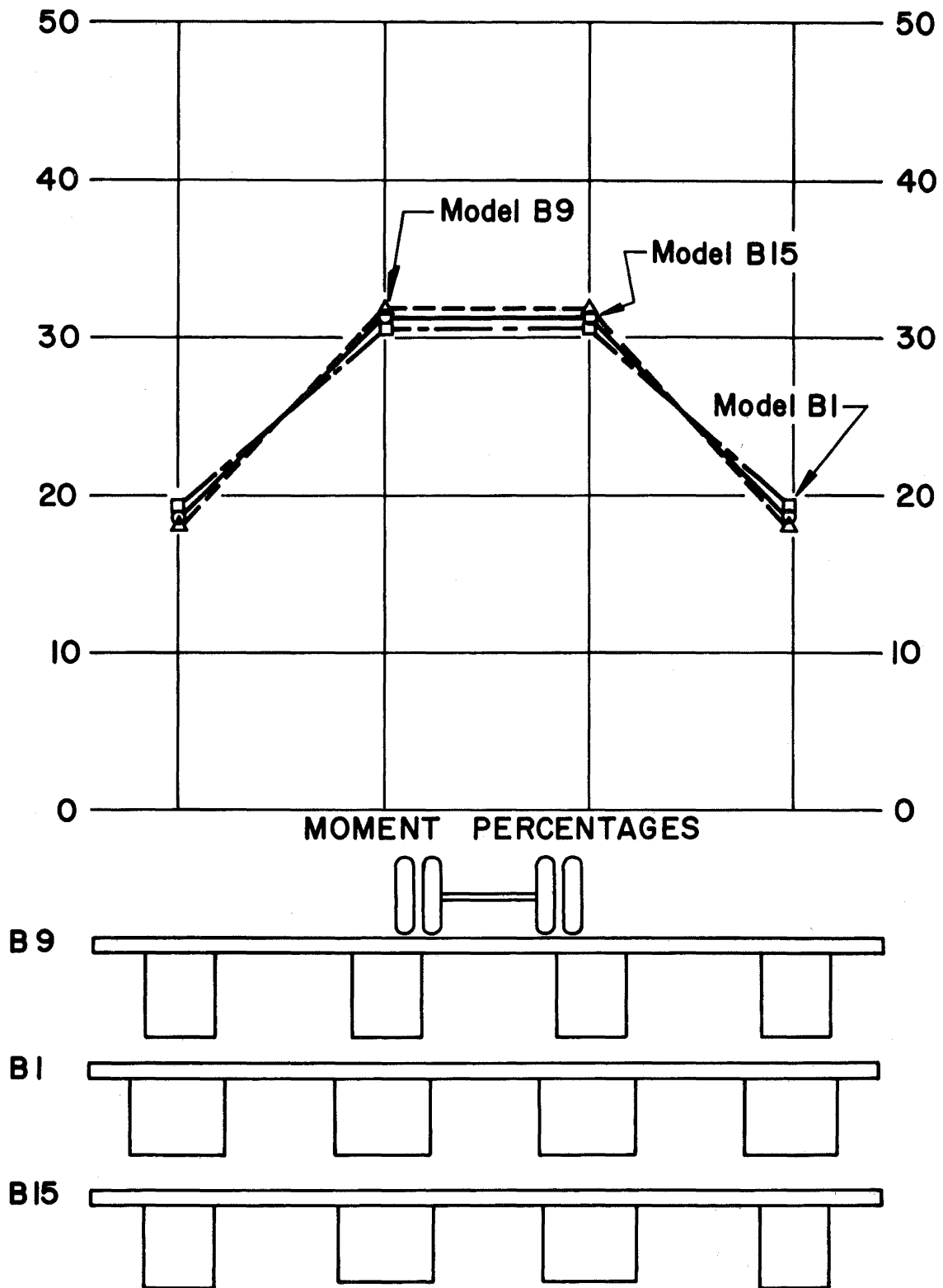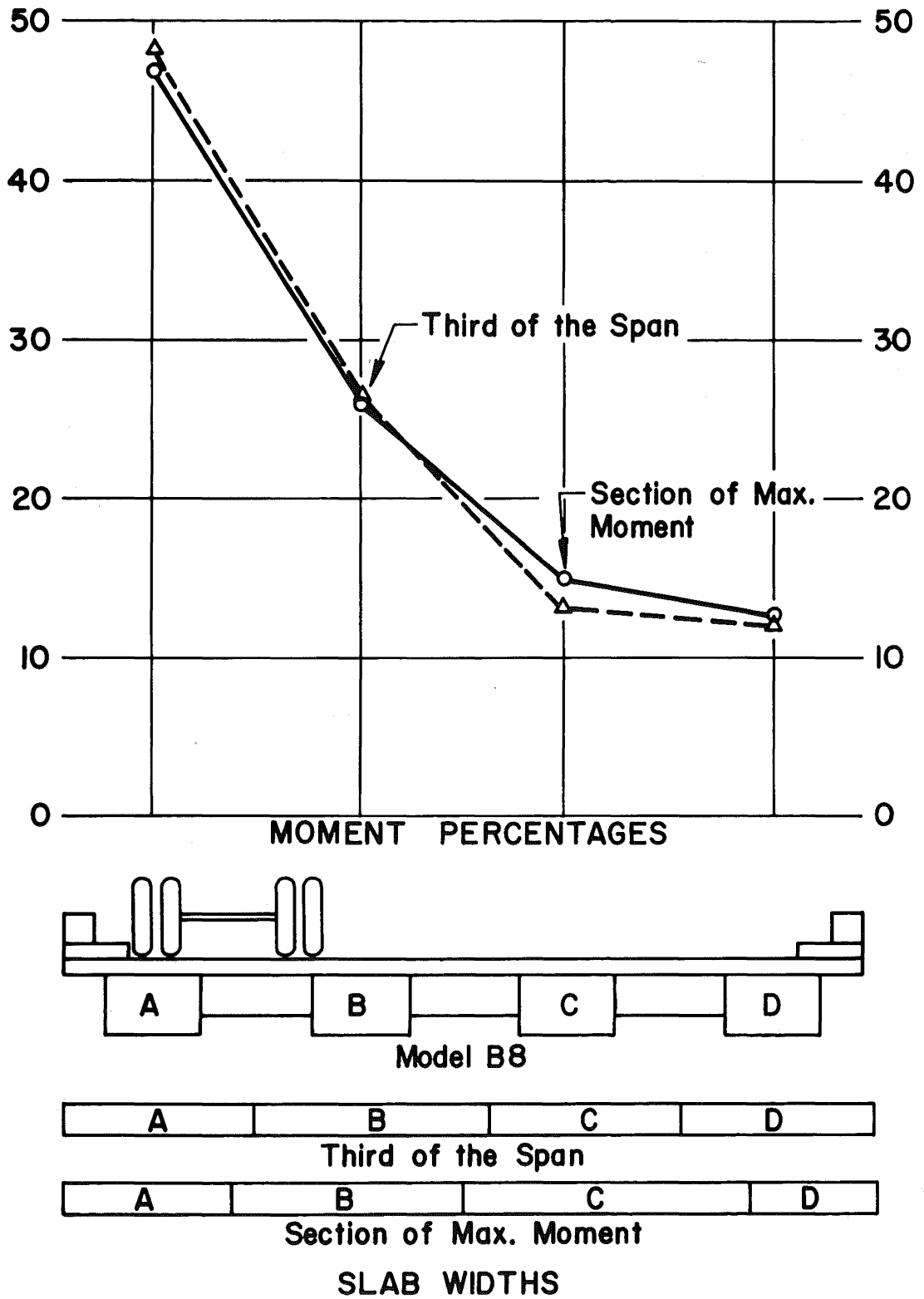Fig. 60    Model B8, Third of the Span and Section
of Maximum Moment, Lane 1
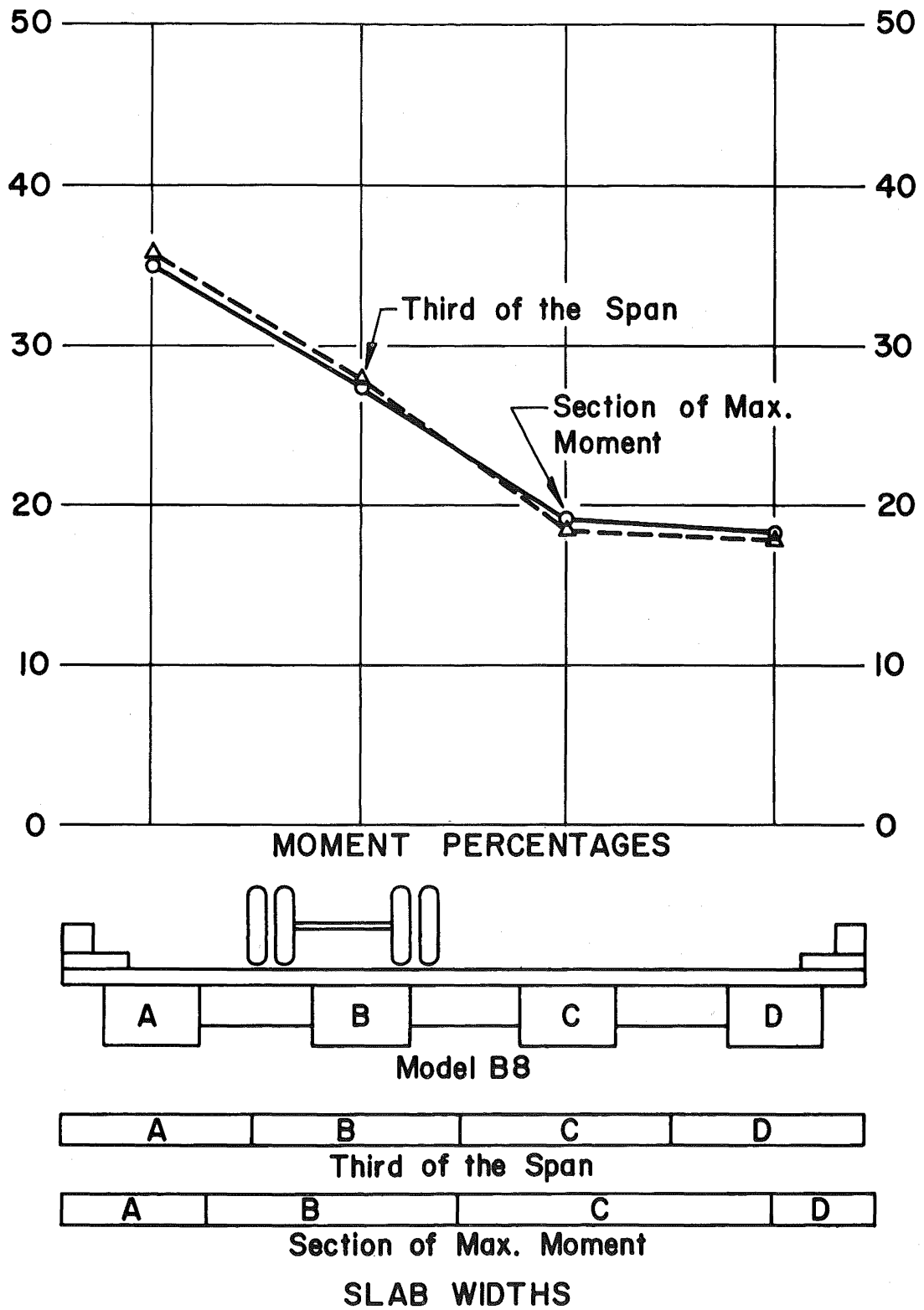
Fig. 61. Model B8, Third of the Span and Section of Maximum Moment, Lane 2
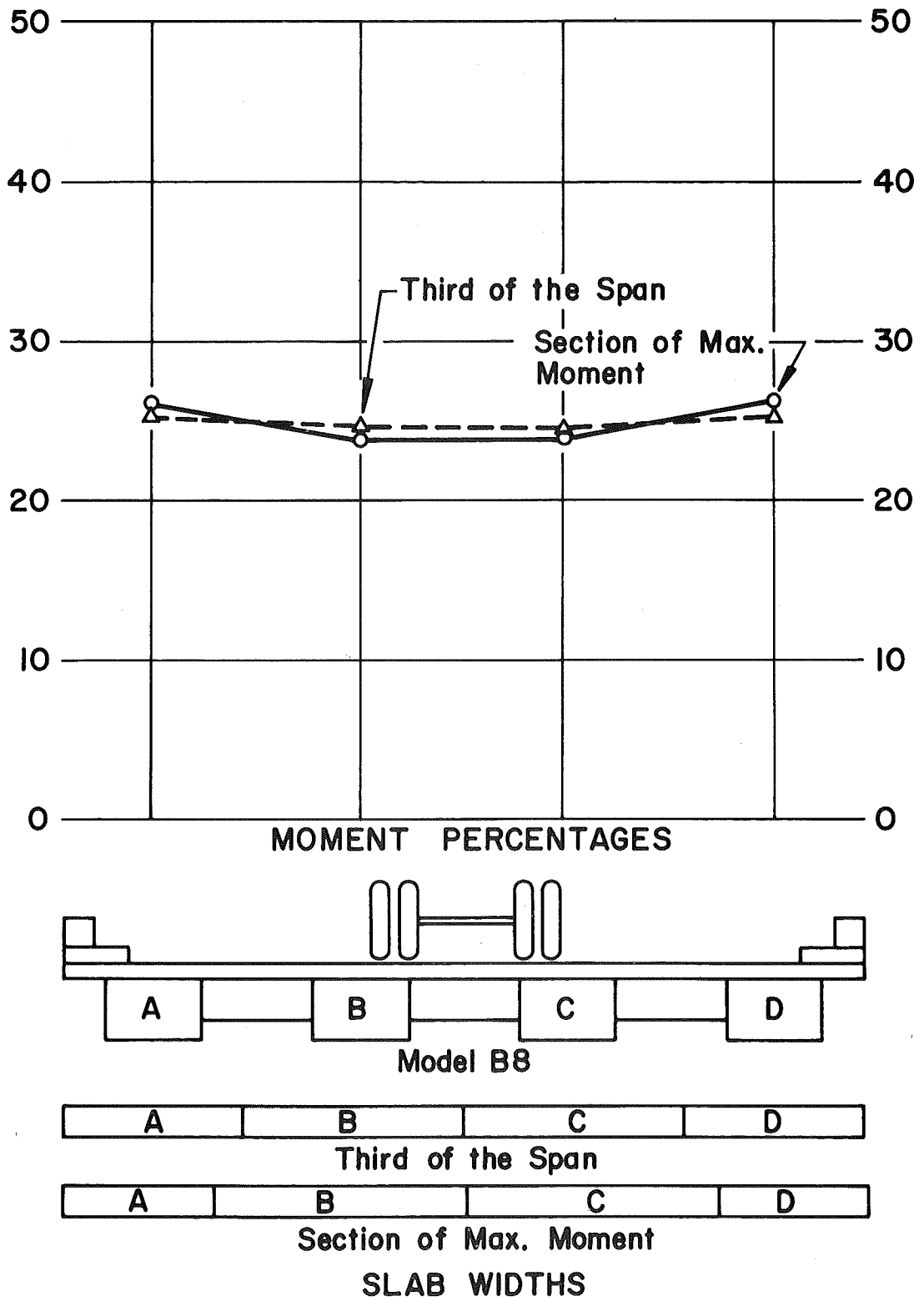
Fig. 62    Model B8, Third of the Span and Section
of Maximum Moment, Lane 3

14. <u>TABLES</u>

Table 1　Material Properties

| MATERIAL | E (lb/in.²) | ν | γ (lb/in.³) |
|---|---|---|---|
| Concrete | Varies with Strength | 0.15 to 0.22 | 0.086 |
| Plexiglas | 450,000* | 0.33* | 0.043 |
| Aluminum | 10,000,000 | 0.33 | 0.098 |
| Polyvinyl　Chloride | 400,000* | 0.33* | 0.045* |

*Typical values from manufacturers.

Table 2　Deflections and Rotations in Model Al and Prototype

| Load on Lane | Beam A | | | Beam B | | |
|---|---|---|---|---|---|---|
| | Model Al | Predicted Prototype | Field Test | Model Al | Predicted Prototype | Field Test |
| DEFLECTIONS IN TEN THOUSANDTHS OF AN INCH | | | | | | |
| 1 | 34 | 544 | 893 | 28 | 448 | 792 |
| 2 | 24 | 384 | 683 | 24 | 384 | 801 |
| 3 | 23 | 368 | 514 | 27 | 432 | 761 |
| 4 | 14 | 224 | 369 | 19 | 304 | 600 |
| 5 | 13 | 208 | 271 | 19 | 304 | 478 |
| ROTATIONS IN MILLIONTHS OF A RADIAN ( (+) ) | | | | | | |
| 1 | -55 | -55 | 52 | -122 | -122 | -393 |
| 2 | 30 | 30 | 54 | -28 | -28 | -58 |
| 3 | 73 | 73 | 156 | 51 | 51 | 134 |
| 4 | 72 | 72 | 97 | 82 | 82 | 190 |
| 5 | 92 | 92 | 106 | 96 | 96 | 193 |

Table 3    Theoretical Values of Flexural and Torsional Moments
of Inertia of Prototype Beams

| Width (ft.) | Depth (in.) | I (in.$^4$) | $I/I_{(3'\times24")}$ | J* (in.$^4$) | $J/J_{(3'\times24")}$ |
|---|---|---|---|---|---|
| 3 | 21 | 2.26 | 0.71 | 9.5 | 0.83 |
| | 24 | 3.20 | 1.00 | 11.5 | 1.00 |
| | 27 | 4.32 | 1.35 | 14.1 | 1.23 |
| | 30 | 5.68 | 1.77 | 16.7 | 1.45 |
| | 33 | 7.24 | 2.26**[1] | 19.5 | 1.70 |
| | 36 | 9.06 | 2.83 | 22.3 | 1.94 |
| | 39 | 11.11 | 3.47 | 25.6 | 2.23 |
| | 42 | 13.50 | 4.22**[2] | 28.8 | 2.50*** |
| | 45 | 16.10 | 5.02 | 32.6 | 2.83 |
| | 48 | 18.90 | 5.90 | 36.1 | 3.14 |
| 4 | 21 | 2.94 | 0.92 | 16.4 | 1.43 |
| | 24 | 4.14 | 1.29 | 20.3 | 1.77 |
| | 27 | 5.58 | 1.74 | 24.3 | 2.11 |
| | 30 | 7.28 | 2.27**[1] | 28.5 | 2.48*** |
| | 33 | 9.24 | 2.89 | 33.2 | 2.89 |
| | 36 | 11.50 | 3.59 | 37.7 | 3.28 |
| | 39 | 14.00 | 4.37**[2] | 42.8 | 3.73 |
| | 42 | 16.90 | 5.28 | 48.0 | 4.17 |
| | 45 | 20.00 | 6.24 | 53.6 | 4.66 |
| | 48 | 23.50 | 7.30 | 59.1 | 5.14 |

*Using Bredt's Formula    **Match of I's    ***Match of J's

Table 4    Ratios of I's/J's of the Sections Adopted

| | 4'x30" | 4'x39" | 4' x 48" |
|---|---|---|---|
| 3'x24" | 2.27 / 2.48 | 4.37 / 3.73 | 7.30 / 5.14 |
| 3'x33" | 1.00 / 1.46 | 1.93 / 2.19 | 3.24 / 3.03 |
| 3'x42" | 0.54 / 0.99 | 1.04 / 1.49 | 1.74 / 2.05 |

Table 5  Models Tested

| Model No. | Number of Beams | Size of Beams | Slab Thick. (in.) | Curbs* | Parapets* | Dia-phragms* | File Comp. Output |
|---|---|---|---|---|---|---|---|
| A1 | 4 | 4x39 | 0.5 | 1 | 1 | 1 | I23 |
| B1 | 4 | 4x39 | 0.5 | 0 | 0 | 0 | a |
| B2 | 4 | 4x39 | 0.5 | 0 | 0 | 1 | n |
| B3 | 4 | 4x39 | 0.5 | 1 | 1 | 0 | m |
| B4 | 4 | 4x39 | 0.5 | 1 | 1 | 1 | e |
| B5 | 4 | 4x30 | 0.5 | 0 | 0 | 0 | k |
| B6 | 4 | 4x30 | 0.5 | 0 | 0 | 1 | l |
| B7 | 4 | 4x30 | 0.5 | 1 | 1 | 0 | j |
| B8 | 4 | 4x30 | 0.5 | 1 | 1 | 1 | i |
| B9 | 4 | 3x42 | 0.5 | 0 | 0 | 0 | o |
| B10 | 4 | 3x42 | 0.5 | 0 | 0 | 1 | r |
| B11 | 4 | 3x42 | 0.5 | 1 | 1 | 0 | p |
| B12 | 4 | 3x42 | 0.5 | 1 | 1 | 1 | q |
| B13 | 4 | 4x39 | 0.375 | 1 | 1 | 1 | g |
| B14 | 4 | 4x39 | 0.625 | 1 | 1 | 1 | f |
| B15 | 4 | 2-3x42 2-4x30 | 0.5 | 0 | 0 | 0 | s |
| B16 | 7 | 3x24 | 0.5 | 0 | 0 | 0 | t |

*Code:  A zero means NO and a one means YES.

## 15.   REFERENCES

1.  American Association of State Highway Officials
    STANDARD SPECIFICATIONS FOR HIGHWAY BRIDGES, Ninth
    Edition, Washington, D. C.  1965.

2.  American Institute of Steel Construction
    DESIGN MANUAL FOR ORTHOTROPIC STEEL PLATE DECK BRIDGES,
    New York, 1963.

3.  American Society for Testing and Materials
    STANDARDS, Part 27, Philadelphia, Pa., 1966.

4.  Carpenter, J. E.
    STRUCTURAL MODEL TESTING; COMPENSATION FOR TIME EFFECT
    IN PLASTICS, Portland Cement Association, Skokie, Ill.,
    Bull. D60, January, 1963.

5.  Dietz, A. G. H. and Campbell, W. H.
    BONDED WIRE STRAIN GAGE TECHNIQUES FOR POLYMETHYL
    METHACRYLATE PLASTICS, Proceedings, Society for Experi-
    mental Stress Analysis, Bridgeport, Conn., Vol. V,
    No. 1, 1947.

6.  Eney, W. J.
    DETERMINING THE DEFLECTION OF STRUCTURES WITH MODELS,
    Civil Engineering, American Society of Civil Engineer-
    ing, Vol. 12, No. 3, New York, March, 1942.

7.  Fang, S. J.
    ESTIMATION OF BENDING MOMENTS IN BOX-BEAM BRIDGES USING
    CROSS-SECTIONAL DEFLECTIONS, Lehigh University, M.S.
    Thesis, Bethlehem, Pa., 1968.

8.  Guilford, A. A. and VanHorn, D. A.
    LATERAL DISTRIBUTION OF VEHICULAR LOADS IN A PRESTRESSED
    CONCRETE BOX-BEAM BRIDGE, BERWICK BRIDGE, Fritz Engineer-
    ing Laboratory Report No. 315.4, Lehigh University,
    October, 1967.

150

9. Hetényi, M.
     HANDBOOK OF EXPERIMENTAL STRESS ANALYSIS, John Wiley
     & Sons, Inc., New York, 1963.


10. Hoel, P. G.
     INTRODUCTION TO MATHEMATICAL STATISTICS, John Wiley
     & Sons, Inc., New York, 1965.


11. Lin, T. Y.
     DESIGN OF PRESTRESSED CONCRETE STRUCTURES, Second
     Edition, John Wiley & Sons, Inc., New York, 1963.


12. Litle, W. A. and Hansen, R. J.
     THE USE OF MODELS IN STRUCTURAL DESIGN, Journal, Boston
     Society of Civil Engineers, Vol. 50, No. 2, April 1963.


13. Massonnet, C.
     COMPLEMENTS A LA METHODE DE CALCUL DES PONTS A POUTRES
     MULTIPLES, (Complements to the Method of Calculation
     for Bridges with Several Longitudinal Beams), Public
     Works of Belgium, Brussels, 1954.


14. Massonnet, C.
     L'ETUDE DES CONSTRUCTIONS SUR MODELES REDUITS SANS
     EMPLOI DE MICROSCOPES, (Study of Structures by Means
     of Small Scale Models without Use of Microscopes), Bull.
     Center of Studies, Research and Scientific Tests for
     Structures of Civil Engineering and Hydraulics, Univer-
     sity of Liège, Belgium, Vol. VI, 1953.


15. Massonnet, C.
     METHODE DE CALCUL DES PONTS A POUTRES MULTIPLES TENANT
     COMPTE DE LEUR RESISTANCE A LA TORSION, (Method of
     Calculation for Bridges with Several Longitudinal Beams,
     Taking into Consideration Their Torsional Resistance),
     Publications IABSE, Zurich, Vol. 10, 1950.


16. Murphy, G.
     SIMILITUDE IN ENGINEERING, Ronald Press, New York, 1950.


17. Natrella, M. G.
     EXPERIMENTAL STATISTICS, National Bureau of Standards
     Handbook 91, Washington, D.C., 1966.

18. Nelson, H. M., Beveridge, A. and Arthur, P. D.
    TESTS ON A MODEL COMPOSITE BRIDGE GIRDER, Publications
    IABSE, Zurich, Vol. 23, 1963.

19. Newmark, N. M. and Siess, C. P.
    RESEARCH ON HIGHWAY-BRIDGE FLOORS, University of Illinois
    Bull. No. 52, 1936-1954.

20. Pennsylvania Department of Highways, Bridge Division
    STANDARDS FOR PRESTRESSED CONCRETE BRIDGES, Harrisburg,
    1964.

21. Reese, R. T.
    LOAD DISTRIBUTION IN HIGHWAY BRIDGE FLOORS:  A SUMMARY
    AND EXAMINATION OF EXISTING METHODS OF ANALYSIS AND
    DESIGN AND CORRESPONDING TEST RESULTS, Brigham Young
    University, M.S. Thesis, Provo, Utah, 1966.

22. Scordelis, A. C.
    ANALYSIS OF SIMPLY SUPPORTED BOX GIRDER BRIDGES, Univer-
    sity of California, Berkeley, 1966.

23. Skeitz, I.
    HANDBOOK OF ADHESIVES, Reinhold Publishing Corp.,
    New York, 1965.

24. Wylie, C. R., Jr.
    ADVANCED ENGINEERING MATHEMATICS, McGraw-Hill, Co.,
    New York, 1960.

Miguel Angel Macías Rendón was born in Monterrey, Nuevo León, México on June 21, 1936. He is the second, and youngest, son of Miguel Angel Macías Valadés and Ana María Rendón de Macías. He received the degree of Ingeniero Civil from the Instituto Tecnológico y de Estudios Superiores de Monterrey in 1957.

In September 1957, the writer became a faculty member in the Civil Engineering Department of the Instituto Tecnológico y de Estudios Superiores de Monterrey. In 1959, he was granted a leave of absence to pursue graduate work at Lehigh University. In 1961, he received the degree of Master of Science in Civil Engineering from Lehigh University, and returned to Monterrey to his teaching and consulting work.

In September, 1964 he was granted a new leave of absence which permitted him to continue his graduate studies at Lehigh University under a scholarship from the Organization of American States. Since September 1965 he has held the titles of Research Assistant, Research Instructor, and Instructor in Civil Engineering.

In 1960, he married the former Romelia Treviño Leal of Monterrey, N.L. They have two children, Romelia Alejandra, and Miguel Angel.